12-2022

Differential Impacts of HHV-6A versus HHV-6B Infection in Differentiated Human Neural Stem Cells

Elham Bahramian
University of Arkansas, Fayetteville

Differential impacts of HHV-6A versus HHV-6B on differentiated human neural stem cells

A dissertation submitted in partial fulfillment
of the requirements for the degree of
Doctor of Philosophy in Cell and Molecular Biology

by

Elham Bahramian
Medical-Tehran University 2012
Bachelor of Science in Clinical Laboratory Science
Azad university-Qom 2016
Master in Cell and Molecular Biology-Microbiology

December 2022
University of Arkansas

This dissertation is approved for recommendation to the Graduate Council.

Ruben Michael Ceballos, Ph.D.
Dissertation Director

Jeannine Marie Durdik, Ph.D.
Committee Member

David S. McNabb, Ph.D.
Committee Member

Nagayasu Nakanishi, Ph.D.
Committee Member

Woodrow L. Shew, Ph.D.
Committee Member

ABSTRACT

Within the family Herpesviridae, sub-family β-herpesvirinae, and genus Roseolovirus, there are only three human herpesviruses that have been described: HHV-6A, HHV-6B, and HHV-7. Initially, HHV-6A and HHV-6B were considered as two variants of the same virus (i.e., HHV6). Despite high overall genetic sequence identity (~90%), HHV-6A and HHV-6B are now recognized as two distinct viruses. Sequence divergence (e.g., >30%) in key coding regions and significant differences in physiological and biochemical profiles (e.g., use of different receptors for viral entry) underscores the conclusion that HHV-6A and HHV-6B are distinct viruses of the β-herpesvirinae. Despite these viruses being implicated as causative agents in several nervous system disorders (e.g., multiple sclerosis, epilepsy, and chronic fatigue syndrome), the mechanisms of action and relative contributions of each virus to neurological dysfunction are unclear. Unresolved questions regarding differences in cell tropism, receptor use and binding affinity (i.e., CD46 versus CD134), host neuro-immunological responses, and relative virulence between HHV-6A versus HHV-6B prevent a complete characterization. Although it has been shown that both HHV-6A and HHV-6B can infect glia (and, recently, cerebellar Purkinje cells), cell tropism of HHV-6A versus HHV-6B for different nerve cell types remains vague. In this study, we show that both viruses can infect different nerve cell types (i.e., glia versus neurons) and different neurotransmitter phenotypes derived from differentiated human neural stem cells. As demonstrated by immunofluorescence, HHV-6A and HHV-6B productively infect VGluT1-containing cells (i.e., glutamatergic neurons) and dopamine-containing cells (i.e., dopaminergic neurons). However, neither virus appears to infect GAD67-containing cells (i.e., GABAergic neurons). As determined by qPCR, the expression of immunological factors (e.g., cytokines) in

cells infected with HHV-6A versus HHV6-B also differs. These data, along with morphometric and image analyses of infected differentiated neural stem cell cultures, indicate that while HHV-6B may have a greater opportunity for transmission, HHV-6A induces more severe cytopathic effects (e.g., syncytia) at the same post-infection end points. Cumulatively, results suggest that HHV-6A is more virulent than HHV-6B in susceptible cells, while neither virus productively infects GABAergic cells. Consistency between these in vitro data and in vivo experiments would provide new insights into potential mechanisms for HHV6-induced epileptogenesis.

ACKNOWLEDGEMENTS

First and foremost, I would like to thank Dr. Ruben Michael Ceballos, my teacher, best advisor, and dissertation committee chair, for his guidance and support, which have made this journey an incredible experience for me. I also thank my other dissertation committee members, Dr. McNab, Dr. Durdik, Dr. Nakanishi, and Dr. Shew. I'd also want to thank all the professors in the biology department who have inspired me with their knowledge and wisdom.

I am thankful to my past and present lab members, from whom I have learned much.

I want to take this opportunity to thank all of my Iranian friends for their genuine friendship and for being like family to me, especially when I was alone in the United States. I couldn't have finished my program without your help.

My parents' support has always been key to my endeavors. I am grateful to have you. Even though you were miles and miles away, your compassion never left me. I'd also want to thank my fantastic sister, role model, teacher, and my best, Hoda, for her endless love and for being a wonderful person in my life. Finally, I would like to thank my best friend, beloved, and brilliant partner, Amin, whose combination of relief and empathy has always balanced my life.

DEDICATION

This dissertation is dedicated to Baba Hojjat and Maman who suffering from our geographic separation. It is also dedicated to my life's love, Amin.

CONTENTS

LIST OF FIGURES

LIST OF PUBLISHED PAPERS

CHAPTER 1 and 2

Bahramian, Elham, Mercede Furr, Jerry T. Wu, and Ruben Michael Ceballos. "Differential impacts of HHV-6A versus HHV-6B on differentiated human neural stem cells." *Frontiers in Immunology*: 3617.

1   CHAPTER I

1.1   INTRODUCTION

1.1.1   Introduction to HHV6 and classification

Human herpesvirus 6 (HHV-6) was isolated in the USA from patients with AIDS In 1986(Salahuddin et al., 1986). In 1987 and 1988, independent samples were isolated from AIDS patients in Africa and were given the names U1102 (from Uganda) and Z29 (from Zaire)(Downing et al., 1987; Lopez et al., 1988). Since more strains from various geographical areas and health centers were discovered, it became evident that all HHV-6 isolates could be divided into two separate groups, each with its unique set of genetic, epidemiological, and biological features(D. Ablashi et al., 1991; Josephs et al., 1988; Schirmer, Wyatt, Yamanishi, Rodriguez, & Frenkel, 1991; Wyatt, Balachandran, & Frenkel, 1990). Particular immunological reactivity with monoclonal antibodies, differential patterns of restriction endonuclease sites, and specific and conserved interstrain variances in DNA sequences were also different between the two groups, as was in vitro tropism for certain T cell lines(Iyengar, Levine, Ablashi, Neequaye, & Pearson, 1991; Josephs et al., 1988).

HHV-6 is a member of the Herpesviridae family's β-Herpesvirinae subfamily, where it was placed due to genetic similarities with human cytomegalovirus (HCMV)(Yamanishi, 2007). The distinctions between HHV-6A and HHV-6B, as well as their connections to the other of the

herpesvirus family, have recently been confirmed using genomic sequencing(Dominguez et al.,

1999). It, like HHV-7, belongs to the Roseolovirus genus, and infection is widespread

worldwide(Caselli & Di Luca, 2007).

1.1.2 HHV6 Genome

HHV-6A and HHV-6B exhibit substantial sequence identity (ranging from 75% to 95%

depending on the genome area under study) but differ in the genome sequence, cell tropism,

growth characteristics, antigenic features, epidemiology, and disease association(D. Ablashi et

al., 1991; Aubin et al., 1993; Greninger et al., 2018). The HHV-6 genome is constituted of a

double-stranded linear DNA segment of approximately 160 Kb in length, with minor variations

between strains 6A (about 156 Kb for the GS strain) and 6B. (about 161 Kb long for the Z29

strain)(Finkel et al., 2020). The virus genome was sequenced in 1995 and contains over 100 open

reading frames (ORFs), the majority of which are found in the unique region (U), which is

surrounded by 8–9 Kb direct repeats (DR, DRL left, and DRR right), each contains 9 ORFs, viral

DNA packaging elements (pac1 and pac2), and human telomere-like (TAACCC)

repeats(Gompels et al., 1995). HHV6 integration into germline cells can result in the viral

genome being passed down from generation to generation in roughly 1% of the human

population; this condition is known as inherited chromosomally integrated HHV6 (iciHHV6).

U94 transcripts were detected in the majority (54.5%) of PBMC obtained from 11 iciHHV-6

patients, indicating that U94 plays a part during integration(Strenger et al., 2014). Both HHV6A and HHV6B include telomere-like repeats at the ends of their genomes, which are believed to be crucial in establishing latency via viral genome integration into human chromosomes(Arbuckle et al., 2010; Arbuckle et al., 2013).

DRs and the right end of the U region, covering ORFs U86 to U100, are the most diverged areas in HHV6-A and HHV6-B(Engdahl et al., 2019a). The HHV-6A and HHV-6B immediate-early 1 (IE1) proteins, encoded by the U90–U89 genes, have just 62 % homology(Stanton, Wilkinson, & Fox, 2003). The nucleotide sequences of these two areas are 85 % and 72 % identical, respectively(Dominguez et al., 1999). The most variable genes include the immediate-early 1 (IE1) gene (U90–U89), specific segments of the glycoprotein B (U39) and glycoprotein H (U48) genes, and U94, which is employed to differentiate between 6A and 6B species(Achour et al., 2008; Rapp, Krug, Inoue, Dambaugh, & Pellett, 2000). The U94 gene is found in the antisense strand of the viral genome and has no analogs in any other known human herpesviruses, including the closely related -herpesviruses HHV-7 and HCMV(Dominguez et al., 1999). The HHV-6 U94 gene is a spliced gene that encodes a 490-amino-acid protein that's also highly conserved across species, with only ten amino acid residues differing(Rapp et al., 2000).

1.1.3 HHV-6 Biology feature, Epidemiology and Disease association

Although both HHV-6A and HHV-6B have been shown to have a significant CD4+ T-lymphocyte tropism in vitro and in vivo, their ability to infect cytotoxic effector cells differs significantly(Chi et al., 2012; Dagna, Pritchett, & Lusso, 2013; Lusso et al., 1988; Takahashi et al., 1989). Although HHV-6A has been shown to infect CD8+ T cells successfully, natural killer (NK) cells, and gamma/delta T cells, HHV-6B has been shown to infect these cells inefficiently(Grivel et al., 2003; Martin, Schub, Dillinger, & Moosmann, 2012).

Both HHV-6A and HHV-6B utilize different cell receptors: HHV-6A makes use of CD46(Santoro et al., 1999), which is found on all nucleated cells, whereas HHV-6B makes use of CD134(Tang et al., 2013), which is located on T-lymphocytes. HHV-6B can bind to CD46 but prefers CD134. HHV-6A and HHV-6B have a broader cell tropism, infecting not only T- and B-lymphocytes but also macrophages, natural killer (NK) cells, vascular and lymphatic endothelium cells, thyroid, salivary gland, endometrial, skin, fibroblasts, oligodendrocytes, and neurons(Caruso et al., 2003; Caselli & Di Luca, 2007; Caselli et al., 2019; Caselli et al., 2012; Kondo, Kondo, Okuno, Takahashi, & Yamanishi, 1991; Luppi, Barozzi, Maiorana, Marasca, & Torelli, 1994; Marci et al., 2016; Rizzo et al., 2017; Robert et al., 1996). The distribution of HHV6 A and HHV6 B differ in human tissue. We can detect HHV6 from peripheral blood mononuclear cells (PBMCs) of healthy adults, also, GI tract of solid organ transplant patients, saliva and salivary glands, renal tubular cells, thyroid, skin, and the central nervous

system(Boutolleau et al., 2006; Chapenko et al., 2012; Levine, Jahan, Murari, Manak, & Jaffe, 1992; Luppi et al., 1994; Reddy & Manna, 2005).

The amino acid sequence identity of the HHV-6A and HHV-6B gO gene products is 76.8%, substantially lower than the identity of other glycoproteins. The reduced identity implies that the gH–gL–gO complex may convey at least some of the various biological features that drive HHV-6A and HHV-6B to target different cells(Bates et al., 2009; Tang, Hayashi, Maeki, Yamanishi, & Mori, 2011). Cellular tropism may also be related to the ability of viral chemokines to chemoattract various cellular populations. U83B, an HHV-6B chemokine, is CCR2-specific and can chemoattract cells with this receptor, such as monocytic cells and some T cell subpopulations, for latent or lytic infection. U83A, the HHV-6A chemokine, has a broader selectivity for CCR1, CCR4, CCR5, CCR6, and CCR8, which are present on monocytic/macrophage, dendritic, and NK cells, as well as activated and skin-homing T cells(Catusse, Parry, Dewin, & Gompels, 2007; Clark, Catusse, Stacey, Borrow, & Gompels, 2013; Dewin, Catusse, & Gompels, 2006; Lüttichau et al., 2003). U83 is also one of the few hypervariable genes exclusive to HHV-6A and HHV-6B and not shared with the related HHV-7, encoding significant differences for these viruses(French et al., 1999). The HHV-6A and HHV-6B glycoprotein-encoding genes that encode gQ (U97, 98, 99, and 100) have just 72.1 % sequence identity(Isegawa et al., 1999). As a result, this glycoprotein might play a role in the differences between HHV-6A and HHV-6B infections. gQ1 has epitopes identified by

neutralizing antibodies and is a target for virus-specific neutralizing antibodies, along with gB

and gH(Kawabata et al., 2011; Maeki & Mori, 2012; Oyaizu et al., 2012; B Pfeiffer et al., 1993;

Brian Pfeiffer, Thomson, & Chandran, 1995; Tang et al., 2010).

As with all other human herpesviruses, HHV-6 causes both active and latent infections. The vast

majority of known primary infections and reactivation events are caused by HHV-6B, which

infects newborns in their first two years of life and causes roseola infantum, a condition

characterized by fever, diarrhea, and a mild skin rash(Tanaka et al., 1994; Yamanishi et al.,

1988). As a result of this mild disease, febrile seizures and epilepsy might occur. Primary HHV-

6B infection in adults, on the other hand, is uncommon and can be followed by a mononucleosis-

like syndrome with persistent lymphadenopathy(Akashi et al., 1993). The epidemiology and

clinical consequences of HHV-6A, which has long been considered to be less common than

HHV-6B, are less well recognized, and its etiologic role in initial infection and subsequent

disease remains unclear(Tesini, Epstein, & Caserta, 2014). Recent data, based on expensive

serological screening with a technology capable of differentiating between the two species,

suggest that HHV-6A is indeed relatively widespread(Engdahl et al., 2019b).

Primary HHV-6 infection causes a life-long latent disease in the host, which can reactivate,

especially during immunological disorders(Scotet et al., 1999). HHV-6A/B reactivation in adults

has been associated with a number of disorders, while the causative relationships remain

unknown. HHV-6A/6B-associated pathologies include immunocompromised patients' neurological disorders such as encephalitis, seizures, ataxia, and mild dementia, with HHV-6A being more prevalent in cognitive dysfunctions and HHV-6B being more common in encephalitis and seizures(Agut, Bonnafous, & Gautheret-Dejean, 2015; Caselli et al., 2020; Montoya et al., 2012; Pantry & Medveczky, 2017).

1.1.4   HHV6 and Immune system

The most efficient replication of the virus is CD4+ cells. We can detect both HHV6A and HHV6B in lymphocytes, monocytes, and macrophages; however, there are some differences in their ability to infect cytotoxic effector cells. For instance, HHV6A is able to infect CD8+ T cells, natural killer (NK) cells, and gamma/delta T cells(Krueger & Ablashi, 2006; Lusso et al., 1991; Lusso, Garzino-Demo, Crowley, & Malnati, 1995). However, HHV6B infection of these cells is relatively ineffective(Grivel et al., 2003). HHV6A is able to infect and induce CPE on HSB-2 cells, and HHV6B is able to infect and cause CPE on MOLt-3 cells(D. Ablashi et al., 1991; D. V. Ablashi et al., 1988; L. Li et al., 2011).

Immunoglobulin M (IgM) responses arise in children with primary HHV-6 infection on day five of illness, while immunoglobulin G (IgG) responses appear at around one week(Yamanishi et al., 1990). The IgM antibody only lasts for two to three weeks, but the IgG response lasts much longer. When the speed of viral isolation slows down, a low-level neutralizing antibody begins to

develop about day 3 of the illness and reaches its peak 2 to 4 weeks later(Asano et al., 1989;

Kumagai et al., 2006). Even while the immune response to HHV-6 is often sensitive and

specific, IgM has also been found in around 5% of healthy persons and has been reported to

cross-react with HHV-7, limiting the use of this test for the diagnosis of HHV-6 infection or

reactivation(Kumagai et al., 2006). It has also been shown that HV-6-specific CD4+ and CD8+

T-cell responses play a part in the immunological reaction to HHV-6(de Pagter et al., 2012;

Nastke et al., 2012).

After infecting PBMCs, HHV-6 interacts with the immune system in several ways, including by

upregulating CD4, suppressing cytokines, type I interferons, and having an impact on NK cell

function(Kumagai et al., 2006; Lusso, 2006; Yoshida, Torigoe, & Yamada, 2002). There have

been contradictory findings on the functional consequence of in vitro HHV-6 infection of

dendritic cells(Kakimoto, Hasegawa, Fujita, & Yasukawa, 2002; Smith et al., 2005). Following

HHV-6 infection, T cells undergo apoptosis both in vitro and in vivo, in addition to the

previously reported cell lysis(Inoue, Yasukawa, & Fujita, 1997; Yasukawa, Inoue, Ohminami,

Terada, & Fujita, 1998). Aside from the immunological response to HHV-6, the viral genome

contains various components with immunologic regulatory action, including two chemokine

receptor homologs (U12 and U51) and two potential chemokines (U22 and U83)(Lusso, 2006). It

has been proposed that HHV-6 may accelerate viral replication in infected cells, increase the

number of relevant virus susceptible cells, or avoid the host immune response to infection by using these proteins(CASERTA).

1.1.5 HHV6 and Nervous system

Both viruses are neurotropic, and they've been linked to neurological disorders in humans. HHV-6B has previously been associated with several forms of seizures, epilepsy, and encephalitis. HHV-6A has been found in serum, urine, and CSF from individuals with multiple sclerosis and, anecdotally, from the saliva of a child suffering from severe seizures(Akhyani et al., 2000; Alenda et al., 2014; Bartolini et al., 2018).

By attaching to the ubiquitous complement regulator CD46, HHV-6A and HHV-6B may infect a variety of cell types(De Bolle, Van Loon, De Clercq, & Naesens, 2005).

Data revealing the intensity of HHV-6A vs. HHV-6B in patients with neurological diseases(Boutolleau et al., 2006; Crawford, Kadom, Santi, Mariani, & Lavenstein, 2007; De Bolle, Naesens, & De Clercq, 2005). and DNA and mRNA of HHV6-A mostly found in patients with neuroinflammatory diseases such as multiple sclerosis (MS) rather than HHV6 B(Álvarez-Lafuente, De las Heras, Bartolomé, Picazo, & Arroyo, 2004; Alvarez-Lafuente et al., 2010; Dominguez-Mozo et al., 2012; Soldan et al., 1997). Active HHV-6A infection has been discovered in blood and CSF of individuals with relapsing/remitting MS and HHV-6A has been found primarily in the CNS of a fraction of MS patients(Akhyani et al., 2000; Álvarez-Lafuente,

Heras, Bartolomé, García-Montojo, & Arroyo, 2006). In another study, Crawford et al. identified

HHV6-A in 72 % of pediatric glial tumors(Crawford et al., 2009). HHV-6B infection, on the

other hand, is frequently linked to an elevated risk of temporal lobe epilepsy(Epstein et al., 2012;

J.-M. Li et al., 2011). It's been proposed that HHV-6A and HHV-6B bind to CD46 via distinct

isoforms of CD46(Hansen, Bundgaard, Biltoft, Rossen, & Höllsberg, 2017). However, certain

strains of HHV-6B employ a different receptor called CD134(Tang et al., 2013). During early

viremia or retrograde neuronal propagation the virus can penetrate the CNS and establish

persistent latency in brain tissue as well as tonsils/salivary glands(Donati et al., 2003; Harberts et

al., 2011).

HHV6 infects and establishes latency in the CNS; however, it is unknown which cell types are

more susceptible (or permissive) to certain strains of the virus. The reactivation of latent HHV6

is linked to neurological diseases. Electron microscopy revealed HHV6B infection of

oligodendrocytes (EM)(Albright et al., 1998). Histology analyses suggest both HHV6A and

HHV6B infect oligodendrocytes *in vivo*(Challoner et al., 1995; Opsahl & Kennedy, 2005).

Immunohistochemical studies found HHV6 antigens in cells expressing the astrocyte marker

glial fibrillary acidic protein (GFAP) in people with temporal lobe epilepsy. In addition to

oligodendrocytes, HHV6 has been reported to infect human astrocytes *in vivo*(Donati et al.,

2003). Both HHV6A and HHV6B appear to adsorb to astrocytes *in vitro*(Fotheringham,

Williams, Akhyani, & Jacobson, 2008). A study published recently demonstrated that HHV-6A

and HHV-6B infect Purkinje cells(Prusty et al., 2018). We also showed that both HHV6-A and HHV6-B are able to infect Glia and neuron (e.g., glutamatergic cells, dopaminergic), but they are not able to infect GABAergic cells (Bahramian et al., 2022).

1.2   HHV6 Association with Epilepsy

The prevalence of HHV6 Infection in individuals known to have seizure disorders was recently assessed by a literature review. The inquiry reported 21% of children with febrile seizures could be positive for active HHV-6 Infection, and some children with more severe forms of seizure like status epilepticus are positive for HHV-6(Mohammadpour Touserkani et al., 2017).

Founding the existence of the virus in the brain tissue of people suffering from temporal lobe epilepsy (TLE) has sparked controversy about the virus's role in TLE. According to research(Epstein et al., 2012), the presence of HHV-6B in the brain tissue of TLE patients was not different from the control group. They also looked at prior similar trials, and HHV-6 levels in the TLE group were not higher than in the non-TLE group. Despite the fact that the viral load in their samples was considerably more significant in the TLE group compared to the control group (P < 0.001).

Herpesviruses can induce neuronal damage and death, particularly in immunocompromised hosts, altering neuronal circuits with changes at the receptor, ligand, and channel levels, eventually contributing to epileptogenesis(Löscher & Brandt, 2010; Vezzani et al., 2016).

Following that, I focused on the hypothesis that HHV-6 infection is associated with seizures and

epilepsy.

1.2.1 Dormant interneuron hypothesis

Temporal lobe epilepsy is the most frequent kind of epilepsy in adults, and it is generally

resistant to anticonvulsant therapy. Its pathogenesis is unknown(Engel, Wilson, & Lopez-

Rodriguez, 2002). In experimental TLE models, acute neuronal cell loss occurs in many limbic

locations, including the formation of the hippocampus. The dentate gyrus's hilar region and layer

III of the entorhinal cortex (EC) are the most impacted neurons in this area(Du, Eid, Lothman,

Kohler, & Schwarcz, 1995; Gorter et al., 2003). Some subpopulations of GABAergic

interneurons appear less sensitive than the surrounding primary cells in these locations(Sloviter

et al., 2003).

Layer II stellate cells are hyperexcitable in animal models of temporal lobe epilepsy(Tolner et

al., 2005). Their hyperexcitability appears unaffected by changes in intrinsic electrophysiological

features, which are comparable to controls(R. S. Jones, 1994). Downstream granule cells in the

dentate gyrus get excessive, synchronous, excitatory synaptic input as a result of layer II stellate

cells' hyperexcitability, which may be identified as large-amplitude field EPSPs that mirror

interictal EEG spikes in patients(Bragin, Jando, Nadasdy, Van Landeghem, & Buzsáki, 1995;

Kobayashi, Wen, & Buckmaster, 2003; Wilson et al., 1991). The dormant interneuron theory

was initially suggested in the hippocampus as an epileptogenic etiology(Bekenstein & Lothman, 1993). The altered function is considered to be caused by a decrease in inhibition mediated by gamma-aminobutyric acid (GABA), which happens when GABAergic basket interneurons in animal hippocampal slices models of the condition become "dormant" as a result of being separated from excitatory inputs. (Bekenstein & Lothman, 1993). It was later proposed as a mechanism for layer II stellate cell hyperexcitability in the entorhinal cortex(Schwarcz, Eid, & Du, 2000). This hypothesis is supported by other research findings(Tolner et al., 2005).

Glutamate appears to have a role in seizures and epileptogenesis during SE in both animal models and humans. SE is linked to excessive acetylcholine buildup and subsequent recruitment of excitatory glutamatergic signaling when induced by high sublethal to lethal dosages of nerve agents(Lallement et al., 1991). SE-induced glutamate release overstimulates glutamate receptors, particularly NMDARs, resulting in long-term seizure activity and seizure-induced brain injury(Dorandeu, Dhote, Barbier, Baccus, & Testylier, 2013). GABA receptors are internalized during prolonged SE, while NMDARs move to neuronal synapses, resulting in decreased inhibition and hyperexcitability (Naylor, Liu, Niquet, & Wasterlain, 2013). Because of these differences in receptor localization, GABAergic neurotransmission-targeting drugs are unlikely to reduce seizures associated with protracted SE. However, NMDAR antagonists, in combination with GABA agonists and other therapies, can frequently successfully attenuate experimental SE(Barker-Haliski & White, 2015).

One of the crucial roles of astrocytes in the CNS is the regulation of the excitatory neurotransmitter glutamate. Dysregulation of glutamate can result in elevated glutamate in the cerebral spinal fluid (CSF) and increased extracellular levels of glutamate, which is an indication of dysfunction in glutamate signaling, uptake, and/or metabolism(Fotheringham et al., 2008). HHV6-B infected astrocytes were found in resected brain tissue from patients with epilepsy of unknown cause. HHV-6 infected astrocytes also display morphological abnormalities, suggesting that the process of astrocyte infection may produce a change in cell function, contributing to this illness in patients. According to research, functional alterations in virus-infected astrocytes that produce glutamate transporter (EAAT2) dysregulation may create secondary damage to the hippocampus, which might lead to epilepsy, or more particularly, MTLE. Testing this hypothesis on MTLE patients found that the highest HHV-6 viral load was found in the hippocampus of surgical brain resections. However, the exact mechanism of Infection is unclear(Fotheringham et al., 2007). Loss of Astroglia glutamine synthetase, changes in glutaminase and glutamate dehydrogenase, and other abnormalities in the brain's glutamate-glutamine cycle are common in epileptics(Eid et al., 2016).

So astroglia this function as a result of HHV6 infection may change the level of glutamate, and excessive glutamate can cause overstimulates glutamate receptors, particularly NMDARs, resulting in long-term seizure activity injury and GABA receptors are internalized during prolonged SE.

1.2.2   Cholinergic Dysfunction in Temporal Lobe Epilepsy

Seizures in people with mesial temporal lobe epilepsy (TLE) are frequently triggered in the entorhinal cortex, hippocampal, or amygdala(Lopes da Silva, Witter, Beijing, & Lohman, 1990). The entorhinal cortex (EC) takes information from the perirhinal and post rhinal cortices and sends it to various parts of the hippocampus (HIP)(Dugladze, Heinemann, & Gloveli, 2001). Fibers from the lateral EC innervate the dentate gyrus's outer third, whereas fibers from the medial EC innervate the dentate gyrus's middle third of granule cell dendrites. Cells in layer III of the EC project straight into the subiculum, CA1, and, most likely, CA3 areas, where some pyramidal cells get activated while the majority are suppressed by feed-forward inhibition(Empson & Heinemann, 1995). HIP output from the CA1 and CA2 regions, as well as the subiculum, reaches the deep levels of the EC and synoptically activates superficial layer III and layer II cells(Gloveli, Egorov, Schmitz, Heinemann, & Müller, 1999). The EC–HIP complex has two main modes of operation: closed-loop mode, in which the EC's input to the HIP is quiet, and open-loop mode, in which the EC's information can activate various cells in the HIP(Hasselmo & Bower, 1993). Extensive experimental data suggests that acetylcholine (ACh) release is a critical regulator of the EC–HIP working mode. As a result, in the closed loop mode, ACh release is modest. When novelty detection, information storage, and retrieval are permitted in the open loop mode, ACh release increases, resulting in theta and nested gamma oscillations, which are theorized to bind parallel-processed information and promote information

storage(Friedman, Behrens, & Heinemann, 2007). The EC–HIP complex receives a significant amount of cholinergic input, which comes predominantly from the basal forebrain via the fimbria-fornix. The activation of this pathway causes an increase in ACh levels in the HIP(Milner, Loy, & Amaral, 1983). Cholinergic fibers are numerous in the stratum orients of CA1 and the dentate hilus, and they provide input to many, if not all, interneurons. At the single cell level in the HIP, ACh was shown to lower conductance of a number of potassium channels via muscarinic receptors, that is, G protein-coupled receptors, resulting in delayed depolarization(Benardo & Prince, 1982), reduced firing adaptability and enhanced action potential back propagation along dendrites(Tsubokawa & Ross, 1996).

It has frequently been reported that the levels of ACh in various epilepsy models were reduced in epileptic tissue. This behavior might be caused by increased or decreased production of the ACh-hydrolyzing enzyme, acetylcholinesterase (AChE). It is reasonable to expect that the density of receptors, AChE levels, and the density of cholinergic innervation all fluctuate significantly in TLE(Friedman et al., 2007). For example, Misra, Kalita et al., reported AChE activity and muscarinic 2 M2 receptor levels were considerably lower in the acute phases of Japanese encephalitis (JE) and herpes simplex encephalitis (HSE) when compared to controls, and AChE activity was much lower in HSE than in JE. After a year, both AChE and M2 receptor levels increased dramatically in JE, but not in HSE, where AChE activity increased, but M2 receptors did not(Misra, Kalita, & Chauhan, 2019).

The activation of muscarinic receptors causes an increase in intracellular Ca2+(Egorov & Müller, 1999). This shows that ACh may have a function in initiating gene expression and excitotoxicity. Likewise, excitotoxic cells in the EC collect three times more Ca2+ after a seizure-like event than more resistant layer II cells. Furthermore, in the HIP, muscarinic-dependent increased excitability is linked to altered gene expression, which may be inhibited by intracellular Ca2+chelators(Kaufer, Friedman, Seidman, & Soreq, 1998). This mechanism has been linked to increased sensitivity to AChE inhibitors and muscarinic antagonists and has been found to be long lasting(Meshorer et al., 2002).

Increased excitability causes intracellular Ca2+-dependent changes in gene expression of important cholinergic proteins, such as decreased expression of the ACh synthesizing protein, choline-acetyltransferase (CHAT), and the coregulated vesicular ACh transporter (VACHT). The most remarkable of these alterations is the long-term up-regulation of AChE caused by the splicing of AChE pre-mRNA to form the distinct AChE-R mRNA and protein. It's likely that AChE-R is controlled as a "feedback mechanism" to minimize the amount of ACh released, raising the seizure threshold and restricting seizure propagation. While such modifications might result in decreased cholinergic functions, physiological evidence demonstrates increased cholinergic responses under identical settings, indicating that alternative processes are at

work(Meshorer et al., 2002). As evidenced by pentylenetetrazole-induced generalized seizures, these may include altered receptor expression/distribution or enhanced receptor efficacy to G-proteins(Potier & Psarropoulou, 2001).

It has been demonstrated that in rats infected with Borna disease virus (BDV), choline acetyltransferase (ChAT) decreases in the number of ChAT-positive fibers, eventually leading to an almost total loss of cholinergic fibers, particularly in the hippocampus and neocortex(Gies, Bilzer, Stitz, & Staiger, 1998).

There has been no research on the effect of HHV6 viral infection on human cholinergic cells; however, since that other herpes viruses (HSE) and BDV could cause dysfunction in cholinergic cells, there is a chance that infection with HHV6 will impair the cholinergic cells' normal activity.

1.2.3 Neuroinflammatory pathways in epilepsy

Neuroinflammation response is not only triggered during infections, autoimmunity, and toxicity but also caused an increase in neuronal activity, like epileptic seizures. The term "neurogenic neuroinflammation" was used to characterize neuroinflammatory pathways triggered by neuronal activity(Xanthos & Sandkühler, 2014). Inflammatory reactions are triggered by viral infections in both immune and non-immune cells. Infections and infestations are among the leading causes of seizures and acquired epilepsy(Ngugi et al., 2013). Status epilepticus can be caused by a wide

range of CNS pathogens, including bacterial (e.g. typical bacterial meningitis, tuberculosis (TB)), viral (e.g. herpes simplex, HHV-6), parasitic (e.g. cerebral toxoplasmosis, NCC, malaria), fungal (e.g. candidiasis, coccidioidomycosis, aspergillosis), and prion infections (CJD)(Lowenstein, Walker, & Waterhouse, 2014). The likelihood of developing epilepsy following infection is determined by the infectious agent, the severity of brain damage, age, genetic factors, and a variety of other unknown parameters(Michael & Solomon, 2012). Various brain alterations occur during the latent phase between infection and the emergence of epilepsy, including impairment of blood–brain barrier (BBB) integrity, neuronal hyperexcitability, neuronal loss and gliosis, molecular and structural reorganization, and epigenetic reprogramming, which may eventually result in spontaneous recurrent epileptic seizures(Löscher & Brandt, 2010).

By attaching to the ubiquitous complement regulator CD46 and CD134(Santoro et al., 1999; Tang et al., 2013), HHV-6 can alter the adaptive immune response. In our previous study, we showed the expression of bothCD46 and CD134 in human neural stem cells (Bahramian at al., 2022). Complement activation has been suggested to play a crucial role in neuroinflammation produced by HHV-6 infection, similar to what has been shown in individuals with multiple sclerosis who are infected with the virus(Alvarez-Lafuente et al., 2009).

TLRs are an integral part of innate immune system receptors, which sense specific molecular

patterns from pathogens and activate immune responses(Johnson et al., 2005; Murakami et al.,

2010). TLR family members are characterized structurally by the presence of a leucine-rich

repeat (LRR) domain in their extracellular domain and a TIR domain in their intracellular

domain(Huang, 2021). TLRs can be grouped into families according to the types of ligands they

recognize. Peptidoglycan and bacterial lipoproteins are recognized by TLR2, and heterodimers

are composed of TLR2 and either TLR1 or TLR6. TLR4 homodimers also bind

lipopolysaccharides. (B. W. Jones et al., 2001). In addition, viral and bacterial nucleic acids are

recognized by TLR3, TLR7, TLR8, and TLR9. For example, TLR3 recognizes double stranded

RNA (dsRNA) and TLR9 binds bacterial and viral DNA containing cytosine–phosphate–

guanine (CpG) dideoxynucleoside motifs(Ohto et al., 2015). Toll-like receptor 9 (TLR9) may

be activated by roseolovirus infection in addition to CD46 (or CD134) expression for virus

entry(Bowman, Rasley, Tranguch, & Marriott, 2003). Through several TLR-associated adaptor

proteins, such as MAL/TIRAP (MyD88-adaptor-like/TIR-associated protein), MyD88

(myeloid differentiation factor 88), TRIF (Toll-receptor-associated activator of interferon),

and TRAM (Toll-receptor-associated molecule), ligand binding to TLRs can result in

activation of protein kinases, which, in turn, results in upregulation of transcription factors

associated with inflammatory responses(Beutler, 2004). Although the stimulation pathways

may be different, the resultant signaling cascades ultimately involve Toll/interleukin (IL)–1

receptor (TIR) domain, which is present in the cytosolic region of all TLRs, as well as the members of the IL-1 receptor family, domain-containing adapters, like MyD88. MyD88 involvement always results in subsequent activation of Nuclear Factor-κB (NF-κB), which controls the expression of inflammatory cytokine genes(Stevens et al., 2008; Trinchieri & Sher, 2007). TLR9 has been shown to be expressed in both mice and human microglial cells and astrocytes. Furthermore, the findings show that HHV-6A may trigger human TLR9 in addition to murine TLR9. In an animal model of multiple sclerosis, TLR9 was also demonstrated to be an essential regulator of an autoimmune process(Bowman et al., 2003). These findings imply that HHV-6A can cause neuroinflammation via TLR9, which could have therapeutic implications since TLR9 inhibitors could be utilized to reduce the generation of proinflammatory chemokines and slow CNS pathogenesis(Reynaud, Jégou, Welsch, & Horvat, 2014).

Herpesviruses can induce direct neuronal damage and death, particularly in immunocompromised hosts, resulting in cytokine release and activation of the innate and adaptive immune systems(Vezzani et al., 2016). HHV-6 has the ability to infect astrocytes and oligodendrocytes *in vivo*(Opsahl & Kennedy, 2005). IL-1β, interferon (IFN)-α, and tumor necrosis factor (TNF)-a are among the cytokines that have increased production. After stimulation with TNF-α, IL-1β, and IFNγ, HHV-6 infection increased the production of various proinflammatory cytokines, including chemokines such as chemokine ligand (CCL)-2, CCL-5,

and C-X-C motif chemokine (CXCL)-2, according to transcriptional microarray study on infected astrocytes(Meeuwsen et al., 2005).

Our data show a remarkable increase in IL-10 expression concomitant with the upregulation of TLR9 gene expression in cultures infected with HHV-6A. Changes in CD46 functions were identified, such as a significant reduction in CD46-induced IL-10 production by T cells(Alvarez-Lafuente et al., 2009). Even though we detected a substantial rise in IL-10 following HHV6-A infection in human neural stem cell culture, this was suggested to be related to a lack of T cells in vitro for suppressing IL-10 production. Because of its anti-inflammatory action, a rise in IL-10 may explain the absence of an increase in other inflammatory cytokines in HHV6-A infected cells. However, we found no increase in IL-10 in HHV6-B-infected cells.

Other researches indicate that the transcription factor NF-kB may have a role in the development of MTLE in individuals infected with HHV-6(J.-M. Li et al., 2011). This protein complex has been linked to cancer, inflammatory diseases, and viral infections(Hayden, West, & Ghosh, 2006).

1.2.4   Gliosis and neuronal loss

Glial fibrillary acidic protein (GFAP) and CCL-2 , also known as Monocyte Chemoattractant Protein-1 (MCP-1), were found to be upregulated in the amygdala of MTLE patients with HHV-6 infection, with a positive correlation with viral load and in resected epileptogenic tissue from

the hippocampus(Kawamura et al., 2015; Xu et al., 2011). Upregulation of GFAP and CCL-2 is

linked to astrogliosis and neuronal cell death, which might play a role in the development of

MTLE. (Ortinski et al., 2010; Robel et al., 2015). CCL-2 is a protein involved in the control of

macrophage and monocyte migration and invasion. HHV-6 can cause persistent alterations in

MTLE by establishing latent infection in these cells and facilitating the migration of infected

cells into the amygdala by upregulating CCL-2(Bartolini, 2020).

1.3   Goals of This Project

Even though I detailed the historical record of HHV6, and there are now two separate strains and

information on neurological disfunction associated with HHV6, there is still much unknown

about this system, and many fundamental issues remain unanswered. The study on HSV1, EBV,

and CMV is ten years above that on HHV6, so our result on HHV6 may look basic, but it needs

to be essential since we do not know as much about HHV6 as we do about other viruses in this

family.

Since fundamental knowledge such as cell tropism, relative virulence, and cellular responses are

unknown, we used culture neurons, especially human neural stem cells, to investigate possible

distinctions between these two strains.

The second chapter investigates HHV6 cell tropism, cytopathic impact, morphological changes,

and relative pathogenicity in human neural stem cells. The third chapter explores the virus's

transcriptome alterations and immunological consequences. In the last chapter, I briefly cover our newly launched multielectrode array project, our preliminary data, and the project's future direction. These studies were carried out to establish whether HHV6-A and HHV6-B differed from one another. Even if they may be linked to epilepsy, our main concern is whether they are distinct from one another.

1.4 References

Ablashi, D., Balachandran, N., Josephs, S., Hung, C., Krueger, G., Kramarsky, B., . . . Gallo, R. (1991). Genomic polymorphism, growth properties, and immunologic variations in human herpesvirus-6 isolates. *Virology, 184*(2), 545-552.

Ablashi, D. V., Lusso, P., Hung, C. L., Salahuddin, S. Z., Josephs, S. F., Llana, T., . . . Gallo, R. C. (1988). Utilization of human hematopoietic cell lines for the propagation and characterization of HBLV (human herpesvirus 6). *International journal of cancer, 42*(5), 787-791.

Achour, A., Malet, I., Le Gal, F., Dehée, A., Gautheret-Dejean, A., Bonnafous, P., & Agut, H. (2008). Variability of gB and gH genes of human herpesvirus-6 among clinical specimens. *Journal of medical virology, 80*(7), 1211-1221.

Adams, M. J., & Carstens, E. (2012). Ratification vote on taxonomic proposals to the International Committee on Taxonomy of Viruses (2012). *Archives of virology, 157*(7), 1411-1422.

Agut, H., Bonnafous, P., & Gautheret-Dejean, A. (2015). Laboratory and clinical aspects of human herpesvirus 6 infections. *Clinical microbiology reviews, 28*(2), 313-335.

Akashi, K., Eizuru, Y., Sumiyoshi, Y., Minematsu, T., Hara, S., Harada, M., . . . Minamishima, Y. (1993). Severe infectious mononucleosis-like syndrome and primary human herpesvirus 6 infection in an adult. *New England Journal of Medicine, 329*(3), 168-171.

Akhyani, N., Berti, R., Brennan, M. B., Soldan, S. S., Eaton, J. M., McFarland, H. F., &

    Jacobson, S. (2000). Tissue distribution and variant characterization of human

    Herpesvirus (HHV)—6: Increased prevalence of HHV-6A in patients with multiple

    sclerosis. *The Journal of infectious diseases, 182*(5), 1321-1325.

Akira, S., & Sato, S. (2003). Toll-like receptors and their signaling mechanisms. *Scandinavian*

    journal of infectious diseases, 35(9), 555-562.

Albright, A. V., Lavi, E., Black, J. B., Goldberg, S., O'Connor, M. J., & Gonzalez-Scarano, F.

    (1998). The effect of human herpesvirus-6 (HHV-6) on cultured human neural cells:

    oligodendrocytes and microglia. *Journal of neurovirology, 4*(5), 486-494.

Alenda, R., Álvarez-Lafuente, R., Costa-Frossard, L., Arroyo, R., Mirete, S., Álvarez-Cermeño,

    J., & Villar, L. (2014). Identification of the major HHV-6 antigen recognized by

    cerebrospinal fluid IgG in multiple sclerosis. *European journal of neurology, 21*(8),

    1096-1101.

Alkharsah, K. R. (2018). VEGF upregulation in viral infections and its possible therapeutic

    implications. *International journal of molecular sciences, 19*(6), 1642.

Álvarez-Lafuente, R., De las Heras, V., Bartolomé, M., Picazo, J. J., & Arroyo, R. (2004).

    Relapsing-remitting multiple sclerosis and human herpesvirus 6 active infection. *Archives*

    of neurology, 61(10), 1523-1527.

Alvarez-Lafuente, R., Garcia-Montojo, M., De Las Heras, V., Dominguez-Mozo, M., Bartolome,

    M., & Arroyo, R. (2009). CD46 expression and HHV-6 infection in patients with

    multiple sclerosis. *Acta neurologica scandinavica, 120*(4), 246-250.

Álvarez-Lafuente, R., Heras, V. D., Bartolomé, M., García-Montojo, M., & Arroyo, R. (2006).

    Human herpesvirus 6 and multiple sclerosis: a one-year follow-up study. *Brain*

    Pathology, 16(1), 20-27.

Alvarez-Lafuente, R., Martinez, A., Garcia-Montojo, M., Mas, A., De Las Heras, V.,

    Dominguez-Mozo, M., . . . Gomez De La Concha, E. (2010). MHC2TA rs4774C and

    HHV-6A active replication in multiple sclerosis patients. *European journal of neurology,*

    17(1), 129-135.

Alzaid, A., Castro, R., Wang, T., Secombes, C. J., Boudinot, P., Macqueen, D. J., & Martin, S.

    A. (2016). Cross talk between growth and immunity: coupling of the IGF Axis to

    conserved cytokine pathways in rainbow trout. *Endocrinology, 157*(5), 1942-1955.

Arbuckle, J. H., Medveczky, M. M., Luka, J., Hadley, S. H., Luegmayr, A., Ablashi, D., . . .

    Montoya, J. G. (2010). The latent human herpesvirus-6A genome specifically integrates

    in telomeres of human chromosomes in vivo and in vitro. *Proceedings of the National*

    Academy of Sciences, 107(12), 5563-5568.

Arbuckle, J. H., Pantry, S. N., Medveczky, M. M., Prichett, J., Loomis, K. S., Ablashi, D., & Medveczky, P. G. (2013). Mapping the telomere integrated genome of human herpesvirus 6A and 6B. *Virology, 442*(1), 3-11.

Asakura, K., Hayashi, S., Ojima, A., Taniguchi, T., Miyamoto, N., Nakamori, C., . . . Honda, Y. (2015). Improvement of acquisition and analysis methods in multi-electrode array experiments with iPS cell-derived cardiomyocytes. *Journal of pharmacological and toxicological methods, 75*, 17-26.

Asano, Y., Yoshikawa, T., Suga, S., Yazaki, T., Hata, T., Nagai, T., . . . Yoshida, S. (1989). Viremia and neutralizing antibody response in infants with exanthem subitum. *The Journal of pediatrics, 114*(4), 535-539.

Aubin, J.-T., Agut, H., Collandre, H., Yamanishi, K., Chandran, B., Montagnier, L., & Jean-Marie, H. (1993). Antigenic and genetic differentiation of the two putative types of human herpes virus 6. *Journal of virological methods, 41*(2), 223-234.

Bar-Gad, I., Ritov, Y. a., Vaadia, E., & Bergman, H. (2001). Failure in identification of overlapping spikes from multiple neuron activity causes artificial correlations. *Journal of neuroscience methods, 107*(1-2), 1-13.

Barker-Haliski, M., & White, H. S. (2015). Glutamatergic mechanisms associated with seizures and epilepsy. *Cold Spring Harbor perspectives in medicine, 5*(8), a022863.

Bartolini, L. (2020). Mechanisms of neuroinflammation in epilepsy linked to HHV-6 infection. *Drug Discovery Today: Disease Models, 32*, 53-57.

Bartolini, L., Piras, E., Sullivan, K., Gillen, S., Bumbut, A., Lin, C.-T. M., . . . Chamberlain, J. M. (2018). Detection of HHV-6 and EBV and cytokine levels in saliva from children with seizures: results of a multi-center cross-sectional study. *Frontiers in neurology*, 834.

Bartolini, L., Theodore, W. H., Jacobson, S., & Gaillard, W. D. (2019). Infection with HHV-6 and its role in epilepsy. *Epilepsy research, 153*, 34-39.

Bates, M., Monze, M., Bima, H., Kapambwe, M., Clark, D., Kasolo, F. C., & Gompels, U. A. (2009). Predominant human herpesvirus 6 variant A infant infections in an HIV-1 endemic region of Sub-Saharan Africa. *Journal of medical virology, 81*(5), 779-789.

Beal, M. F. (1992). Mechanisms of excitotoxicity in neurologic diseases. *The FASEB journal, 6*(15), 3338-3344.

Bekenstein, J. W., & Lothman, E. W. (1993). Dormancy of inhibitory interneurons in a model of temporal lobe epilepsy. *Science, 259*(5091), 97-100.

Benardo, L. S., & Prince, D. A. (1982). Cholinergic excitation of mammalian hippocampal pyramidal cells. *Brain research, 249*(2), 315-331.

Beutler, B. (2004). Inferences, questions and possibilities in Toll-like receptor signalling. *Nature, 430*(6996), 257-263.

Boutolleau, D., Duros, C., Bonnafous, P., Caïola, D., Karras, A., De Castro, N., . . . Agut, H.

(2006). Identification of human herpesvirus 6 variants A and B by primer-specific real-

time PCR may help to revisit their respective role in pathology. *Journal of Clinical*

Virology, 35(3), 257-263.

Bowman, C. C., Rasley, A., Tranguch, S. L., & Marriott, I. (2003). Cultured astrocytes express

toll-like receptors for bacterial products. *Glia, 43*(3), 281-291.

Bragin, A., Jando, G., Nadasdy, Z., Van Landeghem, M., & Buzsáki, G. (1995). Dentate EEG

spikes and associated interneuronal population bursts in the hippocampal hilar region of

the rat. *Journal of neurophysiology, 73*(4), 1691-1705.

Brown, E. N., Kass, R. E., & Mitra, P. P. (2004). Multiple neural spike train data analysis: state-

of-the-art and future challenges. *Nature neuroscience, 7*(5), 456-461.

Burke, D., Kiernan, M. C., & Bostock, H. (2001). Excitability of human axons. *Clinical*

neurophysiology, 112(9), 1575-1585.

Buzsáki, G., Anastassiou, C. A., & Koch, C. (2012). The origin of extracellular fields and

currents—EEG, ECoG, LFP and spikes. *Nature Reviews Neuroscience, 13*(6), 407-420.

Caruso, A., Favilli, F., Rotola, A., Comar, M., Horejsh, D., Alessandri, G., . . . Fiorentini, S.

(2003). Human herpesvirus-6 modulates RANTES production in primary human

endothelial cell cultures. *Journal of medical virology, 70*(3), 451-458.

Caselli, E., D'Accolti, M., Caccuri, F., Soffritti, I., Gentili, V., Bortolotti, D., . . . Zani, A.

(2020). The U94 Gene of Human Herpesvirus 6: A Narrative Review of Its Role and

Potential Functions. *Cells, 9*(12), 2608.

Caselli, E., & Di Luca, D. (2007). Molecular biology and clinical associations of Roseoloviruses

human herpesvirus 6 and human herpesvirus 7. *Microbiologica-Quarterly Journal of*

Microbiological Sciences, 30(3), 173-188.

Caselli, E., Soffritti, I., D'Accolti, M., Bortolotti, D., Rizzo, R., Sighinolfi, G., . . . Ferri, C.

(2019). HHV-6A infection and systemic sclerosis: Clues of a possible association.

Microorganisms, 8(1), 39.

Caselli, E., Zatelli, M. C., Rizzo, R., Benedetti, S., Martorelli, D., Trasforini, G., . . . Dolcetti, R.

(2012). Virologic and immunologic evidence supporting an association between HHV-6

and Hashimoto's thyroiditis.

CASERTA, M. T. Infections of the Central Nervous System.

Castañeda-Cabral, J. L., Beas-Zárate, C., Rocha-Arrieta, L. L., Orozco-Suárez, S. A., Alonso-

Vanegas, M., Guevara-Guzmán, R., & Ureña-Guerrero, M. E. (2019). Increased protein

expression of VEGF-A, VEGF-B, VEGF-C and their receptors in the temporal neocortex

of pharmacoresistant temporal lobe epilepsy patients. *Journal of neuroimmunology, 328*,

68-72.

Catusse, J., Parry, C. M., Dewin, D. R., & Gompels, U. A. (2007). Inhibition of HIV-1 infection

    by viral chemokine U83A via high-affinity CCR5 interactions that block human

    chemokine-induced leukocyte chemotaxis and receptor internalization. *Blood, 109*(9),

    3633-3639.

Challoner, P. B., Smith, K. T., Parker, J. D., MacLeod, D. L., Coulter, S. N., Rose, T. M., . . .

    Chang, M. (1995). Plaque-associated expression of human herpesvirus 6 in multiple

    sclerosis. *Proceedings of the National Academy of Sciences, 92*(16), 7440-7444.

Chapenko, S., Trociukas, I., Donina, S., Chistyakov, M., Sultanova, A., Gravelsina, S., . . .

    Murovska, M. (2012). Relationship between beta-herpesviruses reactivation and

    development of complications after autologous peripheral blood stem cell transplantation.

    Journal of medical virology, 84(12), 1953-1960.

Chi, J., Wang, F., Li, L., Feng, D., Qin, J., Xie, F., . . . Yao, K. (2012). The role of MAPK in

    CD4+ T cells toll-like receptor 9-mediated signaling following HHV-6 infection.

    Virology, 422(1), 92-98.

Clark, D., Catusse, J., Stacey, A., Borrow, P., & Gompels, U. (2013). Activation of CCR2+

    human proinflammatory monocytes by human herpesvirus-6B chemokine N-terminal

    peptide. *Journal of General Virology, 94*(7), 1624-1635.

Crawford, J. R., Kadom, N., Santi, M. R., Mariani, B., & Lavenstein, B. L. (2007). Human

herpesvirus 6 rhombencephalitis in immunocompetent children. *Journal of child*

neurology, 22(11), 1260-1268.

Crawford, J. R., Santi, M. R., Thorarinsdottir, H. K., Cornelison, R., Rushing, E. J., Zhang, H., . .

. MacDonald, T. J. (2009). Detection of human herpesvirus-6 variants in pediatric brain

tumors: association of viral antigen in low grade gliomas. *Journal of Clinical Virology,*

46(1), 37-42.

Dagna, L., Pritchett, J. C., & Lusso, P. (2013). Immunomodulation and immunosuppression by

human herpesvirus 6A and 6B. *Future virology, 8*(3), 273-287.

De Bolle, L., Naesens, L., & De Clercq, E. (2005). Update on human herpesvirus 6 biology,

clinical features, and therapy. *Clinical microbiology reviews, 18*(1), 217-245.

De Bolle, L., Van Loon, J., De Clercq, E., & Naesens, L. (2005). Quantitative analysis of human

herpesvirus 6 cell tropism. *Journal of medical virology, 75*(1), 76-85.

De Filippis, L., Foglieni, C., Silva, S., Vescovi, A., Lusso, P., & Malnati, M. S. (2006).

Differentiated human neural stem cells: a new ex vivo model to study HHV-6 infection of

the central nervous system. *Journal of Clinical Virology, 37*, S27-S32.

de Pagter, A., Boelens, J., Scherrenburg, J., Vroom-de Blank, T., Tesselaar, K., Nanlohy, N., . . .

van Baarle, D. (2012). First analysis of human herpesvirus 6T-cell responses: specific

boosting after HHV6 reactivation in stem cell transplantation recipients. *Clinical immunology, 144*(3), 179-189.

Denys, A., Udalova, I. A., Smith, C., Williams, L. M., Ciesielski, C. J., Campbell, J., . . . Foxwell, B. M. (2002). Evidence for a dual mechanism for IL-10 suppression of TNF-α production that does not involve inhibition of p38 mitogen-activated protein kinase or NF-κB in primary human macrophages. *The Journal of Immunology, 168*(10), 4837-4845.

Dewin, D. R., Catusse, J., & Gompels, U. A. (2006). Identification and characterization of U83A viral chemokine, a broad and potent β-chemokine agonist for human CCRs with unique selectivity and inhibition by spliced isoform. *The Journal of Immunology, 176*(1), 544-556.

Dominguez-Mozo, M. I., Garcia-Montojo, M., De Las Heras, V., Garcia-Martinez, A., Arias-Leal, A. M., Casanova, I., . . . Alvarez-Lafuente, R. (2012). MHC2TA mRNA levels and human herpesvirus 6 in multiple sclerosis patients treated with interferon beta along two-year follow-up. *BMC neurology, 12*(1), 1-6.

Dominguez, G., Dambaugh, T. R., Stamey, F. R., Dewhurst, S., Inoue, N., & Pellett, P. E. (1999). Human herpesvirus 6B genome sequence: coding content and comparison with human herpesvirus 6A. *Journal of virology, 73*(10), 8040-8052.

Donati, D., Akhyani, N., Fogdell–Hahn, A., Cermelli, C., Cassiani-Ingoni, R., Vortmeyer, A., ... Sato, S. (2003). Detection of human herpesvirus-6 in mesial temporal lobe epilepsy surgical brain resections. *Neurology, 61*(10), 1405-1411.

Dorandeu, F., Dhote, F., Barbier, L., Baccus, B., & Testylier, G. (2013). Treatment of status epilepticus with ketamine, are we there yet? *CNS Neuroscience & Therapeutics, 19*(6), 411-427.

Downing, R. G., Sewankambo, N., Serwadda, D., Honess, R., Crawford, D., Jarrett, R. t., & Griffin, B. (1987). Isolation of human lymphotropic herpesviruses from Uganda. *The Lancet, 330*(8555), 390.

Du, F., Eid, T., Lothman, E., Kohler, C., & Schwarcz, R. (1995). Preferential neuronal loss in layer III of the medial entorhinal cortex in rat models of temporal lobe epilepsy. *Journal of Neuroscience, 15*(10), 6301-6313.

Dugladze, T., Heinemann, U., & Gloveli, T. (2001). Entorhinal cortex projection cells to the hippocampal formation in vitro. *Brain research, 905*(1-2), 224-231.

Egert, U., Banach, K., & Meyer, T. (2006). Analysis of cardiac myocyte activity dynamics with micro-electrode arrays *Advances in network electrophysiology* (pp. 274-290): Springer.

Egert, U., & Meyer, T. (2005). Heart on a chip—extracellular multielectrode recordings from cardiac myocytes in vitro *Practical methods in cardiovascular research* (pp. 432-453): Springer.

Egorov, A. V., & Müller, W. (1999). Subcellular muscarinic enhancement of excitability and

    Ca2+-signals in CA1-dendrites in rat hippocampal slice. *Neuroscience letters, 261*(1-2),

    77-80.

Eid, T., Gruenbaum, S. E., Dhaher, R., Lee, T.-S. W., Zhou, Y., & Danbolt, N. C. (2016). The

    glutamate–glutamine cycle in epilepsy. *The glutamate/GABA-glutamine cycle*, 351-400.

Empson, R. M., & Heinemann, U. (1995). The perforant path projection to hippocampal area

    CA1 in the rat hippocampal-entorhinal cortex combined slice. *The Journal of physiology,*

    484(3), 707-720.

Engdahl, E., Gustafsson, R., Huang, J., Biström, M., Lima Bomfim, I., Stridh, P., . . . Michel, A.

    (2019a). Increased serological response against human herpesvirus 6A is associated with

    risk for multiple sclerosis. *Frontiers in immunology*, 2715.

Engdahl, E., Gustafsson, R., Huang, J., Biström, M., Lima Bomfim, I., Stridh, P., . . . Michel, A.

    (2019b). Increased serological response against human herpesvirus 6A is associated with

    risk for multiple sclerosis. *Frontiers in immunology, 10*, 2715.

Engel, J., Wilson, C., & Lopez-Rodriguez, F. (2002). Limbic connectivity: anatomical substrates

    of behavioural disturbances in epilepsy. *The neuropsychiatry of epilepsy*, 18-38.

Epstein, L. G., Shinnar, S., Hesdorffer, D. C., Nordli, D. R., Hamidullah, A., Benn, E. K., . . .

    Moshe, S. L. (2012). Human herpesvirus 6 and 7 in febrile status epilepticus: the

    FEBSTAT study. *Epilepsia, 53*(9), 1481-1488.

Erickson, J., Tooker, A., Tai, Y.-C., & Pine, J. (2008). Caged neuron MEA: A system for long-term investigation of cultured neural network connectivity. *Journal of neuroscience methods, 175*(1), 1-16.

Fee, M. S., Mitra, P. P., & Kleinfeld, D. (1996). Automatic sorting of multiple unit neuronal signals in the presence of anisotropic and non-Gaussian variability. *Journal of neuroscience methods, 69*(2), 175-188.

Ferrara, N., Gerber, H. P., & LeCouter, J. (2003). The biology of VEGF and its receptors. *Nat Med, 9*(6), 669-676. doi:10.1038/nm0603-669

Finkel, Y., Schmiedel, D., Tai-Schmiedel, J., Nachshon, A., Winkler, R., Dobesova, M., . . . Stern-Ginossar, N. (2020). Comprehensive annotations of human herpesvirus 6A and 6B genomes reveal novel and conserved genomic features. *Elife, 9*, e50960.

Fotheringham, J., Donati, D., Akhyani, N., Fogdell-Hahn, A., Vortmeyer, A., Heiss, J. D., . . . Gaillard, W. D. (2007). Association of human herpesvirus-6B with mesial temporal lobe epilepsy. *PLoS Medicine, 4*(5), e180.

Fotheringham, J., Williams, E. L., Akhyani, N., & Jacobson, S. (2008). Human herpesvirus 6 (HHV-6) induces dysregulation of glutamate uptake and transporter expression in astrocytes. *Journal of Neuroimmune Pharmacology, 3*(2), 105-116.

French, C., Menegazzi, P., Nicholson, L., Macaulay, H., DiLuca, D., & Gompels, U. (1999). Novel, nonconsensus cellular splicing regulates expression of a gene encoding a

chemokine-like protein that shows high variation and is specific for human herpesvirus 6. *Virology, 262*(1), 139-151.

Friedman, A., Behrens, C. J., & Heinemann, U. (2007). Cholinergic dysfunction in temporal lobe epilepsy. *Epilepsia, 48*, 126-130.

Gies, U., Bilzer, T., Stitz, L., & Staiger, J. (1998). Disturbance of the cortical cholinergic innervation in Borna disease prior to encephalitis. *Brain Pathology, 8*(1), 39-48.

Gloveli, T., Egorov, A. V., Schmitz, D., Heinemann, U., & Müller, W. (1999). Carbachol-induced changes in excitability and [Ca2+] i signalling in projection cells of medial entorhinal cortex layers II and III. *European Journal of Neuroscience, 11*(10), 3626-3636.

Gompels, U., Nicholas, J., Lawrence, G., Jones, M., Thomson, B., Martin, M., . . . Macaulay, H. (1995). The DNA sequence of human herpesvirus-6: structure, coding content, and genome evolution. *Virology, 209*(1), 29-51.

Gorter, J. A., Pereira, P. M. G., Van Vliet, E. A., Aronica, E., Da Silva, F. H. L., & Lucassen, P. J. (2003). Neuronal cell death in a rat model for mesial temporal lobe epilepsy is induced by the initial status epilepticus and not by later repeated spontaneous seizures. *Epilepsia, 44*(5), 647-658.

Greninger, A. L., Knudsen, G. M., Roychoudhury, P., Hanson, D. J., Sedlak, R. H., Xie, H., . . .

    Boeckh, M. (2018). Comparative genomic, transcriptomic, and proteomic reannotation of

    human herpesvirus 6. *BMC genomics, 19*(1), 1-17.

Grivel, J.-C., Santoro, F., Chen, S., Fagá, G., Malnati, M. S., Ito, Y., . . . Lusso, P. (2003).

    Pathogenic effects of human herpesvirus 6 in human lymphoid tissue ex vivo. *Journal of*

    virology, 77(15), 8280-8289.

Gross, G. W., Rhoades, B. K., Azzazy, H. M., & Wu, M.-C. (1995). The use of neuronal

    networks on multielectrode arrays as biosensors. *Biosensors and Bioelectronics, 10*(6-7),

    553-567.

Hall, C. B., Caserta, M. T., Schnabel, K. C., Long, C., Epstein, L. G., Insel, R. A., & Dewhurst,

    S. (1998). Persistence of human herpesvirus 6 according to site and variant: possible

    greater neurotropism of variant A. *Clinical infectious diseases, 26*(1), 132-137.

Hansen, A. S., Bundgaard, B. B., Biltoft, M., Rossen, L. S., & Höllsberg, P. (2017). Divergent

    tropism of HHV-6AGS and HHV-6BPL1 in T cells expressing different CD46 isoform

    patterns. *Virology, 502*, 160-170.

Harberts, E., Yao, K., Wohler, J. E., Maric, D., Ohayon, J., Henkin, R., & Jacobson, S. (2011).

    Human herpesvirus-6 entry into the central nervous system through the olfactory

    pathway. *Proceedings of the National Academy of Sciences, 108*(33), 13734-13739.

Hasselmo, M. E., & Bower, J. M. (1993). Acetylcholine and memory. *Trends in neurosciences, 16*(6), 218-222.

Hayden, M., West, A., & Ghosh, S. (2006). NF-κB and the immune response. *Oncogene, 25*(51), 6758-6780.

Howell, K. B., Tiedemann, K., Haeusler, G., Mackay, M. T., Kornberg, A. J., Freeman, J. L., & Harvey, A. S. (2012). Symptomatic generalized epilepsy after HHV6 posttransplant acute limbic encephalitis in children. *Epilepsia, 53*(7), e122-e126.

Huang, X. (2021). *Human IPSC-Derived Kupffer Cell-Based Model for Immune Mediated Toxicity and Nonalcoholic Steatohepatitis.* National University of Singapore (Singapore).

Inoue, Y., Yasukawa, M., & Fujita, S. (1997). Induction of T-cell apoptosis by human herpesvirus 6. *Journal of virology, 71*(5), 3751-3759.

Isegawa, Y., Mukai, T., Nakano, K., Kagawa, M., Chen, J., Mori, Y., . . . Hata, A. (1999). Comparison of the complete DNA sequences of human herpesvirus 6 variants A and B. *Journal of virology, 73*(10), 8053-8063.

Isegawa, Y., Ping, Z., Nakano, K., Sugimoto, N., & Yamanishi, K. (1998). Human herpesvirus 6 open reading frame U12 encodes a functional β-chemokine receptor. *Journal of virology, 72*(7), 6104-6112.

Iyengar, S., Levine, P. H., Ablashi, D., Neequaye, J., & Pearson, G. R. (1991).

Sero-epidemiological investigations on human herpesvirus 6 (HHV-6) infections using a

newly developed early antigen assay. *International journal of cancer, 49*(4), 551-557.

Johnson, A. C., Heinzel, F. P., Diaconu, E., Sun, Y., Hise, A. G., Golenbock, D., . . . Pearlman,

E. (2005). Activation of toll-like receptor (TLR) 2, TLR4, and TLR9 in the mammalian

cornea induces MyD88-dependent corneal inflammation. *Investigative ophthalmology &

visual science, 46*(2), 589-595.

Jones, B. W., Means, T. K., Heldwein, K. A., Keen, M. A., Hill, P. J., Belisle, J. T., & Fenton,

M. J. (2001). Different Toll-like receptor agonists induce distinct macrophage responses.

Journal of leukocyte biology, 69(6), 1036-1044.

Jones, R. S. (1994). Synaptic and intrinsic properties of neurons of origin of the perforant path in

layer II of the rat entorhinal cortex in vitro. *Hippocampus, 4*(3), 335-353.

Josephs, S. F., Ablashi, D. V., Salahuddin, S. Z., Kramarsky, B., Franza Jr, B. R., Pellett, P., . . .

Gallo, R. C. (1988). Molecular studies of HHV-6. *Journal of virological methods, 21*(1-

4), 179-190.

Kakimoto, M., Hasegawa, A., Fujita, S., & Yasukawa, M. (2002). Phenotypic and functional

alterations of dendritic cells induced by human herpesvirus 6 infection. *Journal of

virology, 76*(20), 10338-10345.

Kapucu, F. E., Tanskanen, J. M., Mikkonen, J. E., Ylä-Outinen, L., Narkilahti, S., & Hyttinen, J.

    A. (2012). Burst analysis tool for developing neuronal networks exhibiting highly

    varying action potential dynamics. *Frontiers in computational neuroscience, 6*, 38.

Kaufer, D., Friedman, A., Seidman, S., & Soreq, H. (1998). Acute stress facilitates long-lasting

    changes in cholinergic gene expression. *Nature, 393*(6683), 373-377.

Kawabata, A., Oyaizu, H., Maeki, T., Tang, H., Yamanishi, K., & Mori, Y. (2011). Analysis of a

    neutralizing antibody for human herpesvirus 6B reveals a role for glycoprotein Q1 in

    viral entry. *Journal of virology, 85*(24), 12962-12971.

Kawamura, Y., Nakayama, A., Kato, T., Miura, H., Ishihara, N., Ihira, M., . . . Yoshikawa, T.

    (2015). Pathogenic role of human herpesvirus 6B infection in mesial temporal lobe

    epilepsy. *The Journal of infectious diseases, 212*(7), 1014-1021.

Kobayashi, M., Wen, X., & Buckmaster, P. S. (2003). Reduced inhibition and increased output

    of layer II neurons in the medial entorhinal cortex in a model of temporal lobe epilepsy.

    Journal of Neuroscience, 23(24), 8471-8479.

Kondo, K., Kondo, T., Okuno, T., Takahashi, M., & Yamanishi, K. (1991). Latent human

    herpesvirus 6 infection of human monocytes/macrophages. *Journal of General Virology,*

    72(6), 1401-1408.

Krueger, G., & Ablashi, D. V. (2006). Human herpesvirus-6: general virology, epidemiology,

    and clinical pathology.

Kumagai, T., Yoshikawa, T., Yoshida, M., Okui, T., Ihira, M., Nagata, N., . . . Ichihara, K.

(2006). Time course characteristics of human herpesvirus 6 specific cellular immune

response and natural killer cell activity in patients with exanthema subitum. *Journal of*

medical virology, 78(6), 792-799.

Lallement, G., Carpentier, P., Collet, A., Pernot-Marino, I., Baubichon, D., & Blanchet, G.

(1991). Effects of soman-induced seizures on different extracellular amino acid levels

and on glutamate uptake in rat hippocampus. *Brain research, 563*(1-2), 234-240.

Leigh, R., Oyelusi, W., Wiehler, S., Koetzler, R., Zaheer, R. S., Newton, R., & Proud, D. (2008).

Human rhinovirus infection enhances airway epithelial cell production of growth factors

involved in airway remodeling. *Journal of Allergy and Clinical Immunology, 121*(5),

1238-1245. e1234.

Levine, P. H., Jahan, N., Murari, P., Manak, M., & Jaffe, E. S. (1992). Detection of human

herpesvirus 6 in tissues involved by sinus histiocytosis with massive lymphadenopathy

(Rosai-Dorfman disease). *Journal of Infectious Diseases, 166*(2), 291-295.

Li, J.-M., Lei, D., Peng, F., Zeng, Y.-J., Li, L., Xia, Z.-L., . . . Zhou, D. (2011). Detection of

human herpes virus 6B in patients with mesial temporal lobe epilepsy in West China and

the possible association with elevated NF-κB expression. *Epilepsy research, 94*(1-2), 1-9.

Li, L., Gu, B., Zhou, F., Chi, J., Wang, F., Peng, G., . . . Lu, S. (2011). Human herpesvirus 6

   suppresses T cell proliferation through induction of cell cycle arrest in infected cells in

   the G2/M phase. *Journal of virology, 85*(13), 6774-6783.

Liu, D., Wang, X., Wang, Y., Wang, P., Fan, D., Chen, S., . . . Luan, G. (2018). Detection of

   EBV and HHV6 in the Brain Tissue of Patients with Rasmussen's Encephalitis.

   Virologica Sinica, 33(5), 402-409.

Lopes da Silva, F., Witter, M. P., Boeijinga, P. H., & Lohman, A. (1990). Anatomic organization

   and physiology of the limbic cortex. *Physiological reviews, 70*(2), 453-511.

Lopez, C., Pellett, P., Stewart, J., Goldsmith, C., Sanderlin, K., Black, J., . . . Feorino, P. (1988).

   Characteristics of human herpesvirus-6. *The Journal of infectious diseases, 157*(6), 1271-

   1273.

Löscher, W., & Brandt, C. (2010). Prevention or modification of epileptogenesis after brain

   insults: experimental approaches and translational research. *Pharmacological reviews,

   62*(4), 668-700.

Lowenstein, D. H., Walker, M., & Waterhouse, E. (2014). Status Epilepticus in the Setting of

   Acute Encephalitis: Status Epilepticus in the Setting of Acute Encephalitis. *Epilepsy

   Currents, 14*(2_suppl), 43-49.

Luppi, M., Barozzi, P., Maiorana, A., Marasca, R., & Torelli, G. (1994). Human herpesvirus 6

   infection in normal human brain tissue. *Journal of Infectious Diseases, 169*(4), 943-944.

Lusso, P. (2006). HHV-6 and the immune system: mechanisms of immunomodulation and viral

    escape. *Journal of Clinical Virology, 37*, S4-S10.

Lusso, P., De Maria, A., Malnati, M., Lori, F., DeRocco, S. E., Baseler, M., & Gallo, R. C.

    (1991). Induction of CD4 and susceptibility to HIV-1 infection in human CD8+ T

    lymphocytes by human herpesvirus 6. *Nature, 349*(6309), 533-535.

Lusso, P., Garzino-Demo, A., Crowley, R. W., & Malnati, M. S. (1995). Infection of

    gamma/delta T lymphocytes by human herpesvirus 6: transcriptional induction of CD4

    and susceptibility to HIV infection. *The Journal of experimental medicine, 181*(4), 1303-

    1310.

Lusso, P., Markham, P. D., Tschachler, E., di Marzo Veronese, F., Salahuddin, S. Z., Ablashi, D.

    V., . . . Gallo, R. C. (1988). In vitro cellular tropism of human B-lymphotropic virus

    (human herpesvirus-6). *The Journal of experimental medicine, 167*(5), 1659-1670.

Lüttichau, H. R., Clark-Lewis, I., Jensen, P. Ø., Moser, C., Gerstoft, J., & Schwartz, T. W.

    (2003). A highly selective CCR2 chemokine agonist encoded by human herpesvirus 6.

    Journal of Biological Chemistry, 278(13), 10928-10933.

Maeki, T., & Mori, Y. (2012). Features of human herpesvirus-6A and-6B entry. *Advances in

    Virology, 2012*.

Marci, R., Gentili, V., Bortolotti, D., Lo Monte, G., Caselli, E., Bolzani, S., . . . Rizzo, R. (2016).

Presence of HHV-6A in endometrial epithelial cells from women with primary

unexplained infertility. *PLoS One, 11*(7), e0158304.

Martin, L. K., Schub, A., Dillinger, S., & Moosmann, A. (2012). Specific CD 8+ T cells

recognize human herpesvirus 6 B. *European journal of immunology, 42*(11), 2901-2912.

Meeuwsen, S., Persoon-Deen, C., Bsibsi, M., Bajramovic, J. J., Ravid, R., De Bolle, L., & van

Noort, J. M. (2005). Modulation of the cytokine network in human adult astrocytes by

human herpesvirus-6A. *Journal of neuroimmunology, 164*(1-2), 37-47.

Meiry, G., Reisner, Y., Feld, Y., Goldberg, S., Rosen, M., Ziv, N., & Binah, O. (2001).

Evolution of action potential propagation and repolarization in cultured neonatal rat

ventricular myocytes. *Journal of cardiovascular electrophysiology, 12*(11), 1269-1277.

Meshorer, E., Erb, C., Gazit, R., Pavlovsky, L., Kaufer, D., Friedman, A., . . . Soreq, H. (2002).

Alternative splicing and neuritic mRNA translocation under long-term neuronal

hypersensitivity. *Science, 295*(5554), 508-512.

Miccoli, B., Lopez, C. M., Goikoetxea, E., Putzeys, J., Sekeri, M., Krylychkina, O., . . .

Reumers, V. (2019). High-density electrical recording and impedance imaging with a

multi-modal CMOS multi-electrode array chip. *Frontiers in Neuroscience, 13*, 641.

Michael, B. D., & Solomon, T. (2012). Seizures and encephalitis: clinical features, management,

and potential pathophysiologic mechanisms. *Epilepsia, 53*, 63-71.

Milne, R. S., Mattick, C., Nicholson, L., Devaraj, P., Alcami, A., & Gompels, U. A. (2000). RANTES binding and down-regulation by a novel human herpesvirus-6 β chemokine receptor. *The Journal of Immunology, 164*(5), 2396-2404.

Milner, T., Loy, R., & Amaral, D. G. (1983). An anatomical study of the development of the septo-hippocampal projection in the rat. *Developmental Brain Research, 8*(2-3), 343-371.

Minerbi, A., Kahana, R., Goldfeld, L., Kaufman, M., Marom, S., & Ziv, N. E. (2009). Long-term relationships between synaptic tenacity, synaptic remodeling, and network activity. *PLoS biology, 7*(6), e1000136.

Misra, U. K., Kalita, J., & Chauhan, P. S. (2019). Evaluation of cholinergic functions in patients with Japanese encephalitis and Herpes simplex encephalitis. *Brain research, 1707*, 227-232.

Mohammadpour Touserkani, F., Gaínza-Lein, M., Jafarpour, S., Brinegar, K., Kapur, K., & Loddenkemper, T. (2017). HHV-6 and seizure: A systematic review and meta-analysis. *Journal of medical virology, 89*(1), 161-169.

Montoya, J. G., Neely, M. N., Gupta, S., Lunn, M. R., Loomis, K. S., Pritchett, J. C., . . . Medveczky, P. G. (2012). Antiviral therapy of two patients with chromosomally-integrated human herpesvirus-6A presenting with cognitive dysfunction. *Journal of Clinical Virology, 55*(1), 40-45.

Mori, D., Khanam, W., Sheikh, R. A., Tabib, S., Ikebe, E., Hossain, M. M., . . . Ahmed, K.

    (2017). Increased serum vascular endothelial growth factor is associated with acute viral

    encephalitis in Bangladeshi children. *Scientific reports, 7*(1), 1-7.

Murakami, Y., Tanimoto, K., Fujiwara, H., An, J., Suemori, K., Ochi, T., . . . Yasukawa, M.

    (2010). Human herpesvirus 6 infection impairs Toll-like receptor signaling. *Virology*

    journal, 7(1), 1-5.

Nastke, M.-D., Becerra, A., Yin, L., Dominguez-Amorocho, O., Gibson, L., Stern, L. J., &

    Calvo-Calle, J. M. (2012). Human CD4+ T cell response to human herpesvirus 6. *Journal*

    of virology, 86(9), 4776-4792.

Naylor, D. E., Liu, H., Niquet, J., & Wasterlain, C. G. (2013). Rapid surface accumulation of

    NMDA receptors increases glutamatergic excitation during status epilepticus.

    Neurobiology of disease, 54, 225-238.

Ngugi, A. K., Bottomley, C., Kleinschmidt, I., Wagner, R. G., Kakooza-Mwesige, A., Ae-

    Ngibise, K., . . . Odhiambo, R. (2013). Prevalence of active convulsive epilepsy in sub-

    Saharan Africa and associated risk factors: cross-sectional and case-control studies. *The*

    Lancet Neurology, 12(3), 253-263.

Ohto, U., Shibata, T., Tanji, H., Ishida, H., Krayukhina, E., Uchiyama, S., . . . Shimizu, T.

    (2015). Structural basis of CpG and inhibitory DNA recognition by Toll-like receptor 9.

    Nature, 520(7549), 702-705.

Opsahl, M. L., & Kennedy, P. G. (2005). Early and late HHV-6 gene transcripts in multiple

    sclerosis lesions and normal appearing white matter. *Brain, 128*(3), 516-527.

Ortinski, P. I., Dong, J., Mungenast, A., Yue, C., Takano, H., Watson, D. J., . . . Coulter, D. A.

    (2010). Selective induction of astrocytic gliosis generates deficits in neuronal inhibition.

    Nature neuroscience, 13(5), 584-591.

Oyaizu, H., Tang, H., Ota, M., Takenaka, N., Ozono, K., Yamanishi, K., & Mori, Y. (2012).

    Complementation of the function of glycoprotein H of human herpesvirus 6 variant A by

    glycoprotein H of variant B in the virus life cycle. *Journal of virology, 86*(16), 8492-

    8498.

Pantry, S. N., & Medveczky, P. G. (2017). Latency, integration, and reactivation of human

    herpesvirus-6. *Viruses, 9*(7), 194.

Pfeiffer, B., Berneman, Z., Neipel, F., Chang, C., Tirwatnapong, S., & Chandran, B. (1993).

    Identification and mapping of the gene encoding the glycoprotein complex gp82-gp105

    of human herpesvirus 6 and mapping of the neutralizing epitope recognized by

    monoclonal antibodies. *Journal of virology, 67*(8), 4611-4620.

Pfeiffer, B., Thomson, B., & Chandran, B. (1995). Identification and characterization of a cDNA

    derived from multiple splicing that encodes envelope glycoprotein gp105 of human

    herpesvirus 6. *Journal of virology, 69*(6), 3490-3500.

Potier, S., & Psarropoulou, C. (2001). Endogenous acetylcholine facilitates epileptogenesis in immature rat neocortex. *Neuroscience letters, 302*(1), 25-28.

Prusty, B. K., Gulve, N., Govind, S., Krueger, G. R., Feichtinger, J., Larcombe, L., . . . Toro, C. T. (2018). Active HHV-6 infection of cerebellar purkinje cells in mood disorders. *Frontiers in Microbiology*, 1955.

Rapp, J. C., Krug, L. T., Inoue, N., Dambaugh, T. R., & Pellett, P. E. (2000). U94, the human herpesvirus 6 homolog of the parvovirus nonstructural gene, is highly conserved among isolates and is expressed at low mRNA levels as a spliced transcript. *Virology, 268*(2), 504-516.

Reddy, S., & Manna, P. (2005). Quantitative detection and differentiation of human herpesvirus 6 subtypes in bone marrow transplant patients by using a single real-time polymerase chain reaction assay. *Biology of Blood and Marrow Transplantation, 11*(7), 530-541.

Reynaud, J. M., Jégou, J.-F., Welsch, J. C., & Horvat, B. (2014). Human herpesvirus 6A infection in CD46 transgenic mice: viral persistence in the brain and increased production of proinflammatory chemokines via Toll-like receptor 9. *Journal of virology, 88*(10), 5421-5436.

Rizzo, R., Soffritti, I., D'Accolti, M., Bortolotti, D., Di Luca, D., & Caselli, E. (2017). HHV-6A/6B infection of NK cells modulates the expression of miRNAs and transcription

factors potentially associated to impaired NK activity. *Frontiers in Microbiology, 8,*

2143.

Robel, S., Buckingham, S. C., Boni, J. L., Campbell, S. L., Danbolt, N. C., Riedemann, T., . . .

Sontheimer, H. (2015). Reactive astrogliosis causes the development of spontaneous

seizures. *Journal of Neuroscience, 35*(8), 3330-3345.

Robert, C., Aubin, J.-T., Visse, B., Fillet, A.-M., Huraux, J.-M., & Agut, H. (1996). Difference in

permissiveness of human fibroblast cells to variants A and B of human herpesvirus-6.

Research in virology, 147(4), 219-225.

Salahuddin, S. Z., Ablashi, D. V., Markham, P. D., Josephs, S. F., Sturzenegger, S., Kaplan, M., .

. . Kramarsky, B. (1986). Isolation of a new virus, HBLV, in patients with

lymphoproliferative disorders. *Science, 234*(4776), 596-601.

Santoro, F., Kennedy, P. E., Locatelli, G., Malnati, M. S., Berger, E. A., & Lusso, P. (1999).

CD46 is a cellular receptor for human herpesvirus 6. *Cell, 99*(7), 817-827.

Schirmer, E. C., Wyatt, L. S., Yamanishi, K., Rodriguez, W. J., & Frenkel, N. (1991).

Differentiation between two distinct classes of viruses now classified as human

herpesvirus 6. *Proceedings of the National Academy of Sciences, 88*(13), 5922-5926.

Schwarcz, R., Eid, T., & Du, F. (2000). Neurons in layer III of the entorhinal cortex: A role in

epileptogenesis and epilepsy? *Annals of the New York Academy of Sciences, 911*(1), 328-

342.

Scotet, E., Peyrat, M. A., Saulquin, X., Retiere, C., Couedel, C., Davodeau, F., . . . Lim, A.

(1999). Frequent enrichment for CD8 T cells reactive against common herpes viruses in

chronic inflammatory lesions: towards a reassessment of the physiopathological

significance of T cell clonal expansions found in autoimmune inflammatory processes.

European journal of immunology, 29(3), 973-985.

Shintani, Y., Kapoor, A., Kaneko, M., Smolenski, R. T., D'Acquisto, F., Coppen, S. R., . . .

Takashima, S. (2013). TLR9 mediates cellular protection by modulating energy

metabolism in cardiomyocytes and neurons. *Proceedings of the National Academy of*

Sciences, 110(13), 5109-5114.

Simeonov, S., & Schäffer, T. E. (2019). Ultrafast imaging of cardiomyocyte contractions by

combining scanning ion conductance microscopy with a microelectrode array. *Analytical*

chemistry, 91(15), 9648-9655.

Sloviter, R. S., Zappone, C. A., Harvey, B. D., Bumanglag, A. V., Bender, R. A., & Frotscher,

M. (2003). "Dormant basket cell" hypothesis revisited: relative vulnerabilities of dentate

gyrus mossy cells and inhibitory interneurons after hippocampal status epilepticus in the

rat. *Journal of Comparative Neurology, 459*(1), 44-76.

Smith, A. P., Paolucci, C., Di Lullo, G., Burastero, S. E., Santoro, F., & Lusso, P. (2005). Viral

replication-independent blockade of dendritic cell maturation and interleukin-12

production by human herpesvirus 6. *Journal of virology, 79*(5), 2807-2813.

Soldan, S. S., Berti, R., Salem, N., Secchiero, P., Flamand, L., Calabresi, P. A., . . . Lin, H.-C. (1997). Association of human herpes virus 6 (HHV-6) with multiple sclerosis: increased IgM response to HHV-6 early antigen and detection of serum HHV-6 DNA. *Nature medicine, 3*(12), 1394-1397.

Spira, M. E., & Hai, A. (2013). Multi-electrode array technologies for neuroscience and cardiology. *Nature nanotechnology, 8*(2), 83-94.

Stanton, R., Wilkinson, G. W., & Fox, J. D. (2003). Analysis of human herpesvirus-6 IE1 sequence variation in clinical samples. *Journal of medical virology, 71*(4), 578-584.

Stevens, S. L., Ciesielski, T. M., Marsh, B. J., Yang, T., Homen, D. S., Boule, J.-L., . . . Stenzel-Poore, M. P. (2008). Toll-like receptor 9: a new target of ischemic preconditioning in the brain. *Journal of Cerebral Blood Flow & Metabolism, 28*(5), 1040-1047.

Strenger, V., Caselli, E., Lautenschlager, I., Schwinger, W., Aberle, S., Loginov, R., . . . Urban, C. (2014). Detection of HHV-6-specific mRNA and antigens in PBMCs of individuals with chromosomally integrated HHV-6 (ciHHV-6). *Clinical Microbiology and Infection, 20*(10), 1027-1032.

Takahashi, K., Sonoda, S., Higashi, K., Kondo, T., Takahashi, H., Takahashi, M., & Yamanishi, K. (1989). Predominant CD4 T-lymphocyte tropism of human herpesvirus 6-related virus. *Journal of virology, 63*(7), 3161-3163.

Tanaka, K., Kondo, T., Torigoe, S., Okada, S., Mukai, T., & Yamanishi, K. (1994). Human

 herpesvirus 7: another causal agent for roseola (exanthem subitum). *The Journal of*

 pediatrics, 125(1), 1-5.

Tang, H., Hayashi, M., Maeki, T., Yamanishi, K., & Mori, Y. (2011). Human herpesvirus 6

 glycoprotein complex formation is required for folding and trafficking of the

 gH/gL/gQ1/gQ2 complex and its cellular receptor binding. *Journal of virology, 85*(21),

 11121-11130.

Tang, H., Kawabata, A., Yoshida, M., Oyaizu, H., Maeki, T., Yamanishi, K., & Mori, Y. (2010).

 Human herpesvirus 6 encoded glycoprotein Q1 gene is essential for virus growth.

 Virology, 407(2), 360-367.

Tang, H., & Mori, Y. (2018). Glycoproteins of HHV-6A and HHV-6B. *Human Herpesviruses*,

 145-165.

Tang, H., Serada, S., Kawabata, A., Ota, M., Hayashi, E., Naka, T., . . . Mori, Y. (2013). CD134

 is a cellular receptor specific for human herpesvirus-6B entry. *Proceedings of the*

 National Academy of Sciences, 110(22), 9096-9099.

Tesini, B. L., Epstein, L. G., & Caserta, M. T. (2014). Clinical impact of primary infection with

 roseoloviruses. *Current Opinion in Virology, 9*, 91-96.

Tolner, E. A., Kloosterman, F., van Vliet, E. A., Witter, M. P., da Silva, F. H. L., & Gorter, J. A.

 (2005). Presubiculum stimulation in vivo evokes distinct oscillations in superficial and

deep entorhinal cortex layers in chronic epileptic rats. *Journal of Neuroscience, 25*(38), 8755-8765.

Trinchieri, G., & Sher, A. (2007). Cooperation of Toll-like receptor signals in innate immune defence. *Nature Reviews Immunology, 7*(3), 179-190.

Tsubokawa, H., & Ross, W. N. (1996). IPSPs modulate spike backpropagation and associated [Ca2+] i changes in the dendrites of hippocampal CA1 pyramidal neurons. *Journal of neurophysiology, 76*(5), 2896-2906.

Vezzani, A., Balosso, S., & Ravizza, T. (2019). Neuroinflammatory pathways as treatment targets and biomarkers in epilepsy. *Nature Reviews Neurology, 15*(8), 459-472.

Vezzani, A., Fujinami, R. S., White, H. S., Preux, P.-M., Blümcke, I., Sander, J. W., & Löscher, W. (2016). Infections, inflammation and epilepsy. *Acta neuropathologica, 131*(2), 211-234.

Vinters, H. V., Wang, R., & Wiley, C. A. (1993). Herpesviruses in chronic encephalitis associated with intractable childhood epilepsy. *Human pathology, 24*(8), 871-879.

Vrancken, K., Vervaeke, P., Balzarini, J., & Liekens, S. (2011). Viruses as key regulators of angiogenesis. *Reviews in medical virology, 21*(3), 181-200.

Wang, F.-Z., & Pellett, P. E. (2007). HHV-6A, 6B, and 7: immunobiology and host response. *Human herpesviruses: biology, therapy, and immunoprophylaxis*.

Wilson, C., Isokawa, M., Babb, T., Crandall, P., Levesque, M., & Engel, J. (1991). Functional

connections in the human temporal lobe. *Experimental Brain Research, 85*(1), 174-187.

Wyatt, L. S., Balachandran, N., & Frenkel, N. (1990). Variations in the replication and antigenic

properties of human herpesvirus 6 strains. *Journal of Infectious Diseases, 162*(4), 852-

857.

Xanthos, D. N., & Sandkühler, J. (2014). Neurogenic neuroinflammation: inflammatory CNS

reactions in response to neuronal activity. *Nature Reviews Neuroscience, 15*(1), 43-53.

Xing, Z., Gauldie, J., Cox, G., Baumann, H., Jordana, M., Lei, X.-F., & Achong, M. K. (1998).

IL-6 is an antiinflammatory cytokine required for controlling local or systemic acute

inflammatory responses. *The Journal of clinical investigation, 101*(2), 311-320.

Xu, Z., Xue, T., Zhang, Z., Wang, X., Xu, P., Zhang, J., . . . Wang, L. (2011). Role of signal

transducer and activator of transcription-3 in up-regulation of GFAP after epilepsy.

Neurochemical research, 36(12), 2208-2215.

Yamanishi, K. (2007). Human herpesviruses 6 and 7. *Virology*, 2819-2845.

Yamanishi, K., Kondo, T., Kondo, K., Hayakawa, Y., Kido, S., Takahashi, K., & Takahashi, M.

(1990). Exanthem subitum and human herpesvirus 6 (HHV-6) infection *Immunobiology*

and Prophylaxis of Human Herpesvirus Infections (pp. 29-37): Springer.

Yamanishi, K., Shiraki, K., Kondo, T., Okuno, T., Takahashi, M., Asano, Y., & Kurata, T.

    (1988). Identification of human herpesvirus-6 as a causal agent for exanthem subitum.

    The Lancet, 331(8594), 1065-1067.

Yao, K., Crawford, J. R., Komaroff, A. L., Ablashi, D. V., & Jacobson, S. (2010). Review part 2:

    Human herpesvirus-6 in central nervous system diseases. *Journal of medical virology,*

    82(10), 1669.

Yasukawa, M., Inoue, Y., Ohminami, H., Terada, K., & Fujita, S. (1998). Apoptosis of CD4+ T

    lymphocytes in human herpesvirus-6 infection. *Journal of General Virology, 79*(1), 143-

    147.

Yoshida, M., Torigoe, S., & Yamada, M. (2002). Elucidation of the cross-reactive

    immunoglobulin M response to human herpesviruses 6 and 7 on the basis of neutralizing

    antibodies. *Clinical and Vaccine Immunology, 9*(2), 394-402.

Yoshikawa, T., & Asano, Y. (2000). Central nervous system complications in human

    herpesvirus-6 infection. *Brain and Development, 22*(5), 307-314.

Zitzmann, F. D., Jahnke, H.-G., Nitschke, F., Beck-Sickinger, A. G., Abel, B., Belder, D., &

    Robitzki, A. A. (2017). A novel microfluidic microelectrode chip for a significantly

    enhanced monitoring of NPY-receptor activation in live mode. *Lab on a Chip, 17*(24),

    4294-4302.

2   CHAPTER II

2.1   Abstract

Unresolved questions regarding cell tropism and relative virulence between HHV-6A versus HHV-6B are still unresolved. Even though both HHV-6A and HHV-6B have been shown to infect glia and, more recently, cerebellar Purkinje cells, the cell tropism of HHV-6A vs. HHV-6B for various nerve cell types remains unknown. In this chapter, I demonstrate that both HHV-6A and HHV-6B can infect different nerve cell types (i.e., glia versus neurons) and different neuronal neurotransmitter phenotypes derived from the differentiation of human neural stem cells. I also show that HHV-6A and HHV-6B cause cytopathic effects (CPEs) in nerve cells. However, the time course and intensity of CPEs show differences between HHV-6A and HHV-6B infections and are impacted by a multiplicity of infections (MOI). Immunofluorescence microscopy has shown that both HHV-6A and HHV-6B successfully infect cells expressing VGluT (i.e., glutamatergic neurons) and dopamine (i.e., dopaminergic neurons); however, neither HHV-6A nor HHV-6B infection led in the productive infection of GAD67-containing cells (i.e., GABAergic cells). The reason underlying the apparent resistance of GABAergic cells to HHV-6A and HHV-6B infect on ongoing research. The inhibitory interneuron dysfunction hypothesis for HHV6-driven seizures may be rejected as a viable mechanism for HHV6-induced epileptogenesis if these in vitro studies on differential cell tropism are necessarily in vivo.

2.2   Introduction

Human herpesvirus 6 (HHV-6) variants fall into two sub-groups of viruses, which are now distinguished by the International Committee on Taxonomy of Viruses as distinct virus species, designated as HHV-6A and HHV-6B, in the genus *Roseolovirus*(Adams & Carstens, 2012). Along with human herpesvirus 7 (HHV-7), HHV-6A and HHV-6B are the only characterized human viruses included within the genus Roseolovirus (subfamily β-herpesvirinae, family Herpesviridae). Despite exhibiting approximately 90% overall genome sequence identity(Isegawa et al., 1999). key regions of the HHV-6A and HHV-6B genomes (i.e., immediate-early genes) exhibit only 70% (or less) sequence identity(Dominguez et al., 1999). Beyond notable gene sequence divergence, key coding regions yield homologous proteins with distinguishable amino acid profiles even when the genes exhibit high (e.g., 95%) sequence homology(Achour et al., 2008; Rapp et al., 2000). For example, HHV-6A and HHV-6B envelope glycoproteins (i.e., gH and gB), which are critical for virus-cell surface interactions, exhibit overall high sequence identity between homologous genes but feature distinct amino acid profiles for each of the two species(Achour et al., 2008). This may account for variations in cell tropism (and etiology) between the two viruses(Oyaizu et al., 2012; Tang & Mori, 2018). Among the tissues and organs that are known to harbor HHV-6A and HHV-6B, it is known that both viruses can infect the central nervous system(Boutolleau et al., 2006; De Bolle, Naesens, et al., 2005). Although reports suggest that HHV-6A may be more neurotropic than HHV-6B, this is

mainly based on the prevalence of HHV-6A over HHV-6B in cerebral spinal fluid and blood of

patients with encephalitis, multiple sclerosis, and other neuroinflammatory diseases(Crawford et

al., 2007; Hall et al., 1998). In general, there is a lack of evidence showing the extent of HHV-

6A versus HHV-6B cell tropism in the central nervous system (CNS). It is unknown whether the

brain proper or nerve cells within the spinal column exhibit predisposed susceptibility to one

virus over the other. In the brain, it is unknown if there is predisposition for HHV-6A versus

HHV-6B infection in glia versus neurons. Once it became clear that HHV-6A and HHV-6B

were two distinct viruses, it was demonstrated that both were able to infect

astrocytes(Fotheringham et al., 2008). Since then, a few studies have emerged differentiating

between HHV-6A and HHV-6B infection in select nerve cell types(Liu et al., 2018; Prusty et al.,

2018). However, such studies are limited. The relative virulence of HHV-6A versus HHV-6B on

susceptible nerve cell types and differential susceptibility of specific neuronal neurotransmitter

phenotypes to these two viruses remains unclear. Characterization of infection dynamics and cell

tropism of HHV-6A versus HHV-6B is essential for validating models of HHV6-based

neurological dysfunction. Recently, a study was published demonstrating that HHV-6A and

HHV-6B infect Purkinje cells(Prusty et al., 2018). Although Purkinje cells are GABAergic, this

study did not detect productive HHV-6A or HHV-6B infection in GABAergic cells. In this

study, we provide data from an immunofluorescence (and qPCR) study confirming that both

HHV-6A and HHV-6B infect both GFAP-positive cells (i.e., glia) and βIII-tubulin-positive cells

(i.e., neurons) with notable cytopathic effects. We also show that both viruses can infect different neuronal neurotransmitter phenotypes. However, neither HHV-6A nor HHV-6B appears to infect GABAergic cells.

2.3   Results

For all immunofluorescence, light microscopy, and RT-qPCR experiments, differentiated HNSCs in culture were viable cells at post-differentiation day 7 (PDD7) and were used in experiments through PDD14. After PDD14 cell culture stability was unreliable. By PDD7, cells showed short branching neurites and/or longer processes (see Figs. 4 and 5) and distinct soma morphotypes: oval/round (e.g., tear-drop shapes), square-like (e.g., star shapes), and triangular. There was no apparent correlation between morphotypes and cell type (i.e., glia versus neuron). By PDD7, cells also begin to emit robust electrical discharges as observed using a multi-electrode array culture plate (MEA2100 system, Harvard Bioscience, Inc., Germany; data not shown). During the differentiation process, culture wells are seeded with 5×10^4 cells in suspension. Culture thinning occurs as cells attach to the substrate and undergo the differentiation process. Cultures are considered viable for experiments if there are at least 10,000 cells at PDD7 in the culture wells (well surface area = 0.5 cm^2). This minimum cell density at PDD7 is required since by PDD14 viable cell count decreases by ~70% in uninfected control cultures (N=3, p<0.01). Although there is a substantial loss in cell density over 7 days in

cultured differentiated HNSCs, the cell death rate at either PDD7 or PDD14 over any 2-6 hour period is negligible in uninfected cell cultures (i.e., controls). Therefore, losses in cell density greater than 10% during 2 hours are not likely due to baseline attrition but rather to some treatment (e.g., infection).

For cultures infected with HHV-6A, a 50% loss in viable cells was observed at 2 HPI (N=3, p<0.05) for PDD7 infections. For PDD14 infections with HHV-6A, a 45% loss in viable cells was observed at 2 HPI (N=3, p<0.05). For cultures infected with HHV-6B, a 31% loss in cells was observed at 2 HPI (N=3, p<0.05) for PDD7 infections. For PDD14 infections with HHV-6B, a 54% loss in viable cells was observed at 2 HPI (N=3, p<0.05). Note: Infection assays were typically done at MOI=1.

2.3.1 Both glia and neurons are susceptible to infection by either HHV-6A or HHV-6B

Results from immunofluorescence histochemistry indicate that both HHV-6A and HHV-6B can infect glial fibrillary acidic protein (GFAP)-positive differentiated HNSCs (dHNSCs) in culture. Labeling dHNSC cultures at PDD7 with antibodies against GFAP (anti-GFAP) and HHV6 envelope glycoprotein gB (anti-gB) and co-staining with DAPI (4',6-diamidino-2-phenylindole), reveals coincidence of anti-gB and anti-GFAP fluorescence signals in DAPI-stained cells (Fig. 1). This indicates the susceptibility of glial cells to infection by HHV-6A (Fig. 1, row A) and HHV-6B (Fig. 1, row B). The data also show visible cell aggregation, a cytopathic effect (CPE),

at 2 HPI. Distribution of cells across the substrate is notably more homogenous in the uninfected

controls (Fig. 1, row C). In these mixed cultures of dHNSCs (N=12), ~58% of cells were

identified as glia. Of these GFAP-positive cells, 29.2% were also gB-positive 2 HPI with HHV-

6A (*N*=6; *p*<0.05). Parallel cultures show that 42.3% of GFAP-positive cells were gB-positive in

HHV-6B infected cultures (*N*=6; *p*<0.05). Thus, results show that both HHV-6A and HHV-6B

can infect glia.
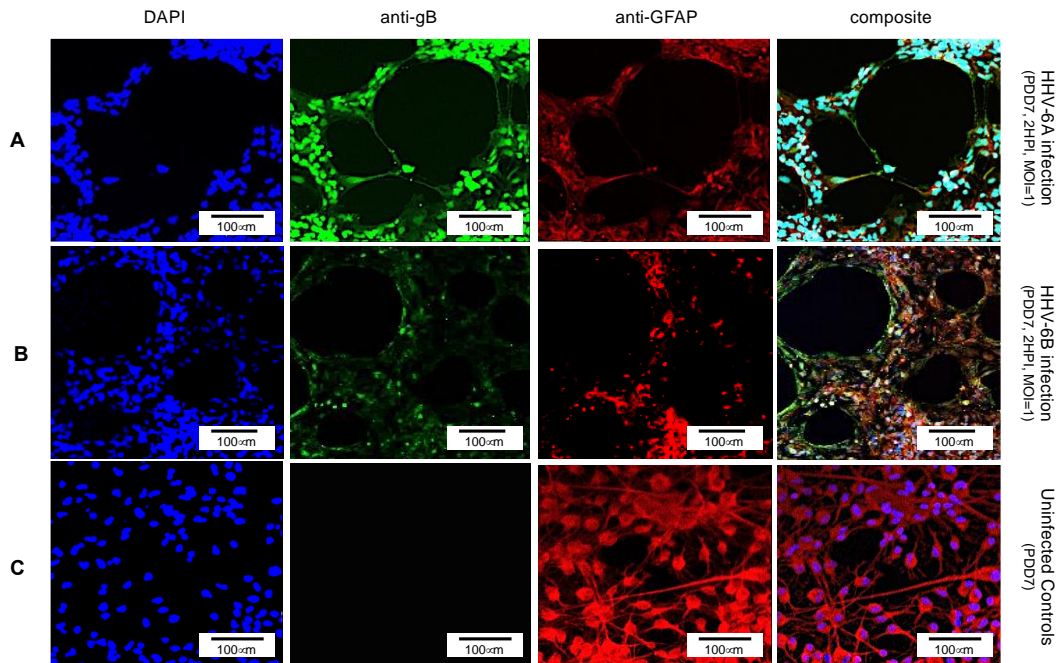
Figure 2-1. Fluorescence microscopy images of differentiated human neural stem cells (dHNSCs) treated with

immunofluorescent antibodies and a fluoro-dye at PDD7: Differentiation to Glial cells. From left to right, DAPI,

anti-gB, anti-GFAP, and composites. PDD7 HNSCs infected with HHV-6A (row A) show gB-positive signals on

GFAP-positive cells (glial cells). PDD7 HNSCs infected with HHV-6B (row B) also show a gB-positive signal on

GFAP-positive cells. Images for uninfected control culture (row C) show well-developed GFAP-positive cells with

homogeneous distribution, many exhibits stellate

Using an antibody for βIII tubulin (a neuron-specific protein), DAPI, and an anti-gB fluoroprobe, immunofluorescence demonstrates neurons are also susceptible to infection by both HHV-6A (Fig. 2, row A) and HHV-6B (Fig. 2, row B). In cells identified as neurons (i.e., βIII tubulin-positive), over 91% and 45.3% were also gB-positive at 2 HPI with HHV-6A (N=6; p<0.05) and HHV-6B (N=6; p<0.05), respectively. These results show that HHV-6A and HHV-6B can infect neurons. Furthermore, fluorescence images from the βIII-tubulin antibody system in uninfected cultures (Fig. 2, row C) show elongated neurite extensions and node formation, further indicating cell differentiation into viable neurons and the formation of cell-cell connectivity. At similar time points, roseolovirus-infected cultures exhibit CPEs (e.g., cell aggregation and neurite disruption).

2.3.2 Infection with either HHV-6A or HHV-6B results in time-dependent cytopathic effects

Productive infection can be verified via transmission electron microscopy (TEM) and quantitative polymerase chain reaction (qPCR). TEM demonstrates the presence of fully assembled HHV-6A virus particles (Fig. 3A) within cells that match the size and morphology of cell-free virions from virus stocks (Fig. 3B). Likewise, HHV-6B virus particles are observed within vacuole-like spaces within dHNSCs (Fig. 3D). These also match the size and shape of HHV-6B virions imaged from virus stocks (Fig. 3E). To demonstrate that these are productive roseolovirus infections as opposed to a *lysis-from-without* phenomenon (Delbruck et al., 1940),

qPCR-based virus titers (i.e., viral genome count per mL) were determined for HHV-6A (Fig. 3C) and HHV-6B (Fig. 3F). Within 2 HPI, the number of detectable viral genomes exceeds the virus density of the inoculum of HHV-6A and HHV-6B used to infect HNSC cultures, thereby demonstrating productive infection (i.e., the production of progeny virus).
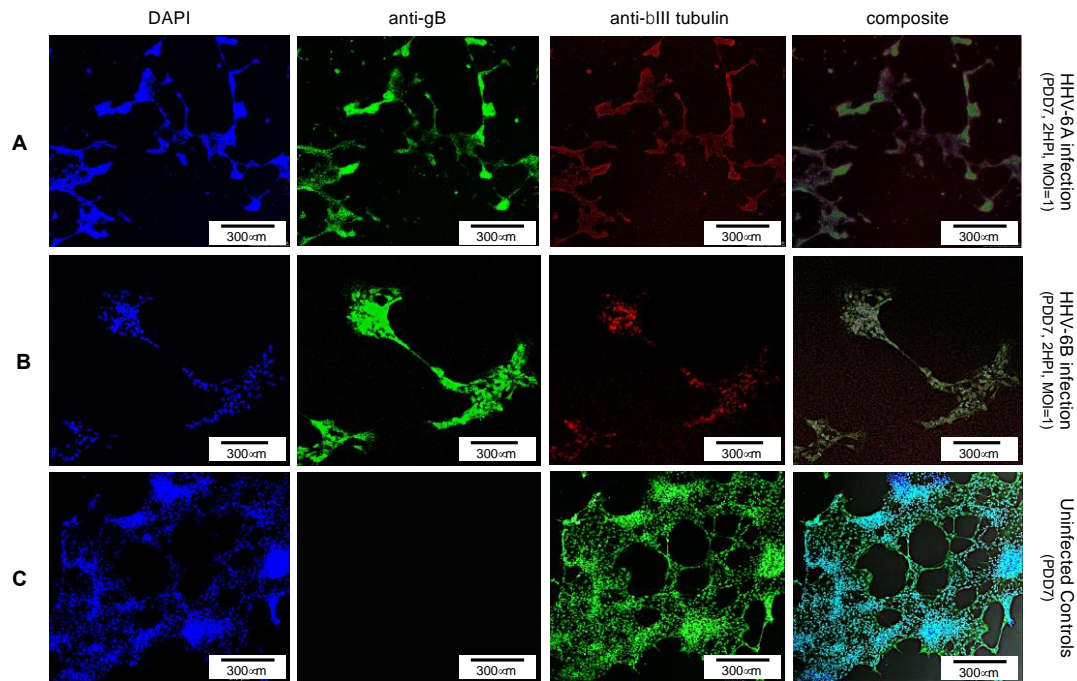
Figure 2-2- Fluorescence microscopy images of differentiated human neural stems cells (dHNSCs) treated with immunofluorescent antibodies and a fluoro-dye at PDD7: Differentiation to Neurons. From left to right, DAPI, anti-gB, anti-βIII tubulin, and composites. PDD7 dHNSCs infected with HHV-6A (row A) show gB-positive signal on βIII tubulin-positive cells. PDD7 HNSCs infected with HHV-6B (row B) also show gB-positive signal on βIII tubulin-positive cells. Images for uninfected control culture (row C) show developed βIII tubulin-positive cells with significant neurite-neurite and neurite-soma connectivity

Figure 2-3 – TEM and qPCR data from HHV6-infected hNSCs. TEM images illustrate: (A) HHV-6A virus particles within a cell; (B) HHV-6A virions in cell-free filtered supernat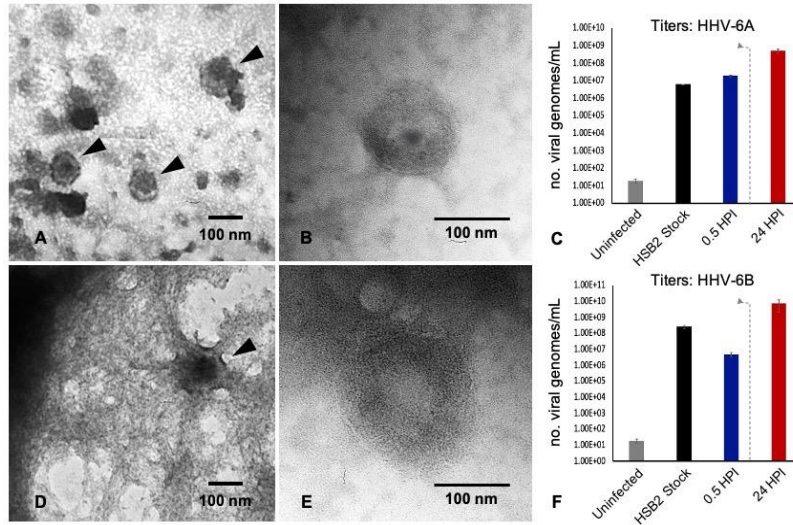ant from cell lysate; (D) HHV-6B virions in a cell; (E) HHV-6B virions in cell-free filtered supernatant. qPCR titer methods show productive virus infection for: (C) HHV-6A and (F) HHV-6B. Uninfected cells show negligible amplification of an HHV6-specific marker (i.e., U22 gene). After 30 min post-infection HHV6 is still present. After a wash at 2 HPI (dashed line) and 22 h incubation (24HPI), titers increase indicating production of progeny virions at densities greater than present immediately after inoculation.

Together, data from TEM, immunofluorescence (using an anti-gB fluorescent antibody system), and qPCR-based quantification of virus titers at different time points during infection provide convincing evidence that both neurons and glia are susceptible to HHV-6A and HHV-6B and result in productive viral infections. Furthermore, both TEM and immunofluorescence data indicate that infection of dHNSCs by either HHV-6A or HHV-6B results in viral-induced CPEs, which manifest as disturbances to cell shape, size, viability, and distribution on culture plates. CPEs often present in two phases: cell aggregation (with notable cell death) and detachment from the culture surface.
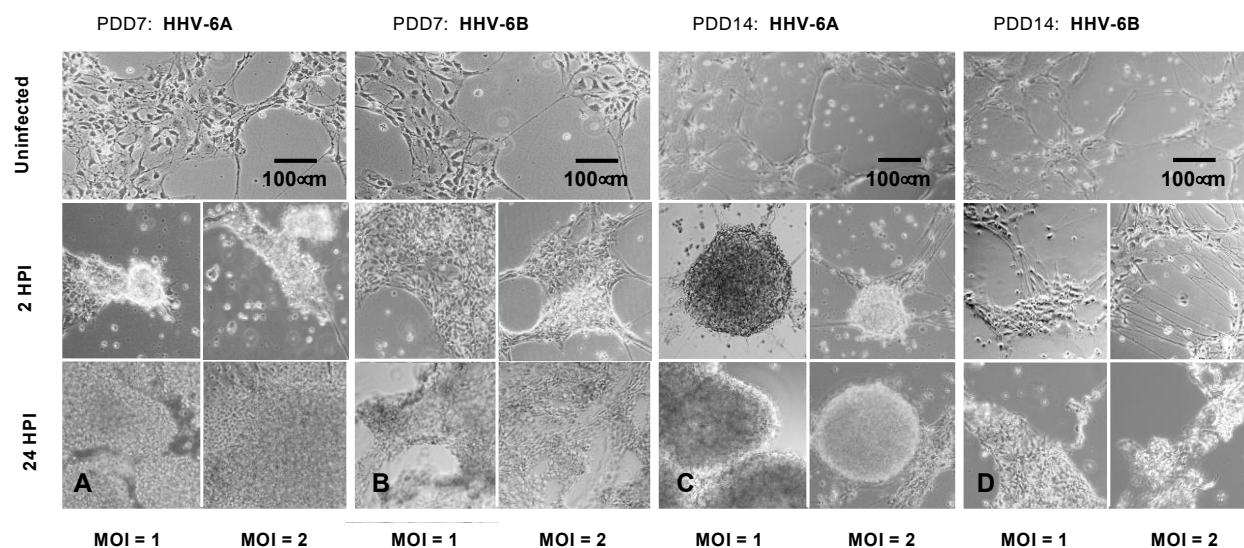
Figure 2-4– Light microscopy of HHV6-induced cytopathic effects (CPEs) on differentiated HNSCs at PDD 7 and 14. (A) Uninfected cultures of HNSCs at PDD7 show healthy cells adhering to the plate surface (top). After two hours post-infection (2HPI) at MOIs = 1, 2 (middle, left, and right, respectively) with HHV-6A, cells begin to aggregate, and at 24HPI with HHV-6A at MOIs = 1, 2 (bottom, left, and right) there is high-density clumping and cell detachment. (B) Uninfected cultures of HNSCs at PDD7 show healthy cells adhering to the plate surface (top). After 2HPI with HHV-6B at MOIs = 1, 2 (middle, left, and right), cells begin to aggregate, and at 24HPI with HHV-6B at MOI = 1, 2 (bottom, left, and right), there is a higher-density aggregation. (C) At PDD14, uninfected healthy cells persist (top); however, at 2HPI at MOIs = 1,2 (middle, left, and right), infection with HHV-6A results in high-density cell aggregation, and at 24HPI, rampant cell death and detachment are observed (bottom, left and right). (D) At PDD14, uninfected cells persist (top); however, HHV-6B infection at MOIs = 1,2 for 2 HPI results in lower-density cell aggregation (middle, left, and right) with higher-density clumping occurring at 24HPI (bottom, left, and right)

Although there is a notable aggregation of cells in both HHV-6A and HHV-6B infected cell cultures (2HPI, MOI=1, or MOI=2), HHV-6A infected cultures produce higher density clumps at

earlier time points for both PDD7 and PDD14 cultures (Fig. 4A and 4C, *middle row*). By 24 HPI, HHV-6A infections yield high-density detached clumps floating in culture (Fig. 4A and 4C, *bottom row*). Although HHV-6B infections induce cell aggregation, cells appear more resistant to forming detached high-density spherical clumps when compared to HHV-6A infections at 2 HPI and 24 HPI (Fig. 4B and 4D). In some trials, HHV-6B infected cultures featured cells that appear to retain morphological integrity at 2HPI (Fig. 4D). These data suggest that the severity and time-course of CPEs may differ between HHV-6A and HHV-6B infections (Fig. 4)
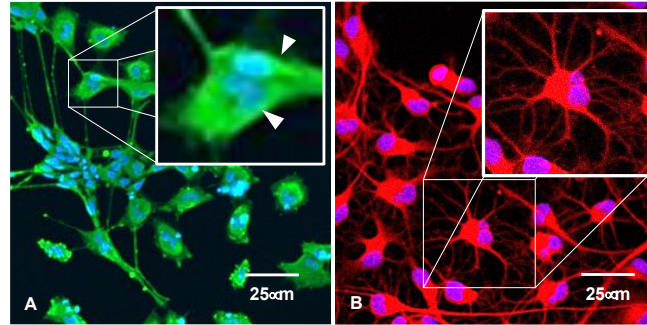
Figure 2-5 -Immunofluorescence suggests syncytia. (A) HHV-6A infection in HNSCs results in syncytia formation as indicated by cell membrane fusion and multinucleated cells (arrows). (B) Uninfected culture shows individual well-bounded dHNSC membranes and the absence of any cell aggregation that would suggest syncytia-like formations.

To determine whether clumping of cellular biomass during the course of HHV6 infection is simply aggregation or *bona fide* viral-induced syncytia formation, fluorescence microscopy was used to detect morphological features characteristic of syncytia (Fig. 5). Results indicate that prior to gross detachment from the culture surface (i.e., 0-2 HPI), morphological features consistent with syncytia occur, including cell fusion and formation of multi-nucleated supercells (Fig. 5A; *arrows*). Syncytia formation was notable in HHV-6A infection. However, no discernable syncytia formation was observed during HHV-6B infection. In uninfected cultures, cells with robust arborized neurites and a single nucleus will persist for weeks (Fig. 5B) and have slightly larger, well-defined somas.

2.3.3   Neurite retraction and morphometrics (HHV-6A versus HHV-6 infected cells)

Initial manual tracing and use of a machine-learning platform (Trainable Weka Segmentation 7) on images taken with a light microscope result in neurite and soma boundary definitions in a pseudo-fluorescence format (Fig. 6A). A pixel-by-pixel assessment by image analysis software

(e.g., Neural Circuit Tracer or NeuronCytoII) produces neuronal reconstructions, from which measurements can be taken including neurite lengths and surface areas of cell soma (Fig. 6B). Morphometric analyses indicate that average neurite length in differentiated HNSCs increases between the time of inoculation (t_0) to 2 hours post-infection (HPI) followed by a precipitous decline (retraction) between 2 HPI and 24 HPI for HHV-6A and HHV-6B infected cells at MOI=1. At MOI=2, the impact on average neurite length is more profound, with a decline from t_0 to 2 HPI in both HHV-6A and HHV-6B infected cell cultures and a precipitous decline from 2 HPI to 24 HPI. Data for MOI=2 suggest that HHV-6B infection results in more significant neurite retraction than HHV-6A. For MOI=2, ~20% (N=39) and ~35% (N=14) decreases in average neurite length for HHV-6A and HHV-6B, respectively, are observed (Fig. 6C). Even at MOI=1, HHV-6B tends to attenuate neurite extension to a greater extent than HHV-6A (N=32, N=20). The magnitude of CPE severity after infection of HNSCs with the virus appears to be MOI-dependent (Fig. 4, MOI = 1 versus MOI = 2). Fewer but notably long neurites extend as high-density cell clumps start to form. (These analyses were conducted by undergraduate student 'Jerry Wu' in the summer program)
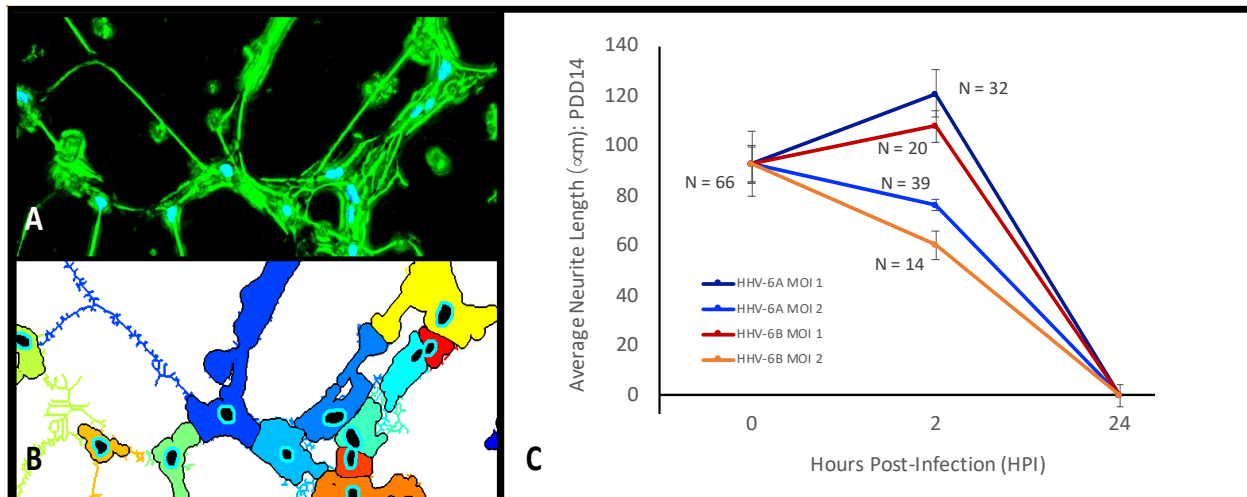
Figure 2-6– Changes in average neurite length and neuronal signaling during the course of an HHV6 infection. (A) Pseudo-fluorescence image generated by Trainabler Weka Segmentation 7 highlights soma boundaries and neurites of neurons from light microscopy images processed via a NeuronJ plug-in to the ImageJ software package. (B) Neuron CytoII software generates neuron and neurite reconstructions for detailed morphometric measurements. (C) Morphometric analysis of average neurite length (ANL) at 2 hours post-infection (HPI) and 24HPI for HHV-6A and HHV-6B infected cells indicate that at MOI = 1, neurites continue to extend from the time of inoculation (t0) through 2HPI for both HHV-6A and HHV-6B infected cells, however, by 24 HPI neurite retraction, cell death, and cell detachment from the culture surface results in insignificant neurites extension. At MOI = 2, there is a decrease in ANL between t0 and 2HPI, with HHV-6B showing more than a 35% decrease in ANL while HHV-6A results in a more modest decrease in ANL (~20%). (This analysis conducted by under graduate student Jerry Wu)

2.3.4 Both glutamatergic and dopaminergic cells are susceptible to either HHV-6A or HHV-6

To determine if either HHV-6A or HHV-6B preferentially infects select neuronal neurotransmitter phenotypes, differentiated neurons were co-labeled with neurotransmitter-specific antibodies.
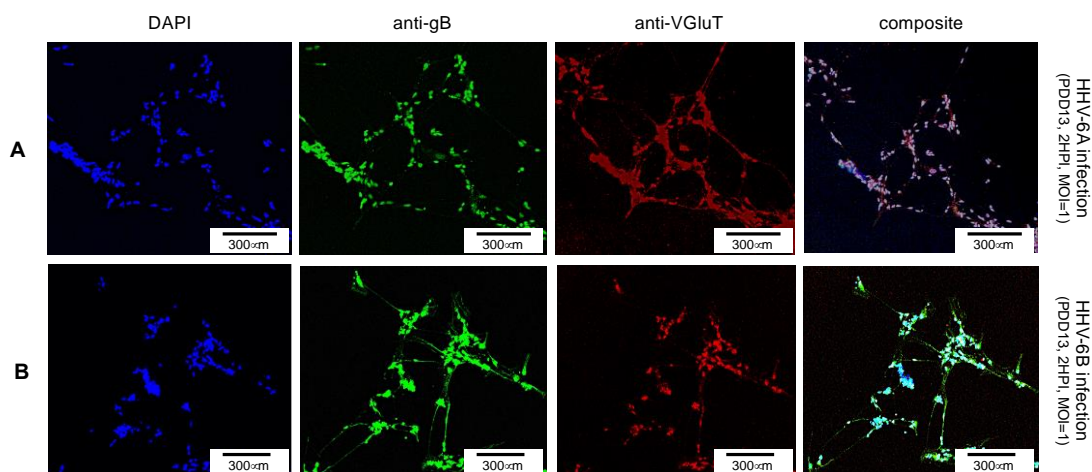
Figure 2-7 -Fluorescence microscopy images of differentiated human neural stems cells (dHNSCs) treated with immunofluorescent antibodies and a fluoro-dye at PDD13: Glutamatergic Neurons. VGluT1-positive dHNSCs at PDD13 (2 HPI, MOI=1) shown (from left to right) by DAPI staining and anti-gB, and anti-VGluT immunofluorescence (with composites) indicate that gB (green) colocalizes with VGlut (red) in DAPI stained (blue) cells for both HHV-6A (row A) and HHV-6B (row B) infected cultures, suggesting susceptibility of glutamatergic neurons to both viruses. (Results were consistent across 6 replicate trials).

For glutamatergic cells, an anti-VGluT1 fluorescent antibody system was used to target the vesicular glutamate transporter (VGluT1), a characteristic protein found in glutamatergic neurons. Simultaneous staining with DAPI and use of the anti-gB fluoroprobe show that VGluT1-positive cells coincide with anti-gB fluorescence signals in dHNSCs infected with HHV-6A (Fig. 7, row A) or HHV-6B (Fig. 7, row B). This reveals that both roseoloviruses can infect of glutamatergic cells. Of cells in mixed cultures identified as glutamatergic (i.e., VGluT1-positive), 96% (N=6, $p<0.05$) and 73% (N=6, $p<0.05$) were gB-positive in HHV-6A and HHV-6B infections, respectively.

For dopaminergic cells, an anti-dopamine (anti-DA) fluorescent antibody system was used to target dopamine directly. Co-staining with DAPI and co-labeling with anti-gB and anti-DA, fluorescence microscopy shows a co-localization of DAPI, anti-gB, and anti-DA signals (Fig. 8).

This suggests that dopaminergic neurons are susceptible to infection by HHV-6A (Fig. 8, row A) and HHV-6B (Fig. 8, row B). Of all cells in mixed cultures labeled dopaminergic (i.e., DA-positive), 89% (N=6, $p<0.05$) and 77% (N=6, $p<0.05$) were gB-positive in HHV-6A and HHV-6B infections, respectively. This demonstrates that both viruses can infect of dopaminergic neurons.

Roseolavirus appears to be widely distributed throughout infected cells. In both VGluT1-positive and DA-positive cells, anti-gB fluorescence was seen within neurites as well as cell soma.

Figure 2-8 Fluorescence microscopy images of differentiated human neural stem cells (dHNSCs) treated with immunofluorescent antibodies and fluoro-dye (DAPI) at PDD7: Dopaminergic Neurons. DA-positive dHNSCs at PDD7 (2HPI, MOI = 1) shown (from left to right) by DAPI staining and anti-gB and anti-DA immunofluorescence (with composites) indicate that gB (green) colocalizes with dopamine (red) in DAPI stained (blue) cells for both HHV-6A (row A) and HHV-6B (row B) infected cultures, suggesting susceptibility of dopaminergic neurons to both viruses. . (Results were consistent across six replicate trials).

2.3.5   Neither HHV-6A nor HHV-6B appears to infect GAD67-positive cells (GABAergic neurons)

To determine whether neurons that synthesize gamma-aminobutyric acid (GABA) were susceptible to infection by HHV-6A or HHV-6B, a fluorescence antibody system against GAD67, a glutamate decarboxylase that is responsible for the overwhelming majority (>90%) of GABA synthesis in the brain, was employed. (GABA is the major inhibitory neurotransmitter in the CNS). Cultures co-stained with DAPI and co-labeled with anti-GAD67 and the anti-gB fluoroprobes failed to show infection of GAD67-positive differentiated HNSCs by either HHV-6A (Fig. 9, row A) or HHV-6B (Fig. 9, row B). Given the unexpected results, multiple time points were examined. However, anti-gB fluorescence was not detected at PDD7 or PDD14 (Fig. 9) or under various MOIs (i.e., MOI=1 and 2). These experiments were repeated multiple times with the same results. For one single trial (out of 5) where differentiation of HNSCs was driven toward GABA-producing cells, a few anti-gB fluorescence patches were observed in HHV-6B infected cultures (Fig. 10).
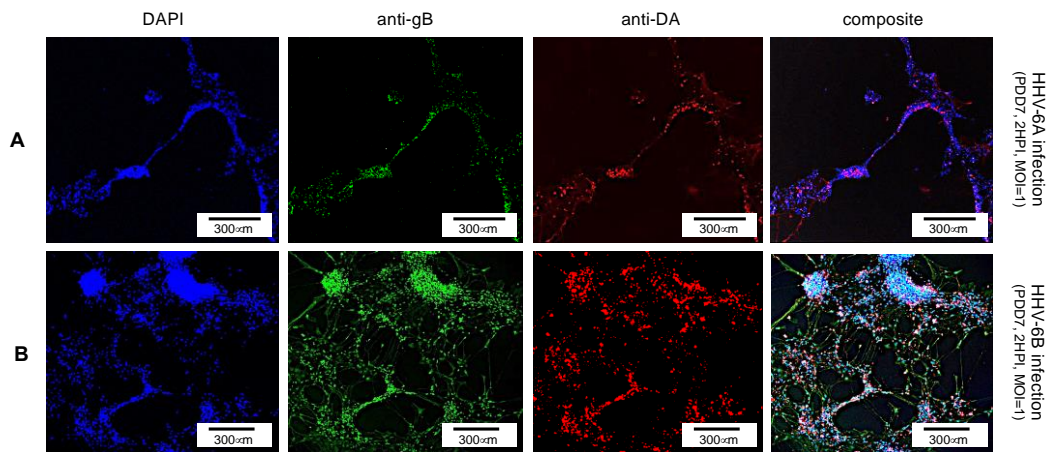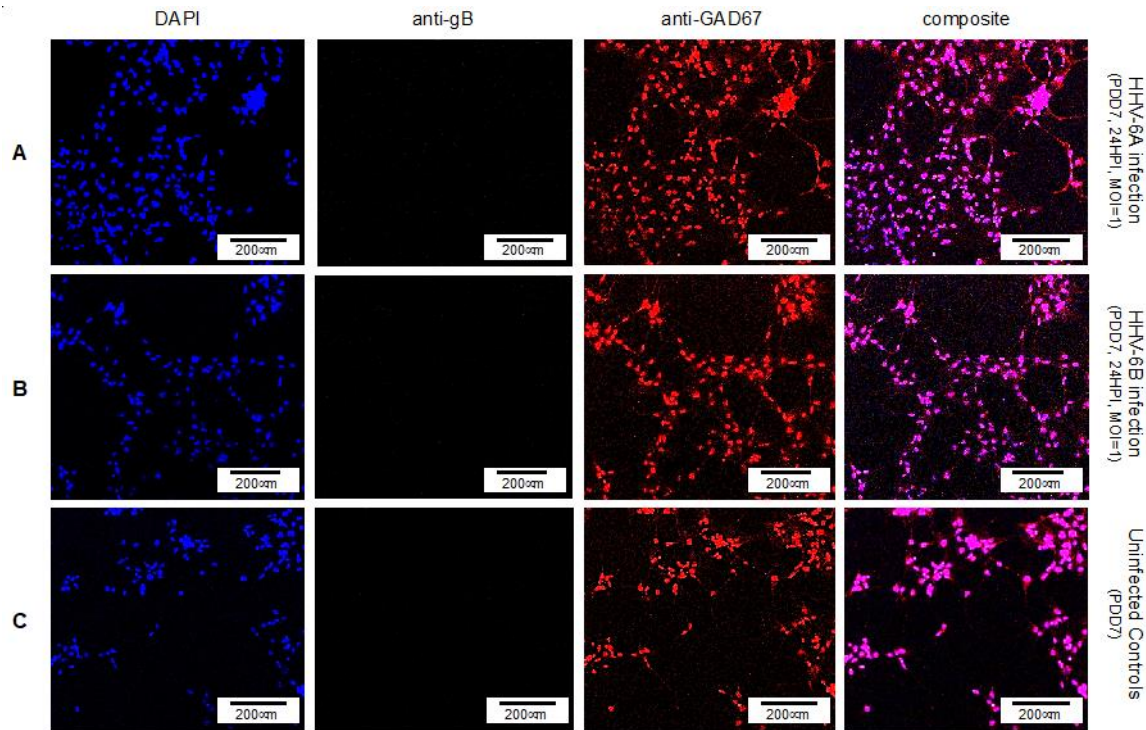
Figure 2-9- Fluorescence microscopy images of differentiated human neural stems cells (dHNSCs) treated with immunofluorescent antibodies and a fluoro-dye (DAPI) at PDD7: GABAergic Neurons. GAD67-positive dHNSCs at PDD7 (2HPI, MOI=1) shown (from left to right) by DAPI dye and anti-GAD67 immunofluorescence (with composites) indicate that gB (green) immunofluorescence does not colocalize with GAD67 (red) in DAPI stained (blue) cells for both HHV-6A (row A) and HHV-6B (row B) infected cultures, suggesting GABAergic neurons are not susceptible to either virus. (Results consistent across 6 replicates).

Initial indications suggested that perhaps HHV-6B can indeed infect GAD67-positive cells. However, upon detailed analysis of immunofluorescence data, the colocalization of the DAPI and anti-gB signals (Fig. 10: A1-D1 and A2-D2, respectively) do not coincide with anti-GAD67 signals, indicating that the anti-gB fluorescence emanates from nearby cells in these mixed cultures. Moreover, for many of the anti-GAD67 fluorescence, there was no overlap with DAPI, suggesting that these could be fluorescence signals from GABA-rich afferents (*see* Fig. 10: A3, B3, C3, D3). Data indicate that >90% of cells were GAD67-positive in HHV-6A and HHV-6B

infected cultures (N=6), yet there was no evidence of coincidence between anti-GAD67 and anti-gB fluorescence.
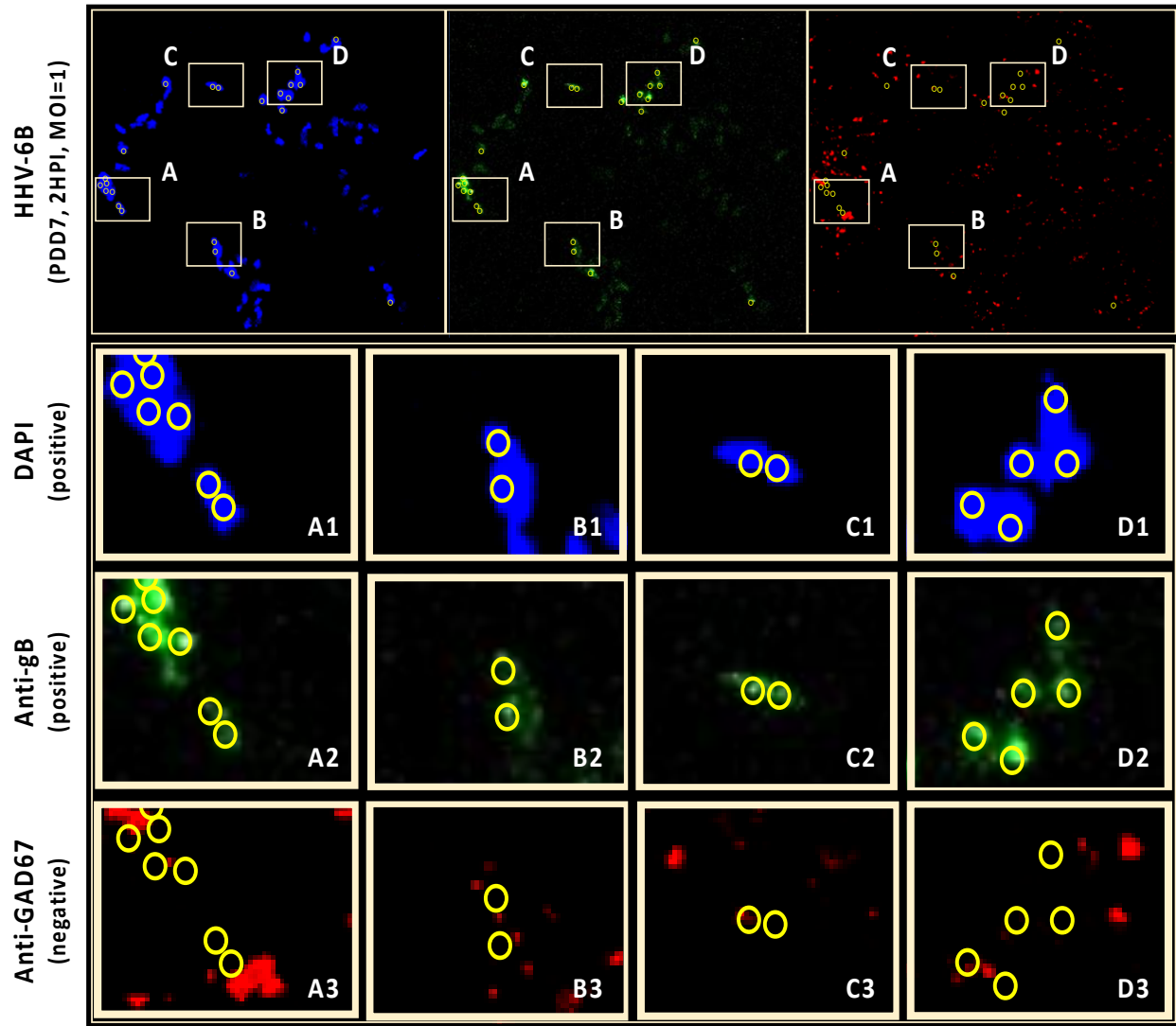
Figure 2-10– Anti-gB/DAPI fluorescence does not colocalize with GAD67-positive cells in mixed cultures. DAPI microscopy images of immunofluorescence and fluorescence staining of differentiated HNSCs at PDD7, MOI = 1, 2HPI challenged with HHV-6B. Out of multiple trials, only one anti-GAD67 positive culture displayed an anti-gB fluorescence signal indicating possible infection of GABA-containing neurons (top). However, upon closer examination of anti-gB cell clusters (regions A-D), it appears that DAPI positive cells (rows A1-D1) and anti-gB positive (rows A2-D2) cells are anti-GAD67 negative (row A3-D3) providing further evidence for GABAergic

neuron resistance to HHV-6 infection. DAPI/anti-gB positive fluorescence is likely from adjacent glial cells or other neuronal neurotransmitter phenotypes in the mixed culture.

2.4 Conclusions

The work performed demonstrates that: (1) both glia cells and neurons are susceptible to infection by HHV-6A or HHV-6B; (2) VGluT1-positive cells (i.e., glutamatergic cells) are susceptible to infection by HHV-6A or HHV-6B; (3) DA-positive cells (i.e., dopaminergic cells) are susceptible to infection by HHV-6A or HHV-6B; (4) GAD67-positive cells (i.e., GABAergic cells) appear to be resistant to infection by HHV-6A or HHV-6B; (5) HHV-6A induces more severe cytopathic effects on differentiated human neural stems cells than HHV-6B for the same time-point post-infection at the same MOI and other equivalent culture conditions.

The cellular and molecular basis for the differences in cell tropism and CPEs is not known. In the subsequent chapter, cellular responses to HHV-6A versus HHV-6B will be explored using immunofluorescence and quantitative polymerase chain reaction (qPCR) methods.

2.4.1 HHV-6A and HHV-6B infect both neurons and glia with different levels of cytopathology

Results from immunofluorescence data demonstrate that both HHV-6A and HHV-6B can infect glia and neurons derived from the differentiation of human neural stem cells (see Figs. 1 and 2). These data are consistent with prior reports demonstrating that HHV6 can infect astrocytes(Fotheringham et al., 2008) and neurons – namely, cerebellar Purkinje cells(Prusty et al., 2018). Results from qPCR and TEM clearly indicate that productive infection of dHNSCs occurs (Fig. 3) when either HHV-6A or HHV-6B is perfused into dHNSC cultures at an MOI of 0.5, 1.0, or 2.0. [Note: MOI is used here to describe the ratio of viral genomes to cells at the

initiation of infection]. Light microscopy and viable cell counts indicate differential impacts of HHV-6A versus HHV-6B on cell cultures (PDD7, 2HPI, MOI=1). Specifically, it appears that HHV-6A induces more severe cytopathic effects that HHV-6B for the same day post-differentiation and post-infection time-point (Fig. 4). For MOIs examined, both HHV-6A and HHV-6B induce cell aggregation and detachment from the surface substrate; however, the magnitude of cell clumping and detachment is greater in HHV-6A infected cultures at both PDD7 and PDD14 (2HPI and 24HPI). Indeed, cells with intact processes are still visible in HHV-6B infected cultures even at MOI=2 at PDD14 (see Fig. 4). Moreover, bona fide syncytia formation was only observed during HHV-6A infection (see Fig. 5). These results suggest that HHV-6A infection may be more detrimental to cell culture than infection with HHV-6B. This is consistent with prior work suggesting that HHV-6A is more virulent in glia(De Bolle, Naesens, et al., 2005).

2.4.2   HHV-6A and HHV-6B infect vGluT[+] and DA^{+} cells, but neither virus infects GAD67^{+} cells

Our results and prior work regarding HHV-6A and HHV-6B cell tropism indicate that HHV6 infects nerve cells(Albright et al., 1998; De Bolle, Naesens, et al., 2005; De Filippis et al., 2006; Donati et al., 2003). An early study showed that HHV-6A and HHV-6B could infect glial cells(Fotheringham et al., 2008). A recent study demonstrated HHV-6A and HHV-6B infections in neurons(Prusty et al., 2018). This latter study only showed HHV-6A and HHV-6B infection in Purkinje cells, which are unique. Although this prior work showed that neurons are susceptible to HHV6 infection, our data provide additional details regarding cell tropism for specific neuronal neurotransmitter phenotypes. Immunofluorescence microscopy shows that VGluT1-positive cells (i.e., glutamatergic neurons) and DA-positive cells (i.e., dopaminergic neurons) are susceptible

to either HHV-6A or HHV-6B (Figs. 7 and 8). Although glutamatergic and dopaminergic cells are susceptible to both viruses, infection assays failed to demonstrate that GAD67-positive cells (i.e., GABAergic neurons) were susceptible to either virus. We were initially skeptical of these results since the study showed that Purkinje cells, which are GABAergic, are susceptible to HHV-6A and HHV-6B. However, repeated trials using immunofluorescence supported by qPCR suggest that GABA neurons derived from dHNSCs are not susceptible to either virus (see Fig. 9). In one infection trial with HHV-6B, a sparse anti-gB fluorescence was observed in mixed cultures with GAD67-positive cells (Fig. 10, top row, middle panel). However, with higher magnification and more detailed analysis, anti-GAD67 emissions do not overlap with anti-gB/DAPI fluorescence. This suggests that HHV-6B is likely infecting cells adjacent to GABA neurons in mixed cultures or anti-gB signals afferents from other cell types on GABAergic cells (e.g., axonal-somatic inputs).

2.4.3   Implications of results for current models of HHV-6 induced epileptogenesis

Several models are proposed as potential mechanisms by which HHV-6 induced seizures can lead to epilepsy (i.e., epileptogenesis). Although neural encephalitis may emerge from primary HHV-6 infections leading to seizures (Bartolini, Theodore, Jacobson, & Gaillard, 2019; Howell et al., 2012; Vinters, Wang, & Wiley, 1993), sub-inflammatory mechanisms have also been proposed. For example, there is some in vitro evidence to suggest that HHV-6 infection of astrocytes can lead to dysfunction in glutamate reuptake from the synapse, leading to hyperexcitation of glutamatergic pathways and thus seizure(Crawford et al., 2007; Eid et al., 2016). Beyond this glutamate reuptake dysfunction hypothesis, other studies have suggested that reactivation of HHV-6 from latency may result in lysis of glutamatergic cells resulting in excess release of glutamate into neuronal circuits associated with seizure induction (e.g., mesial

temporal lobe neural networks). This has been described as an excitotoxicity model(Beal, 1992; Bekenstein & Lothman, 1993; Wang & Pellett, 2007; Yao, Crawford, Komaroff, Ablashi, & Jacobson, 2010). If results observed in cultured dHNSC are generalizable to in vivo conditions, then a glutamatergic excitotoxicity model would be supported by gross glutamatergic cell loss during HHV-6A infection.

Another hypothesis is that GABAergic interneurons, which modulate glutamatergic pathways, could be selectively targeted by HHV-6A or HHV-6B. Disruption of the inhibitory modulation of glutamatergic neurons would, in turn, lead to excess glutamate release and subsequent seizure. If our results regarding a lack of susceptibility of GABAergic neurons to HHV6 are generalizable to in vivo conditions, then this inhibitory (inter)neuron dysfunction hypothesis could be ruled out. Alternatively, HHV6-induced epileptogenesis may involve more than one of these proposed models or another yet to be described mechanism. For example, cholinergic pathways from the peduncular pontine nuclei (PPN) or other tracts may also contribute to seizure induction by hyperexciting glutamatergic targets or inhibiting modulating interneurons. Finally, it is also necessary to explore the impacts of roseolovirus infection on neuronal and neural network signaling. This is the subject of ongoing research in our lab.

2.5   Materials and methods

2.5.1   Cell culture

Culture vessels (i.e., T75 flasks and 8-well microscope chamber slides; Thermofisher Scientific) were coated with CELLStartTM surface substrate (Gibco, Life Technologies Corporation) per supplier protocol. In serum-free medium (SFM) [KnockoutTM DMEM/F-12, 20 ng/mL FGF-2/EGF, 2mM GlutaMAXTM-I, and 2% v/v StemProTM Neural supplement], NIH-approved H9-derived human embryonic stem cells (hESCs) were plated and expanded as a monolayer in CELLStartTM coated vessels. The cultures were maintained at 37°C in a humidified incubator (with 5% CO2). Cells were passaged every 7 days using an accutase cell detachment solution (Sigma-Aldrich) and re-plating at a surface density of 5 x 104 cells/cm2. Using an automated cell counter (Bio-Rad) and Trypan Blue (Thermofisher Scientific), viable cell counts were determined for re-plating cells. Upon re-plating, different media options were used to induce differentiation along desired paths. For example, to facilitate differentiation toward neuron-dense mixed cultures, a seeding density of 2.5 x 104 cells/cm2 was used with a minimal media (MM) [KnockoutTM DMEM/F-12, 2mM GlutaMAXTM-I, and 2% StemProTM Neural Supplement]. Cells were maintained in differentiating conditions for 15-18 days with fresh media change-out every 3-4 days.

2.5.2   Virus preparation

Frozen stocks (-195°C) of HHV-6A strain GS-infected HSB2 cells and HHV-6B strain Z29-infected MOLT-3 cells (courtesy NIH) were thawed and used to infect uninfected HSB2 and MOLT-3 cells. Specifically, 10^6 HHV6-infected cells were mixed with uninfected cells at a ratio of 1:10 in a T150 flask (Thermofisher Scientific) and incubated at 37°C for 2 hr. (5 mL of

media). After 2 hr of incubation fresh media was added (5 mL), and the cells were incubated again at 37°C. Using a light microscope, the culture was checked periodically. When cytopathic effects (CPEs) were noted in more than 80% of cells, the cell suspension was harvested. Aliquots were stored in liquid nitrogen (-195°C) for use in infection assays. Alternatively, cell-free virus suspension was prepared by sonicating cell suspension on ice and centrifuging the lysate at 3500 rpm for 1 hr to pellet cell debris while maintaining virus particles in suspension. The supernatant was extracted and filtered through a 0.45µm filter to remove any remaining cell debris. The virus-containing filtrate was centrifuged at 25,000 rpm at 4°C for 3 hr to pellet the virus. Supernatant was removed, and the virus pellet was resuspended in cold media and stored at -80°C for use in cell-free virus infection assays or for transmission electron microscopy. Virus titers were determined using qPCR.

2.5.3 Transmission electron microscopy (TEM) for cell-free virus

Transmission electron microscopy (TEM) was used for three purposes. First, TEM was used to verify the presence of intact, fully assembled virions from HSB2 and MOLT-3 host cells used for virus storage and propagation. Second, TEM was used to demonstrate the presence of HHV6 virus particles in differentiated HNSCs. Third, TEM was used to validate the presence of virus for qPCR-based titers from storage cells or differentiated HNSCs. For cell-free virus samples, the aforementioned preparation via sonication (or, alternatively, freeze-thaw cycles) was followed by a concentration of virus suspensions (i.e., filtered lysates) using 30kDA MWCO spin concentrator (Sigma-Millipore). From the retentate, ~5µL of concentrated viral suspension was spotted onto a formvar-coated copper grid and incubated for 10 min in a humidity chamber. The sample was then gently rinsed and negatively stained with a 2% solution of uranyl acetate for 30 sec before the excess solution was wicked off of the grid and allowed to air dry for 1 hr.

Samples were placed on grids, and after 2 to 10 minutes, 2% uranyl acetate was added to the grid. Grids were imaged with a Hitachi H-7100 TEM at 75 kV. Images were captured at 60,000–200,000X magnification.

2.5.4 Transmission electron microscopy (TEM) for infected cells

TEM was also used to image virus particles associated with host cells. These included both virus storage cells (HSB2 and MOLT-3 cells) and differentiated HNSCs infected with either HHV6 virus. For virus-infected storage cells in or for virus-infected monolayers of differentiated HNSCs, cells were fixed with a 4% paraformaldehyde (PFA) solution. The samples were place on grids and then gently rinsed and negatively stained with a 2% solution of uranyl acetate. Samples were incubated for 2 hr at 4°C before rinsing with distilled water and wicking off the excess solution from the grid, and allowed to air dry for 1 hr. After air drying for 2 hr., samples were imaged with a Hitachi H-7100 TEM at 75 kV. Images were captured at 60,000– 200,000X magnification. Regions of the grid that showed virions blebbing from membrane or virus particles within the intracellular space were targeted for imaging. Detachment of HNSCs from the surface substrate was required to capture co-localization of virus particles within intact cells.

2.5.5 Light microscopy

The infected cultures were monitored daily via light microscopy to monitor morphological changes. (In each experiment, uninfected cultures served as a control). Light microscopy images were taken from dHNSCs at PDD 7 and PDD 14 at 2 hours post-infection (HPI) and 24 HPI10 using an upright microscope (Primovert, Zeiss) equipped with a color camera (AxioCam 105, Zeiss). Dozens of cells were captured in each image from randomly chosen fields of view for each culture.

2.5.6   Morphometric Analyses

Using light microscopy and an image analysis pipeline that includes a machine learning algorithm to enhance calls on neurite extension, node formation, and other morphometric parameters, cell morphology changes are monitored over the course of infection and at different infection states. Using the NeuronJ plug-in to the ImageJ software package and a machine-learning algorithm, the initial manual tracing of neurons from light microscopy images can be enhanced. This first part of the workflow compares pixel intensity on neurites (and soma boundaries) with adjacent pixel neighborhoods. Using the machine-learning algorithm, Trainabler Weka Segmentation 7, the contrast between nerve cell features and background is enhanced, yielding pseudo-fluorescence images from light microscopy images. Standard tools such as Neural Circuit Tracer or NeuronCytoII are then employed to generate reconstructions of nerve cells allowing for morphometric analysis without fixing cells for traditional immunofluorescence. This workflow requires minimal high-performance computing time and will enable observations and quantification of morphological parameters in real-time while producing quality images (see Fig. 6, panels A-C).

2.5.7   Immunofluorescence and fluorescence microscopy

Immunofluorescence was conducted via a co-labeling approach (two antibody systems per trial) along with the nuclear dye 4,6-diamidino2-phenylindole dihydrochloride (DAPI). The following fluorescence antibody systems (primary antibody/secondary antibody) were used in select pairs: mouse anti-gB (HHV6 envelope glycoprotein gB)/donkey anti-mouse IgG-Alexa Fluor 488; chicken anti-GFAP (Glial Fibrillary Acid Protein)/donkey anti-chicken IgG-Alexa Fluor 680; rabbit anti-βIII tubulin (neuron-specific microtubule protein)/donkey anti-rabbit IgG-Alexa Fluor 568; goat anti-VGluT (vesicular glutamate transporter protein)/donkey anti-goat IgG-Alexa

Fluor 555; chicken anti-GAD67 (glutamate decarboxylase 67)/donkey anti-chicken IgG-Alexa Fluor 680; and, rabbit anti-DA (dopamine)/donkey anti-rabbit IgG-Alexa Fluor 568. The anti-gB antibody (courtesy NIH AIDS reagent program) and fluorescent secondary indicate the presence of HHV6 virus and, when co-localized with other immunofluorescence markers, demonstrate infection in select cell types (i.e., neurons versus glia or distinct neuronal neurotransmitter phenotypes). Signal for anti-gB is usually color-coded green in alignment with emissions during image analysis. Signal for the anti-βIII tubulin fluorescent antibody system (Sigma-Aldrich) is typically color-coded red in alignment with emissions when anti-gB is co-labeled but may also be color-coded green in uninfected controls. Signal for the anti-GFAP fluorescent antibody system (Sigma-Aldrich) is typically color-coded red in alignment with emissions but may also be color-coded green in uninfected controls or when used as a co-label for distinguishing between GFAP-positive cells and βIII tubulin-positive cells in the same image. Signal for anti-VGluT (Abcam), anti-GAD67 (Abcam), and anti-DA (EMD Millipore) fluorescence are typically color-coded red to distinguish neuronal neurotransmitter phenotype from any anti-gB signal (green). All experimental trials used DAPI (blue color code) to locate nuclei of all cells in the mixed cultures regardless of cell type. For all immunofluorescence trials, HNSCs were fixed with 4% PFA in Dulbecco's phosphate buffer solutions (DPBS), then rinsed (3X) with DPBS. Blocking solution (5% donkey serum, 0.1% triton in DPBS) was added for 30 min. at room temperature (RT) after which primary antibodies (abs) were applied. Cells were then incubated for 24 hrs. followed by a series of rinses (3X) with DPBS and then application of secondary antibodies and further incubation. Another series of rinses (3X) with DPBS was followed by the application of DAPI (0.2 nM) and a 20 min incubation at RT. The plates were subjected to a final rinse in DPBS and staged within the confocal fluorescent microscope (Leica). Images were taken using

10X magnification to view the distribution of fluorescent signals across the plates. In infecdted cultures, immunofluorescence was performed at multiple time-points during the differentiation phase (PDD7 and PDD14 preferred) and at several time-points after introduction of viral inocula (e.g., 2HPI and 24HPI). Images for each fluorescent signal were captured, and then images were overlayed using image analysis software to generate composite images.

2.5.8 Quantitative polymerase chain reaction (qPCR)

For quantitative polymerase chain reaction (qPCR)-based virus titers from both storage cell lines (i.e., HSB2 and MOLT-3 cells) as well as infected differentiated HNSCs, the HHV6-specific U22 gene was targeted. Using the following primers (Collot et al., 2002): 397F (5′-TCG AAA TAA GCA TTA ATA GGC ACA CT-3′) and 493R (5′-CGG AGT TAA GGC ATT GGT TGA-3′) – a 99bp fragment of the U22 gene was amplified from viral DNA extracted from infected cell cultures. Amplification was performed using a Rotor-Gene Q real-time fluorescence detector thermocycler (Qiagen) programmed as follows: 94°C for 6 min; followed by 40 cycles of 94°C for 30 sec, 53°C for 30 sec, 72°C for 45 sec; and then a final holding condition of 72°C for 7 min. Verification of the appropriate fragment size (and run quality) was checked via gel electrophoresis. DNA concentration was determined using a micro-volume spectrophotometer (Denovix). The number of viral genomes for each sample was determined by comparing results to a standard curve.

To prepare standards for qPCR analyses, the following procedure was performed for each virus (i.e., HHV-6A and HHV-6B): one copy of the U22 target sequence was cloned into a commercial vector using a TOPO PCR Cloning Kit (Invitrogen) and transformed into competent E. coli. Enrichment of clones was followed by plasmid purification using the QIAprep Spin Miniprep Kit (Qiagen). The resulting plasmid DNA yield was measured by absorbance

spectroscopy (OD260nm). PCR is then employed to amplify the gene of interest (i.e., U22) from the plasmid preparation. PCR product yield is quantified using the Denovix micro-volume spectrophotometer, and then a sample is diluted down to 1 ng/µL, which corresponds to a fragment copy number of 9.216×10^9. From this, subsequent dilutions (10^{-1} through 10^{-9}) are prepared in triplicate. Next, qPCR is used to amplify fragments from these serial dilutions, and the standard curve is generated. For all qPCR trials, 10µL SYBR® Green (Life Technologies, Foster City, USA), 1 µL of unknown DNA sample, 50 nM of forwarding primer, and 50 nM of reverse primer were used in 20 µL total reaction volumes.

2.6 Reference

Achour, A., Malet, I., Le Gal, F., Dehée, A., Gautheret-Dejean, A., Bonnafous, P., & Agut, H. (2008). Variability of gB and gH genes of human herpesvirus-6 among clinical specimens. *Journal of medical virology, 80*(7), 1211-1221.

Adams, M. J., & Carstens, E. (2012). Ratification vote on taxonomic proposals to the International Committee on Taxonomy of Viruses (2012). *Archives of virology, 157*(7), 1411-1422.

Albright, A. V., Lavi, E., Black, J. B., Goldberg, S., O'Connor, M. J., & Gonzalez-Scarano, F. (1998). The effect of human herpesvirus-6 (HHV-6) on cultured human neural cells: oligodendrocytes and microglia. *Journal of neurovirology, 4*(5), 486-494.

Bartolini, L., Theodore, W. H., Jacobson, S., & Gaillard, W. D. (2019). Infection with HHV-6 and its role in epilepsy. *Epilepsy research, 153*, 34-39.

Beal, M. F. (1992). Mechanisms of excitotoxicity in neurologic diseases. *The FASEB journal, 6*(15), 3338-3344.

Bekenstein, J. W., & Lothman, E. W. (1993). Dormancy of inhibitory interneurons in a model of temporal lobe epilepsy. *Science, 259*(5091), 97-100.

Boutolleau, D., Duros, C., Bonnafous, P., Caïola, D., Karras, A., De Castro, N., . . . Agut, H. (2006). Identification of human herpesvirus 6 variants A and B by primer-specific real-time PCR may help to revisit their respective role in pathology. *Journal of Clinical Virology, 35*(3), 257-263.

Crawford, J. R., Kadom, N., Santi, M. R., Mariani, B., & Lavenstein, B. L. (2007). Human herpesvirus 6 rhombencephalitis in immunocompetent children. *Journal of child neurology, 22*(11), 1260-1268.

De Bolle, L., Naesens, L., & De Clercq, E. (2005). Update on human herpesvirus 6 biology, clinical features, and therapy. *Clinical microbiology reviews, 18*(1), 217-245.

De Filippis, L., Foglieni, C., Silva, S., Vescovi, A., Lusso, P., & Malnati, M. S. (2006). Differentiated human neural stem cells: a new ex vivo model to study HHV-6 infection of the central nervous system. *Journal of Clinical Virology, 37*, S27-S32.

Dominguez, G., Dambaugh, T. R., Stamey, F. R., Dewhurst, S., Inoue, N., & Pellett, P. E. (1999). Human herpesvirus 6B genome sequence: coding content and comparison with human herpesvirus 6A. *Journal of virology, 73*(10), 8040-8052.

Donati, D., Akhyani, N., Fogdell–Hahn, A., Cermelli, C., Cassiani-Ingoni, R., Vortmeyer, A., . . . Sato, S. (2003). Detection of human herpesvirus-6 in mesial temporal lobe epilepsy surgical brain resections. *Neurology, 61*(10), 1405-1411.

Eid, T., Gruenbaum, S. E., Dhaher, R., Lee, T.-S. W., Zhou, Y., & Danbolt, N. C. (2016). The glutamate–glutamine cycle in epilepsy. *The glutamate/GABA-glutamine cycle*, 351-400.

Fotheringham, J., Williams, E. L., Akhyani, N., & Jacobson, S. (2008). Human herpesvirus 6 (HHV-6) induces dysregulation of glutamate uptake and transporter expression in astrocytes. *Journal of Neuroimmune Pharmacology, 3*(2), 105-116.

Hall, C. B., Caserta, M. T., Schnabel, K. C., Long, C., Epstein, L. G., Insel, R. A., & Dewhurst, S. (1998). Persistence of human herpesvirus 6 according to site and variant: possible greater neurotropism of variant A. *Clinical infectious diseases, 26*(1), 132-137.

Howell, K. B., Tiedemann, K., Haeusler, G., Mackay, M. T., Kornberg, A. J., Freeman, J. L., & Harvey, A. S. (2012). Symptomatic generalized epilepsy after HHV6 posttransplant acute limbic encephalitis in children. *Epilepsia, 53*(7), e122-e126.

Isegawa, Y., Mukai, T., Nakano, K., Kagawa, M., Chen, J., Mori, Y., . . . Hata, A. (1999). Comparison of the complete DNA sequences of human herpesvirus 6 variants A and B. *Journal of virology, 73*(10), 8053-8063.

Liu, D., Wang, X., Wang, Y., Wang, P., Fan, D., Chen, S., . . . Luan, G. (2018). Detection of EBV and HHV6 in the Brain Tissue of Patients with Rasmussen's Encephalitis. *Virologica Sinica, 33*(5), 402-409.

Oyaizu, H., Tang, H., Ota, M., Takenaka, N., Ozono, K., Yamanishi, K., & Mori, Y. (2012). Complementation of the function of glycoprotein H of human herpesvirus 6 variant A by glycoprotein H of variant B in the virus life cycle. *Journal of virology, 86*(16), 8492-8498.

Prusty, B. K., Gulve, N., Govind, S., Krueger, G. R., Feichtinger, J., Larcombe, L., . . . Toro, C. T. (2018). Active HHV-6 infection of cerebellar purkinje cells in mood disorders. *Frontiers in Microbiology*, 1955.

Rapp, J. C., Krug, L. T., Inoue, N., Dambaugh, T. R., & Pellett, P. E. (2000). U94, the human herpesvirus 6 homolog of the parvovirus nonstructural gene, is highly conserved among isolates and is expressed at low mRNA levels as a spliced transcript. *Virology, 268*(2), 504-516.

Tang, H., & Mori, Y. (2018). Glycoproteins of HHV-6A and HHV-6B. *Human Herpesviruses*, 145-165.

Vinters, H. V., Wang, R., & Wiley, C. A. (1993). Herpesviruses in chronic encephalitis associated with intractable childhood epilepsy. *Human pathology, 24*(8), 871-879.

Wang, F.-Z., & Pellett, P. E. (2007). HHV-6A, 6B, and 7: immunobiology and host response. *Human herpesviruses: biology, therapy, and immunoprophylaxis*.

Yao, K., Crawford, J. R., Komaroff, A. L., Ablashi, D. V., & Jacobson, S. (2010). Review part 2: Human herpesvirus-6 in central nervous system diseases. *Journal of medical virology, 82*(10), 1669.

3 CHAPTER III

3.1 Abstract

Infection with neurotropic viruses like HHV-6, according to a handful of preclinical investigations, can cause infected CNS cells to become implicated in an inflammatory cascade. Clinical studies have established a relationship between HHV-6 infection and various epilepsy syndromes, as well as HHV-6 viral DNA in saliva, blood, CSF, and tissue taken from epileptogenic cells in children and adults with seizures and chronic epilepsy. Inflammation is considered to have a part in the development of an increasing number of acute and chronic neurological disorders. To further understand how HHV-6A and HHV-6B may impact inflammatory pathways in the CNS, we infected cultured human neural stem cells and evaluated the expression of several proinflammatory cytokines and growth factors. Also, expression of HHV6-A and HHV6-B cell surface receptors (CD46, CD134) were evaluated in HHV6 infected GABAergic cells and glutamatergic cells by immunofluorescent staining, and the reverse transcription-polymerase chain reaction (RT-qPCR) confirmed the excretion of HHV6 receptors in mix culture of human neural stem cells.

Our results indicate that the expression of inflammatory cytokines differs between HHV6-A and HHV6-B infected cells. RT-qPCR was performed to determine if HHV-6 infection increases the expression and production of IL-10 and TLR-9 in infected human neural stem cells. Expression and production of IL-10 were markedly increased in HHV6-A infected cells. Other inflammatory cytokines' mRNA expression and protein synthesis may have been suppressed by IL-10 in HHV-6-infected cells. VEGF-C, a growth factor involved in angiogenesis, was another gene product that increased in both HHV6-A and HHV6-B infected cells. Also, insulin-like growth factor binding protein 6 (IGFBP6) over expressed in HHV6-A infected cells.

3.2   Introduction

The central nervous system (CNS) HHV-6 infection is often silent, allowing the virus to stay inside neural cells as a normal CNS commensal. Rarely HHV-6 appear to be linked to encephalopathy, encephalitis, febrile seizures, or neuroinflammation(Yoshikawa & Asano, 2000). HHV-6 has been detected in the oligodendrocytes of MS patients, and CNS tissue, lymphoid tissues, peripheral blood lymphocytes, serum, and urine from MS patients have all demonstrated signs of active HHV-6 infection(Akhyani et al., 2000; Challoner et al., 1995). Despite varied findings of HHV6 infection in the CNS and its association with neurological dieses, it is unclear how HHV-6 might impact its pathogenesis. HVV6 is known for its capacity to alter inflammatory pathways in target cells(Lüttichau et al., 2003). While the U51 region of the viral genome encodes a CCL5 receptor, the U12 region of the viral genome encodes beta chemokine receptors for CCL2, CCL3, CCL4, and CCL5. The viral U83 region also codes for a CCR2 agonist that resembles chemokines(Gompels et al., 1995; Isegawa, Ping, Nakano, Sugimoto, & Yamanishi, 1998; Lüttichau et al., 2003; Milne et al., 2000). HHV-6 may affect the target cell's tendency to create specific mediators or its responsiveness to external stimuli like pro-inflammatory cytokines or chemokines by introducing these chemokine (receptor) mimics(Meeuwsen et al., 2005). Additionally, immunological modulatory effects may result from viral interaction with its cellular receptors. Until 2013, an inhibitory complement receptor, CD46 (cluster of differentiation 46), was considered to be the primary target for HHV-6A attachment to susceptible cell types(Santoro et al., 1999). However, it has been suggested that tumor necrosis factor receptor superfamily member 4 (TNFRSF4), also known as CD134, serves as the primary receptor for HHV-6B entry into susceptible cell types(Tang et al., 2013). Indeed, there may be other yet to be identified cell surface receptors to which HHV-6 virions can bind

with the asymmetric binding affinity between such receptors and HHV-6A versus HHV-6B envelope glycoproteins. This area of research is ongoing.

Because both HHV6-A and HHV6-B are unable to infect GABAergic cells, we studied the excretion of CD46 and CD134 in GABAergic and glutamatergic cells to see if GABAergic cells resistance to HHV6 infection is related to low viral receptor expression in their surface. However, immunofluorescent staining showed the expression of both CD46 and CD134 in the infected GABAergic and glutamatergic cells.

Roseolovirus infection may activate TLR9 in addition to CD46 (or CD134) expression to allow virus entrance(Bowman et al., 2003). TLR9 has been shown to be expressed in both mice and human microglial cells and astrocytes. Furthermore, the findings show that HHV-6A may trigger human TLR9 in addition to murine TLR9. In an animal model of multiple sclerosis, TLR9 was also demonstrated to be an essential regulator of an autoimmune process(Bowman et al., 2003). findings imply that HHV-6A can cause neuroinflammation via TLR9, which could have therapeutic implications since TLR9 inhibitors could be utilized to reduce the generation of proinflammatory chemokines and slow CNS pathogenesis(Reynaud et al., 2014). In this chapter, I provided data that shows TLR9 gene expression increased during HHV6-A infection in human neural stem cells.

To understand how HHV-6 could influence inflammatory processes in the CNS, we infected cultured human neuron stem cells and performed RT-qPCR for different inflammatory cytokines and growth factors. A crucial physiological process called angiogenesis involves the development of new blood vessels from pre-existing ones. It is essential for disease pathology, such as tumor growth, and progression, as well as the creation and healing of wounds. One of the many stimulators engaged in the angiogenesis process is VEGF, which oversees activating

endothelial cells by binding to vascular endothelial growth factor receptors on the cell surface (VEGFR)(Ferrara, Gerber, & LeCouter, 2003). VEGF appears to have an important role in the pathogenesis of a variety of viral infections. As a result, many viruses, such as HSV1, attempt to boost VEGF levels(Alkharsah, 2018). Our result showed that in HHV6-A and HHV6-B infected human neuron stem cells, VEGF gene expression increased.

The IGFBP6 (insulin-like growth factor binding protein 6) IGFBPs were found to be overexpressed in viral infection(Alzaid et al., 2016). Based on our result, IGFBPs overexpressed in HHV6-B infected HNSCs.

3.3 Results

3.3.1 Immunofluorescence indicates both CD134 and CD46 expression in GAD67-positive cells

To determine if the apparent resistance of GAD67-positive cells to roseolovirus infection is due to low receptor expression, immunofluorescence was used to verify the coincidence of GAD67 with CD46 and CD134. CD46 is a receptor known to be used by HHV-6A for cell attachment and entry. CD134 is reported to be the preferred receptor for HHV-6B attachment and entry; however, it has also been shown that HHV-6B can use CD46. Failure to express these "clusters of differentiation" (CD) regulatory proteins in GAD67-positive cells would inhibit HHV-6A or HHV-6B infection. However, immunofluorescence data (Fig. 1A, B) indicate that CD134 and CD46 are coincident with GAD67. These results are consistent with data from VGluT1-positive cultures (Fig. 1C, D).
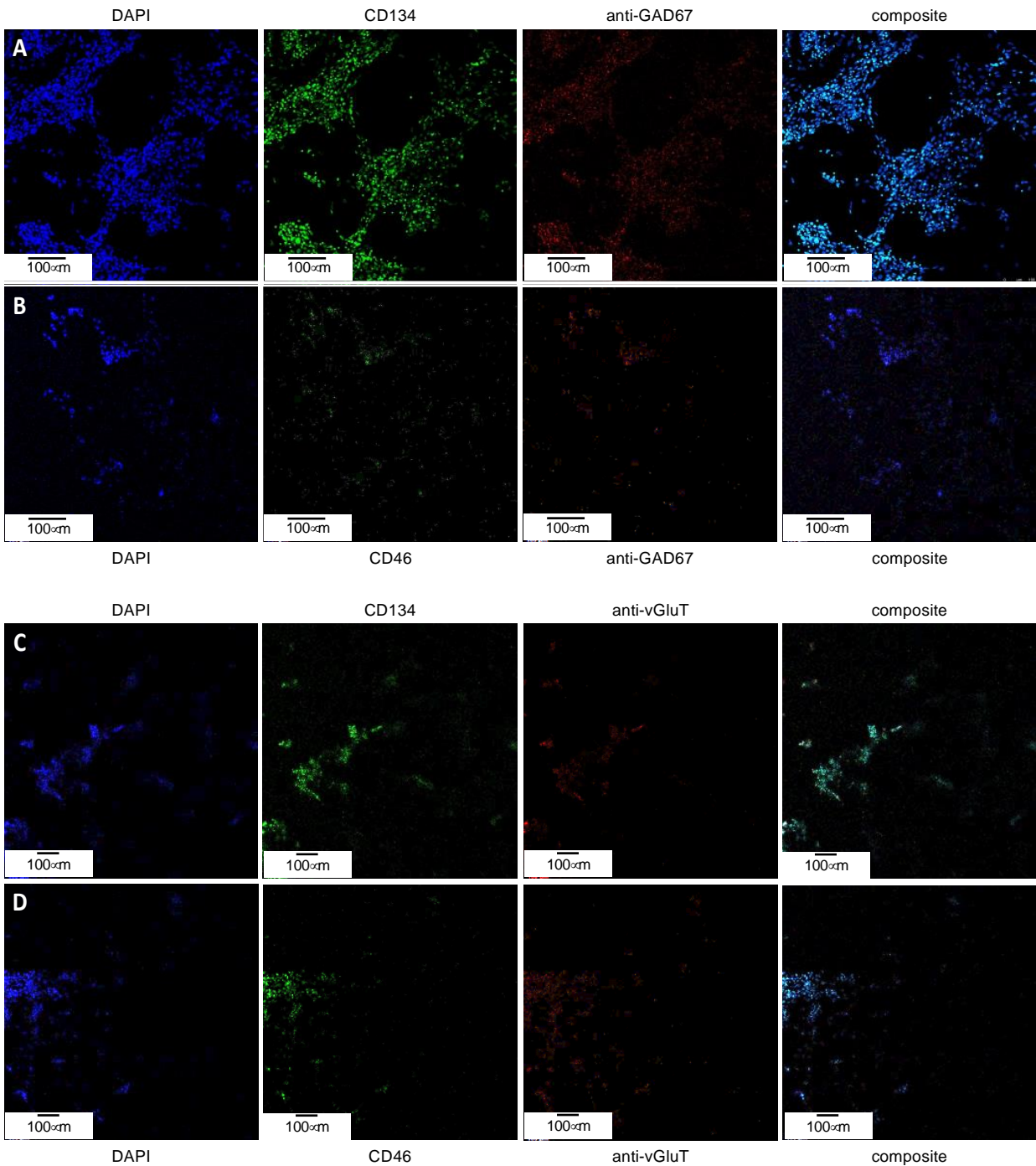
Figure 3-1 CD46 and CD134 colocalize with GAD67-positive and vGluT-positive differentiated H9 stem cells. (A) GAD67-positive (red, mid-right) dHNSCs at PDD7 stained with DAPI (blue, left) exhibit a coincident anti-CD134 immunofluorescence signal (green, mid-left). (B) GAD67-positive (red, mid-right) dHNSCs at PDD7 stained with DAPI (blue, left) also show colocalized anti-CD46 (green, mid-left). Thus, GAD-67-positive cells appear to express

both CD134 and CD46 (composites, right). (C) vGluT-positive (red, mid-right) dHNSCs at PDD7 stained with DAPI (blue, left) also show colocalization of anti-CD134 immunofluorescence signal (green, mid-left). (D) vGluT-positive (red, mid-right) dHNSCs at PDD7 stained with (blue, left) show anti-CD46 immunofluorescence (green, mid-left). This indicates that vGluT-positive cells are also expressing both CD134 and CD46 (composites, right).

Immunofluorescence data indicate that receptor expression in GAD67-positive cells is greater than for VGluT1-positive cells (see Fig. 1), in which productive roseolovirus infection is observed. Moreover, for all cultures examined (N=9), CD134 fluorescent markers appear in greater density than CD46.

To confirm that CD134 is indeed expressed at higher levels than CD46, reverse transcription quantitative polymerase chain reaction (RT-qPCR) was used to determine relative transcription levels of CD134 versus CD46 in cultures infected with HHV-6A or HHV-6B and uninfected controls (Fig. 2). These data indicate that CD134 expression is greater than CD46 expression in both HHV-6A and HHV-6B infected cultures as well as the uninfected control cultures (N=9, $p<0.05$). However, neither CD134 nor CD46 expression is significantly different between HHV-6A versus HHV-6B infected cultures. Interestingly, the expression of both receptors increases significantly during roseolovirus infection (when compared to uninfected controls). During HHV-6A infection, a significant increase in both CD134 and CD46 expression is observed over uninfected controls (N=6, $p<0.05$). Likewise, HHV-6B infections result in a significant increase in CD134 and CD46 expression over uninfected controls (N=6, $p<0.05$). Results are held in mixed cultures and are independent of whether cultures are dominated by glutamatergic, dopaminergic, or GABAergic cell types.
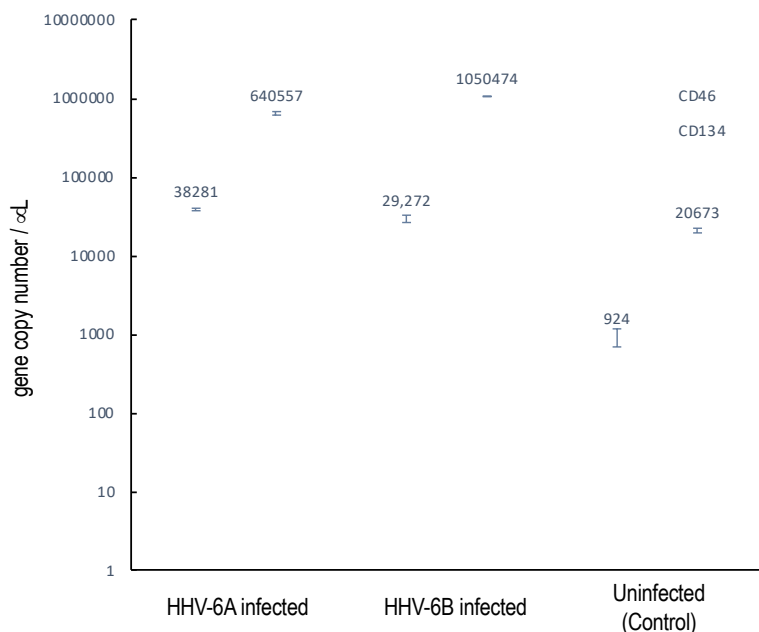
Figure 3-2 CD134 and CD46 gene expression in HHV6 infected cells. Using RT-qPCR CD134 and CD46 mRNA expression was determined for dHNSCs (i.e., H9 cells) after infection with either HHV-6A or HHV-6B and compared to uninfected controls. After 2 hr post-infection, CD134 (light grey) and CD46 (dark grey) mRNA levels were elevated when compared to uninfected control cultures (far right). CD134 expression levels are greater than CD46 in HHV-6A and HHV-6B infected cultures. CD134 expression is also greater in uninfected cells. These data indicate that cells express CD134 at higher levels and that infection results in overexpression of both CD46 and CD134.

3.3.2 Immunofluorescence and qPCR show that HHV-6A induces a TLR9 and IL-10 response

Toll-like receptors (TLRs) act as early sensors for pathogen detection and initiation of biochemical cascades associated with cellular immunological response to microbial infection (Nie et al., 2018). Although TLR9 is a known pro-inflammatory receptor in immune cells, in non-immune cells, including neurons, TLR9 may play a role in energy metabolism to protect cells during infection (Shintani et al., 2013). To determine if TLR9 expression is impacted during HHV-6A or HHV-6B infection in differentiated human neural stem cells, immunofluorescence was used (*see* Fig. 12). An anti-TLR9 antibody system was used in conjunction with anti-VGluT and anti-GAD67 during separate infections with HHV-6A and

HHV-6B. When compared to uninfected controls, TLR9 signals showed no appreciable difference in fluorescence emissions over HHV-6B infected cells. Moreover, there appeared to be a higher density of TLR9 signal in HHV-6A infected cell cultures than in cultures infected with HHV-6B (Fig 3).

To quantitatively examine TLR9 expression in HHV-6A versus HHV-6B infected differentiated neural stem cell cultures, RT-qPCR was employed (Fig. 4A, dark grey). Consistent with observations from the immunofluorescence assays, which target protein, mRNA levels for TLR9 in HHV-6B infected cell cultures were not significantly different from uninfected control cultures. However, TLR9 gene expression was significantly upregulated in HHV-6A infected cell cultures over HHV-6B infected cell cultures (N=3, $p<0.05$) as well as uninfected controls (N=3, $p<0.05$). These RT-qPCR data (Fig. 4A) are consistent with results from immunofluorescence (Fig. 3).

Since early pro-inflammatory responses initiated by TLR9 (e.g., regulation of IL-1β and TNFα) may be suppressed by IL-10, RT-qPCR was used to determine IL-10 transcript levels under uninfected control conditions and during HHV-6A versus HHV-6B infections (Fig. 4A, light grey). IL-10 mRNA expression levels were not significantly different between the uninfected controls and HHV-6B infected cultures. However, coincident with higher TLR9 expression levels, IL-10 mRNA levels were significantly higher in HHV-6A infected cells than in HHV-6B infected cells (N=3, $p<0.05$) and uninfected controls (N=3, $p<0.05$).
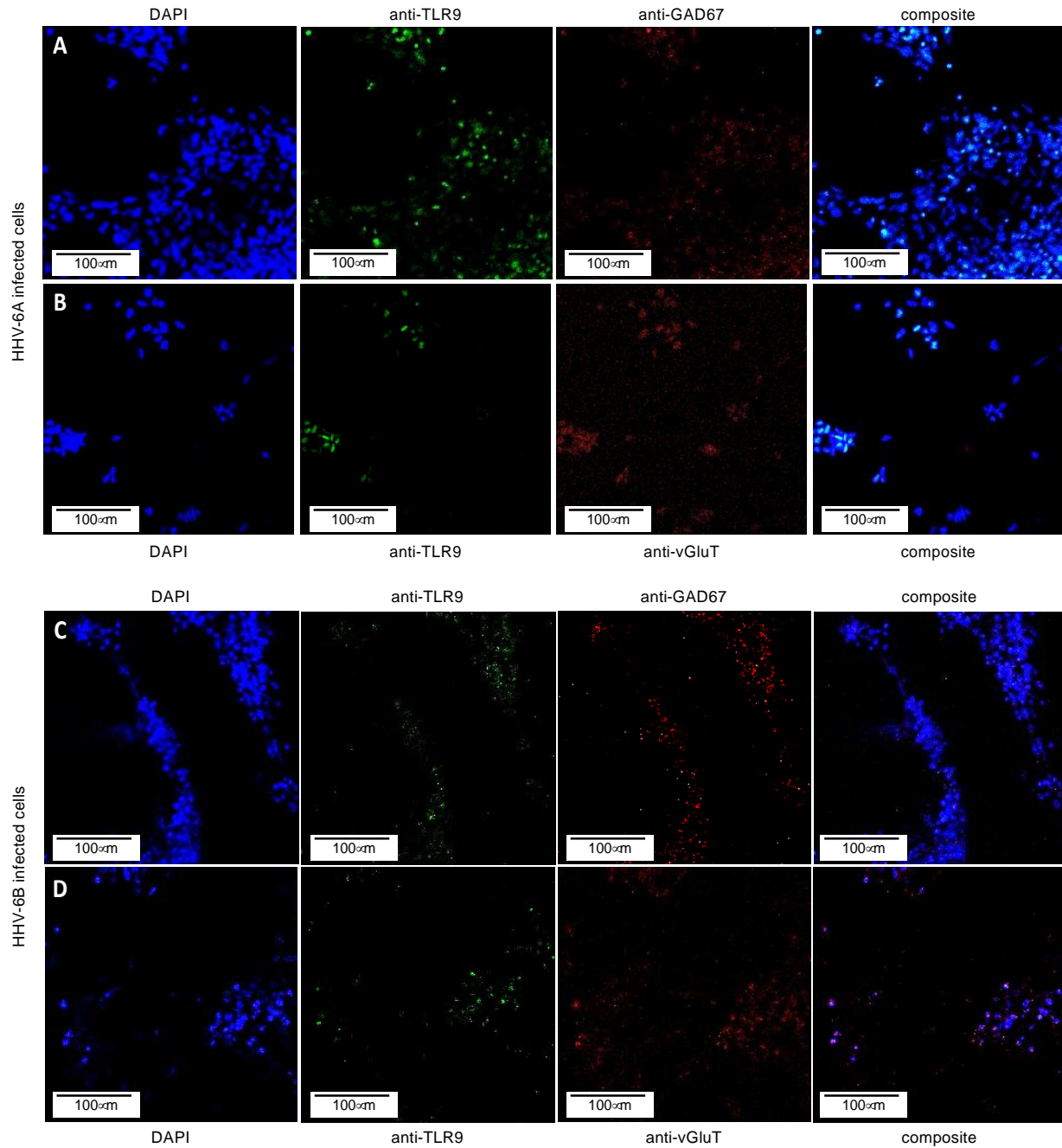
Figure 3-3 TLR9 in HHV6 infected excitatory (vGluT-positive) and inhibitory (GAD67-positive) cells. Immunofluorescence assays indicate that both HHV-6A and HHV-6B infected dHNSCs express TLR9. (A) DAPI stained cells (blue, left) emitting GAD67-positive immunofluorescence signals (red, mid-right) also show signal for anti-TLR9 fluoroprobes (green, mid-left) during HHV-6A infection. (B) HHV-6A infected vGluT-positive neurons (red, mid-right) stained with DAPI (blue, left) also show coincident TLR9 immunofluorescence (green, mid-right).

(C) DAPI stained cells (blue, left) emitting GAD67-positive immunofluorescence signals (red, mid-right) also show a signal for anti-TLR9 fluoroprobes (green, mid-left) during HHV-6B infection. (D)) HHV-6B infected vGluT-positive cells (red, mid-right) stained with DAPI (blue, left) also show coincident TLR9 fluorescence (green, mid-right). [Infections in A-D were performed seven days post-differentiation day (PDD7).
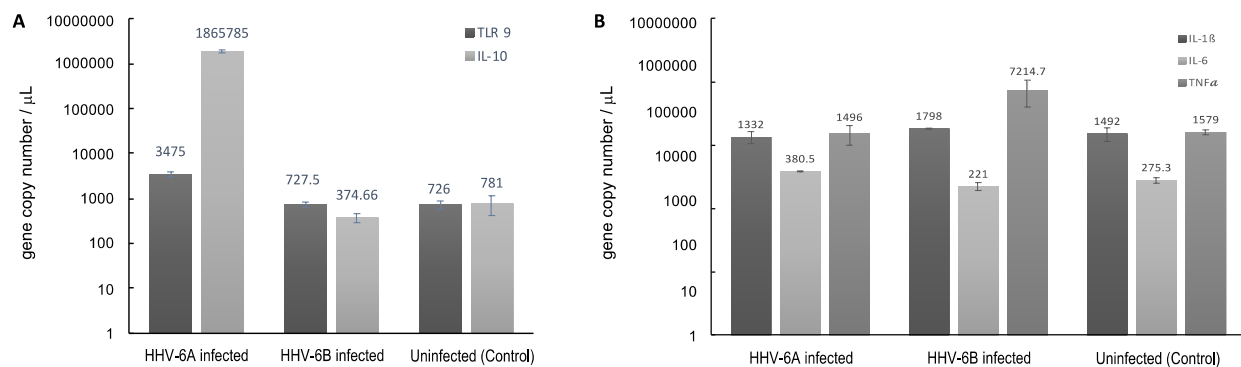

Figure 3-4 Cellular cytokine responses to HHV6 infection in differentiated neural stem cells via RT-qPCR. (A) TLR9 gene expression levels (i.e., mRNA) are elevated in HHV-6A infected cultures, while there is no significant increase in TLR9 gene expression in HHV-6B infected dHNSCs when compared to uninfected controls (*dark grey*). Likewise, a significant increase in IL-10 is observed in HHV-6A infected cultures, while no significant increase in IL-10 gene expression is observed in HHV-6B infected dHNSCs (*light grey*). (B) Gene expression levels of IL-6 are slightly elevated in HHV-6 infected cultures (*light grey*), while no significant difference in IL-6 expression in HHV-6B infected dHNSCs is observed as compared to uninfected controls. TNFα expression is elevated in HHV-6B infected dHNSCs. No significant difference is observed in HHV-6A infected cells when compared to uninfected controls (*medium grey*). No change in IL-1β is noted for either HHV-6A or HHV-6B infected cells (*dark grey*).

There are multiple steps in the immunological response between activation of TLR9 and IL-10 suppression of inflammatory cytokines. RT-qPCR was also used to explore the regulation of other pathway intermediates in HHV-6A versus HHV-6B infections compared to uninfected controls.

3.3.3 Regulation of other immunological factors during HHV-6 infection as detected by qPCR

Given a significant upregulation in the anti-inflammatory cytokine, IL-10, during HHV-6A infection, it was prudent to examine the expression of pro-inflammatory cytokine levels (e.g., IL1β, TNFα). Again, RT-qPCR was performed to determine the impact of HHV-6A versus HHV-6B infection on the expression pro-inflammatory cytokines (Fig. 4B). When compared to uninfected controls, there was no appreciable difference in IL-1β expression levels between HHV-6A or HHV-6B infected cultures (Fig. 4B, dark grey). HHV-6B infected cells exhibited a marked increase in TNFα expression, while HHV-6A infected cells showed no significant difference in TNFα over control (Fig. 4B, medium grey). Neither HHV-6A nor HHV-6B infected cell cultures exhibited notable increases in IL-6 expression (Fig. 4B, light grey).

3.3.4 Regulation of cellular growth factors detected by qPCR during HHV-6 infection

In addition to evoking cytokine responses, viruses are known to upregulate the expression of select cellular growth factors, including insulin-like growth factor binding protein 6 (IGFBP6), which has been shown to be upregulated during HHV-6A infection (Meeuwsen et al., 2005), and vascular endothelial growth factor-C (VEGF-C), which was shown to be upregulated in HHV-1 (a.k.a., HSV-1) infection (Alkharsah, 2018). To determine if these two growth factors are upregulated in response to HHV-6A or HHV-6B infection in differentiated human neural stem cells, RT-qPCR was used to measure transcript levels in infected versus uninfected controls (Fig. 5). For IGFBP6, results from HHV-6B infected cells compared to control were inconclusive; however, IGFBP6 expression was significantly upregulated (N=3, p<0.05) in HHV-6A infected cell cultures (Fig. 14, light grey). Both HHV-6A (N=3, p<0.05) and HHV-6B (N=3, p<0.05) infected cells exhibited increased VEGF levels over uninfected control. However, there was no

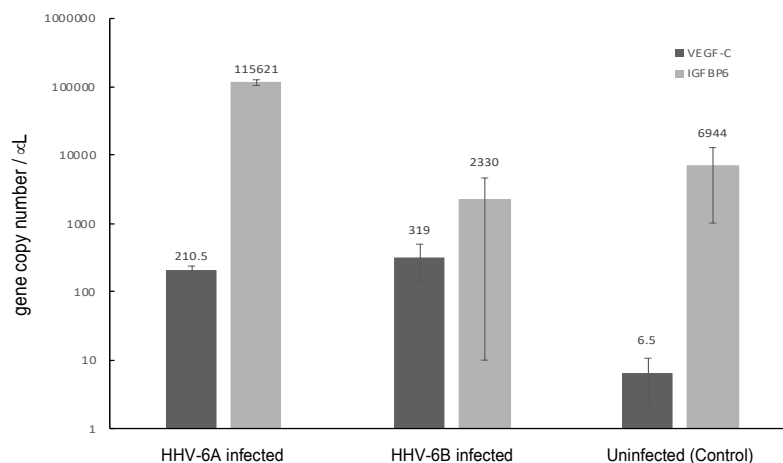significant difference between VEGF levels in HHV-6A versus HHV-6B infected cultures (Fig. 5, dark grey).

Figure 3-5 Growth factor responses to HHV6 infection in differentiated neural stem cells via RT-qPCR. Expression levels of vascular endothelial growth factor C (VEGF-C) and insulin-like growth factor binding protein 6 (IGFBP6) were measured via RT-qPCR during infection with HHV-6A and HHV-6B. Both HHV-6A and HHV-6B infected dHNSCs show elevated expression of VEGF-C compared to uninfected controls (dark grey). HHV-6A infection of dHNSCs also results in increased expression of IGFBP6, while HHV-6B infection does not (light grey).

3.4   Discussion

3.4.1   Cytokine responses differ between cell cultures infected with HHV-6A versus HHV-6B

Viral infections induce inflammatory responses in both immune cells and non-immune cells. Determining the extent to which HHV-6A versus HHV-6B infections upregulates the expression of pro-inflammatory factors (e.g., cytokines) could provide additional insights into relative virulence. To quantify the immunological impacts of HHV-6A versus HHV-6B infection in nerve cell cultures, experiments were performed to investigate potential changes in cytokine expression levels during HHV-6 infections versus uninfected controls. In addition to CD46 (or CD134) expression for virus entry, toll-like receptor 9 (TLR9) may be activated by roseolovirus

infection (Bowman et al., 2003).TLR9 is a major pattern recognition receptor for bacteria and DNA viruses (Slack et al., 2000). Prior work showed that HHV-6A infection in CD4+ T cells not only activates TLR9 but also increases its expression (Chi et al., 2012). In cultures of dHNSCs, our results show a more robust TLR9 fluorescence signal after HHV-6A infection compared to HHV-6B infected cultures (Fig. 3).

This is more evidence of the differential impact of HHV-6A versus HHV-6B on susceptible nerve cells.

These results are consistent with prior work that show an increase in TLR9 expression in microglia and astrocytes from both mice and humans upon infection with HHV-6A(Bowman et al., 2003). TLR9 activation is known to coincide with the activation (and upregulated expression) of cytokines, including interleukin-1β (IL-1β), tumor necrosis factor α (TNFα), and IL-6(Akira & Sato, 2003). In response to the activation of pro-inflammatory factors (e.g., TLR9, IL-β TNFα), IL-10 may be upregulated as an anti-inflammatory reaction, especially in neurons(Shintani et al., 2013). Interestingly, our data show a remarkable increase in IL-10 expression concomitant with the upregulation of TLR9 gene expression in cultures infected with HHV-6A. IL-10 upregulation may serve to inhibit a robust IL-1β pro-inflammatory response in HHV-6A infected cells (see Fig. 4A). This IL-10 increase may account for the negligible change in IL-1β after HHV-6A infection (Fig. 13B). Upon examination of pro-inflammatory cytokine expression (i.e., IL1β and TNFα), IL-1β was not elevated under any condition; however, HHV-6B infection appears to increase TNFα (Fig. 4B). It would be anticipated that in addition to attenuating IL-1β, IL-10 would also temper TNFα levels(Denys et al., 2002). However, our results do not support this in dHNSCs infected with HHV-6B. More detailed time-course of infection studies will be needed to relate IL-10 activation/expression with changes in other

cytokine levels (e.g., IL-1β and TNFα). Interestingly IL-6 may act as either a pro-inflammatory cytokine (like IL1β and TNFα) under conditions of chronic inflammation or as an anti-inflammatory cytokine (like IL-10) during acute inflammatory responses(Xing et al., 1998). Results from our in vitro HHV6 infection assays yield mixed results with regards to IL-6 (Fig. 4). Specifically, IL-6 is upregulated in HHV-6A infection but shows no significant change in HHV-6B infected cells. Cumulatively, these results demonstrate a differential effect in cytokine regulation between HHV-6A versus HHV-6B infections in differentiated human neural stem cells.

3.4.2 Growth factor levels differ between cell cultures infected with HHV-6A versus HHV-6B

In addition to cytokine responses, it is known that select cellular growth factors can be activated or upregulated during viral infection(Leigh et al., 2008; Vrancken, Vervaeke, Balzarini, & Liekens, 2011). Both vascular endothelial growth factor-C (VEGF-C) and insulin-like growth factor binding protein-6 (IGFBP-6) have been shown to be upregulated during herpesvirus infections(Meeuwsen et al., 2005). VEGFs are responsible for activating endothelial cells by attaching to vascular endothelial growth factor receptors on the cell surface(Ferrara et al., 2003). VEGF appears to play a role in the pathogenesis of several viral diseases, including those involving HHV nervous system infections.

For example, it was shown that HHV-1 (a.k.a., HSV1) infection can enhance VEGF expression(Alkharsah, 2018). It was also shown that patients with virus-positive encephalitis exhibit higher levels of VEGF-C in serum than patients with virus-negative encephalitis(Mori et al., 2017). Specific to roseoloviruses, it has been reported that VEGF-C is continuously activated in HHV-6 infected astrocytes at twice the level compared to uninfected controls(Meeuwsen et

al., 2005). Our results show that both HHV-6A and HHV-6B infection can elevate VEGF-C levels in dHNSCs. This is notable since VEGF-C protein levels were found to be elevated in the temporal neocortex of patients with temporal lobe epilepsy(Castañeda-Cabral et al., 2019). It is notable for our results that both HHV-6A and HHV-6B elevate VEGF mRNA to comparable levels over uninfected controls (Fig. 5, dark grey). Likewise, it has been shown that IGFBPs are overexpressed in response to viral infection as a result of inflammatory cytokine activation(Alzaid et al., 2016). For example, HHV-6A has been shown to increase IGFBP-6 expression in astrocytes (Meeuwsen et al., 2005). Our results indicate that IGFBP-6 is also overexpressed in HHV-6A infected dHNSCs but not in cultures infected with HHV-6B (Fig. 5, light grey). Cumulatively, these results add growth factor regulation to the list of differential impacts on HHV-6A versus HHV-6B infected nerve cell cultures.

3.5   Conclusion

The research presented in this chapter demonstrated that: (1) HHV6-A and HHV6-B receptors (CD46 and Cd 134) express in both GABAergic and Glutamatergic neuron cells; (2) toll-like receptor 9 (TLR9) express in neuron cells and that its expression is higher on HHV6-A infected cells than on uninfected control cells and HHV6-B infected cells; (3) Differentiated human neuron stem cells infected with HHV6-A and HHV6-B can exhibit variable cytokine responses; (4) growth factor levels in dHNSCs infected with HHV6-A and HHV6-B vary. The electrophysiological reactions of differentiated human neural stem cells to HHV6-A and HHV6-B will be studied to some level in the next chapter.

3.6   *Materials and methods*

Cell culturing and immunofluorescent staining were performed as described in chapter 1.

3.6.1   mRNA profiling

RNA extraction kit was used to analyze the mRNA profile of HNSCs (Qiagen, Hilden, Germany). Total cellular RNA was collected from uninfected cells at PDD7 and cells infected with HHV6-A and HHV6-B. (PIh24). DNase treatment was conducted to the best of our ability to eliminate DNA contamination using a kit (Ambion™ DNase I). cDNA was synthesized using (iScript Advanced cDNA Synthesis Kit for RT-qPCR, BIORAD, US). H9 cell genomic DNA was utilized (Qiagen DNA extraction kit), and PCR was performed using a particular primer for each cytokine and growth factor (Table.1). Primer for each gene was designed through NCBI and ordered on IDT website. The PCR product concentration was determined using nanodrop, and the PCR product was used as known concentrations to generate a standard curve for calculating each individual cytokine's gene expression levels. Serial dilutions for each cytokine were performed in triplicate. The standard is intended for calculating transcript levels of the same gene in unknown samples using a linear series (log scale). Because both standard and unknown samples were used in the same run, experimental errors are minimized. qPCR primer sequence sets (both forward and reverse) for each target (e.g., IL-1β, IL-6, IL-10, TLR9, TNFα) are provided (see Supplementary Table 1). The following formula was used to determine the transcript copy number:

$$\text{number of copies (molecules)} = \frac{X \text{ ng } (6.0221 \times 10^{23} \text{ molecules/mole})}{N \text{ (660 g/mole) } (1 \times 10^{9} \text{ ng/g})}$$

Such that X represents the amount of amplicon in nanograms, N is the length of the dsDNA amplicon, and 660 g/mole is the average mass of 1 bp dsDNA.

3.7 Reference

Akhyani, N., Berti, R., Brennan, M. B., Soldan, S. S., Eaton, J. M., McFarland, H. F., & Jacobson, S. (2000). Tissue distribution and variant characterization of human Herpesvirus (HHV)—6: Increased prevalence of HHV-6A in patients with multiple sclerosis. *The Journal of infectious diseases, 182*(5), 1321-1325.

Akira, S., & Sato, S. (2003). Toll-like receptors and their signaling mechanisms. *Scandinavian journal of infectious diseases, 35*(9), 555-562.

Alkharsah, K. R. (2018). VEGF upregulation in viral infections and its possible therapeutic implications. *International journal of molecular sciences, 19*(6), 1642.

Alzaid, A., Castro, R., Wang, T., Secombes, C. J., Boudinot, P., Macqueen, D. J., & Martin, S. A. (2016). Cross talk between growth and immunity: coupling of the IGF Axis to conserved cytokine pathways in rainbow trout. *Endocrinology, 157*(5), 1942-1955.

Bowman, C. C., Rasley, A., Tranguch, S. L., & Marriott, I. (2003). Cultured astrocytes express toll-like receptors for bacterial products. *Glia, 43*(3), 281-291.

Castañeda-Cabral, J. L., Beas-Zárate, C., Rocha-Arrieta, L. L., Orozco-Suárez, S. A., Alonso-Vanegas, M., Guevara-Guzmán, R., & Ureña-Guerrero, M. E. (2019). Increased protein expression of VEGF-A, VEGF-B, VEGF-C and their receptors in the temporal neocortex of pharmacoresistant temporal lobe epilepsy patients. *Journal of neuroimmunology, 328*, 68-72.

Challoner, P. B., Smith, K. T., Parker, J. D., MacLeod, D. L., Coulter, S. N., Rose, T. M., . . . Chang, M. (1995). Plaque-associated expression of human herpesvirus 6 in multiple sclerosis. *Proceedings of the National Academy of Sciences, 92*(16), 7440-7444.

Chi, J., Wang, F., Li, L., Feng, D., Qin, J., Xie, F., . . . Yao, K. (2012). The role of MAPK in CD4+ T cells toll-like receptor 9-mediated signaling following HHV-6 infection. *Virology, 422*(1), 92-98.

Denys, A., Udalova, I. A., Smith, C., Williams, L. M., Ciesielski, C. J., Campbell, J., . . . Foxwell, B. M. (2002). Evidence for a dual mechanism for IL-10 suppression of TNF-α production that does not involve inhibition of p38 mitogen-activated protein kinase or NF-κB in primary human macrophages. *The Journal of Immunology, 168*(10), 4837-4845.

Ferrara, N., Gerber, H. P., & LeCouter, J. (2003). The biology of VEGF and its receptors. *Nat Med, 9*(6), 669-676. doi:10.1038/nm0603-669

Gompels, U., Nicholas, J., Lawrence, G., Jones, M., Thomson, B., Martin, M., . . . Macaulay, H. (1995). The DNA sequence of human herpesvirus-6: structure, coding content, and genome evolution. *Virology, 209*(1), 29-51.

Isegawa, Y., Ping, Z., Nakano, K., Sugimoto, N., & Yamanishi, K. (1998). Human herpesvirus 6 open reading frame U12 encodes a functional β-chemokine receptor. *Journal of virology, 72*(7), 6104-6112.

Leigh, R., Oyelusi, W., Wiehler, S., Koetzler, R., Zaheer, R. S., Newton, R., & Proud, D. (2008). Human rhinovirus infection enhances airway epithelial cell production of growth factors involved in airway remodeling. *Journal of Allergy and Clinical Immunology, 121*(5), 1238-1245. e1234.

Lüttichau, H. R., Clark-Lewis, I., Jensen, P. Ø., Moser, C., Gerstoft, J., & Schwartz, T. W. (2003). A highly selective CCR2 chemokine agonist encoded by human herpesvirus 6. *Journal of Biological Chemistry, 278*(13), 10928-10933.

Meeuwsen, S., Persoon-Deen, C., Bsibsi, M., Bajramovic, J. J., Ravid, R., De Bolle, L., & van Noort, J. M. (2005). Modulation of the cytokine network in human adult astrocytes by human herpesvirus-6A. *Journal of neuroimmunology, 164*(1-2), 37-47.

Milne, R. S., Mattick, C., Nicholson, L., Devaraj, P., Alcami, A., & Gompels, U. A. (2000). RANTES binding and down-regulation by a novel human herpesvirus-6 β chemokine receptor. *The Journal of Immunology, 164*(5), 2396-2404.

Mori, D., Khanam, W., Sheikh, R. A., Tabib, S., Ikebe, E., Hossain, M. M., . . . Ahmed, K. (2017). Increased serum vascular endothelial growth factor is associated with acute viral encephalitis in Bangladeshi children. *Scientific reports, 7*(1), 1-7.

Reynaud, J. M., Jégou, J.-F., Welsch, J. C., & Horvat, B. (2014). Human herpesvirus 6A infection in CD46 transgenic mice: viral persistence in the brain and increased production of proinflammatory chemokines via Toll-like receptor 9. *Journal of virology, 88*(10), 5421-5436.

Santoro, F., Kennedy, P. E., Locatelli, G., Malnati, M. S., Berger, E. A., & Lusso, P. (1999). CD46 is a cellular receptor for human herpesvirus 6. *Cell, 99*(7), 817-827.

Shintani, Y., Kapoor, A., Kaneko, M., Smolenski, R. T., D'Acquisto, F., Coppen, S. R., . . . Takashima, S. (2013). TLR9 mediates cellular protection by modulating energy metabolism in cardiomyocytes and neurons. *Proceedings of the National Academy of Sciences, 110*(13), 5109-5114.

Tang, H., Serada, S., Kawabata, A., Ota, M., Hayashi, E., Naka, T., . . . Mori, Y. (2013). CD134 is a cellular receptor specific for human herpesvirus-6B entry. *Proceedings of the National Academy of Sciences, 110*(22), 9096-9099.

Vrancken, K., Vervaeke, P., Balzarini, J., & Liekens, S. (2011). Viruses as key regulators of

angiogenesis. *Reviews in medical virology, 21*(3), 181-200.

Xing, Z., Gauldie, J., Cox, G., Baumann, H., Jordana, M., Lei, X.-F., & Achong, M. K. (1998).

IL-6 is an antiinflammatory cytokine required for controlling local or systemic acute

inflammatory responses. *The Journal of clinical investigation, 101*(2), 311-320.

Yoshikawa, T., & Asano, Y. (2000). Central nervous system complications in human

herpesvirus-6 infection. *Brain and Development, 22*(5), 307-314.

4 Chapter IV

4.1 Abstract

Human induced pluripotent stem (iPS) cell-derived Neurons and multi-electrode array (MEA) devices are often employed to analyze the electrophysiological response to cell stress. We began investigating the impact of HHV6-A and HHV6-B on neuron electrophysiology by recording extracellular voltage changes generated by action potentials in human neuron stem cells (HNSCs).

Membrane proteins, which allow ion transit and transport across the cell membrane, are responsible for electrical impulses traveling down the length of the axon in neurons. A multi electrode array (MEA) can detect this voltage shift generated by extracellular ion flow. Because the electrodes do not hurt the cells, extracellular monitoring has the advantage of never penetrating the cell membrane, allowing for multiple recordings of voltage changes over a more extended period of time.

Voltage measurements in hNSCs could be taken before and after infection with HHV6-A and HHV6-B. Using the MEA system, we can thoroughly examine data from each individual electrode to confirm that the waveforms being collected are not unpredictable, like in the case of a damaged electrode. Following that, uninfected HNSCs and HHV6-A and HHV6-B infected cells were seen and recorded. Preliminary recordings show that neurons' activity decreases the following infection with HHV-6A and HHV-6B.

4.1.1   Introduction

The effect of HHV6-A and HHV6-B on uninfected and infected human neural stem cells (HNSCs) is studied using microelectrode arrays (MEAs). Using the MEA2100 multielectrode plate technology, we can monitor both uninfected (control) and HHV6-infected in vitro neural networks. For example, total firing activity and action potential firing frequency can be measured in a neural culture. Because MEAs are noninvasive, their use with neuronal cultures benefits neurobiology. The system does not require cell penetration to collect extracellular signals; as a result, differences in the behavior of neuronal cultures may be more precisely correlated to external stimuli. Ions pass across the membrane of neurons via proteins ranging from ion channels to ATP-driven pumps. Because there are extracellular alterations, the movement of ions does not require a break-in membrane integrity to be recognized. This is one of the reasons MEAs do not harm the cells they watch; MEAs can detect changes produced by the movement of ions extracellularly(Spira & Hai, 2013). These cells have varied waveforms as well. Different shapes generated by MEA data can be utilized to identify cell types or to distinguish between cells(Fee, Mitra, & Kleinfeld, 1996). This method has also been used to study the propagation of APs in cultured cardiomyocyte sheets or clusters from chicks, mice, or rats by detecting acute spike signals produced from the quick influx of sodium ions (I_{Na}) during the AP's upstroke phase(Egert, Banach, & Meyer, 2006; Egert & Meyer, 2005; Meiry et al., 2001).

These microelectrodes help research naturally electrically excitable cells. These electrodes are often implanted in silicon or glass, which is particularly popular for enabling high-resolution imaging(Minerbi et al., 2009; Zitzmann et al., 2017). MEA is frequently utilized to examine cardiac or neural cells. Systems are not employed to analyze cells that do not respond to an action potential with rapid depolarization and repolarization. These specific electrical cells have

potential surface fluctuations that may be viewed and provide information about the changes. MEAs could detect electrical events such as ions rushing into and out of the cell. Even though neurotransmitters are the primary way which neurons connect, the cell propagates a signal before it reaches another cell via changes in membrane voltage and ion currents(Burke, Kiernan, & Bostock, 2001). The information obtained from the MEA system is frequently changed in how cells fire. Temperature variations, viral infections, exposure to drugs, cell growth stages, etc., are just a few examples of environmental changes that might affect cells surviving and can be modeled by the in vitro culture environment on a MEA. MEA systems may work with a variety of technologies to maintain the stability of the environment. It is feasible to specify appropriate boundaries for describing the key components of cell firing (spikes, bursts, and network bursts). MEAs using in vivo and in vitro procedures can rapidly collect large amounts of data(Asakura et al., 2015; Fee et al., 1996; Kapucu et al., 2012). One of the most beneficial aspects of MEA systems is the ability of single electrodes to be as small as one cell in a culture; electrodes may be as small as 40 µm, and electrodes on a plate often lie only ~200 µm from other electrodes on the plate(Minerbi et al., 2009)(Fig.1). MEA systems can detect and record spontaneous network activity generated by neuronal cultures. The spikes seen by the MEA are actual neurons firing action potentials. Bursts are spikes that rapidly follow each other. One of the challenges with these electrodes is that the neuron-to-electrode ratio is not always one-to-one. While this problem can be handled analytically, the trapped neuron MEA keeps the cell body close to an electrode. Neurites can still protrude and connect to form a neural network. This allows for a more in-depth analysis of some aspects of neurophysiology, such as how neural networks grow and alter over time in diverse contexts(Erickson, Tooker, Tai, & Pine, 2008). Analysis requires the separation of spikes from noise since several neurons may affect a single electrode, potentially interfering

with field potentials(Gross, Rhoades, Azzazy, & Wu, 1995). Data from the MEA can be recorded for extensive periods of time while processing it; however, the lengths typically range from a few seconds to a few minutes. Filters are used to pass through the massive quantity of data produced by each individual electrode in order to get relevant findings. A high pass filter is one of those filters. High pass filters can be used to record only data that exceeds a specified threshold. Variables such as voltage and frequency can be adjusted here. If a voltage high pass filter is employed, only fluctuations in the field potential that surpass a certain magnitude will be exhibited or recorded. High pass filters can aid or impair data depending on their magnitude(Asakura et al., 2015). Filters can also be applied to neuronal bursts. A neural burst occurs when a neuron fires many action potentials in quick sequence. It's critical to set the correct limitations for the experiment, as with the high pass filter. This can be accomplished, for example, by requiring a certain number of spikes per unit of time during bursts(Kapucu et al., 2012). Additionally, frequency filters are utilized, and they have the ability to set a length restriction on the recorded spikes.

A neuron's voltage is the difference in charge between its extracellular and intracellular sides. Current is the passage of charge that causes a voltage change. Changes in local field potentials can be detected by MEAs. Transmembrane potentials and ion currents cause these potentials to alter(Buzsáki, Anastassiou, & Koch, 2012). A single electrode may detect more than one neuron activity. When this happens, a MEA system that works with a microscope comes in handy. MEAs may be combined with microscopes to see neuronal firing while detecting voltage changes(Simeonov & Schäffer, 2019). A neuron impacting an electrode is regularly observed under a microscope. Looking at the waveforms during analysis is another possible method for identifying neurons close to the same electrode. The varied patterns may indicate that an

electrode is sensing electrical changes in two different cells, as shown by the patterns. When two neurons are in contact with the same electrode, different voltages may be generated. In the event that two cells are close enough to one electrode, waves may converge. The presence of another cell might be indicated by this wave interference. This is another reminder of how tricky it may be to choose the ideal action potential threshold. Action potential detection is dropped at thresholds that are too high, while it is also removed at thresholds that are too low(Fee et al., 1996; Miccoli et al., 2019). Since there is no one-size-fits-all strategy for determining which neurons influence an electrode, most approaches for identifying spikes affecting the same electrode fail in certain situations(Bar-Gad, Ritov, Vaadia, & Bergman, 2001).

Understanding the intact networks, spikes, and bursts as well as how they evolve over time, will help us understand how in vitro neural cells respond to HHV-6. Our lab employs the MEA system to cultivate differentiated neural cells in order to learn more about how certain low virulence roseolaviruses (HHV-6A and HHV-6B) affect neuronal signaling.
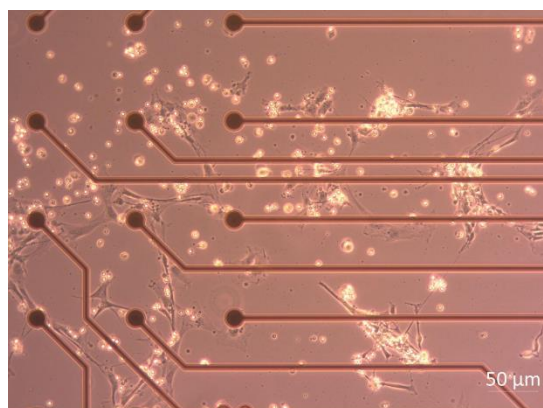

Figure 4-1 A section of a MEA plat with differentiated human neuron stem cells cultured on it

4.2 Results

We detected activity in our differentiated human neural stem cells, suggesting that our culture method worked. Neurons can also be examined using a light microscope, as seen in Fig.1. The ability to see neurons proved helpful in identifying when to infect cells with HHV6. When cells formed long projections and crowded the plate, recordings were conducted to look for electrical activity. After observing the electrical activity from the dHNSCs, we infected the cells with HHV6-A and HHV6-B (Fig. 2). Following the acquisition of raw data, the recordings were analyzed, and the results shown in Fig.3. (All data analysis conducted by honor undergraduate student, Walker Bartels).
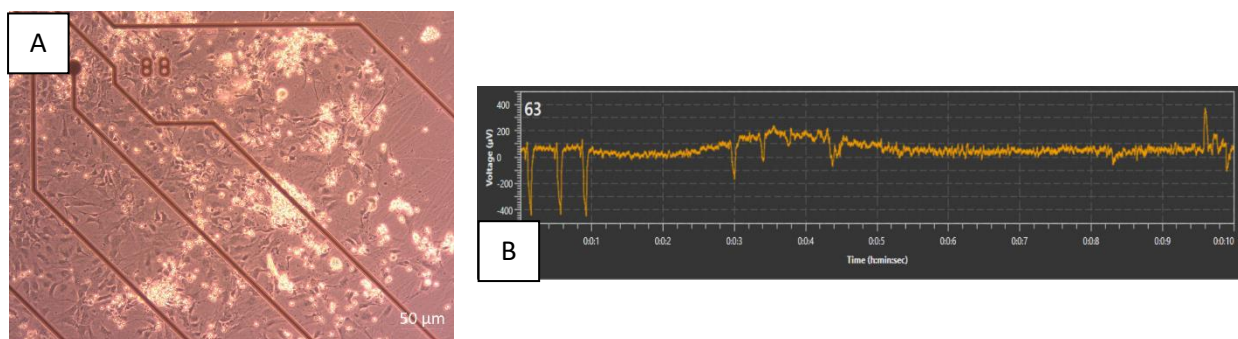

Figure 4-2 A: This image shows the well corner of a MEA plate. An electrode can be seen in the upper left corner, surrounded by several neurons. Long projections were utilized to recognize healthy cells. B: Voltage change recorded in one of the 60 electrodes on our MEA plate with uninfected dHNScs. There are three initial spikes with similar waveforms and voltage levels. These signals indicate that the cells being cultured are healthy and active.
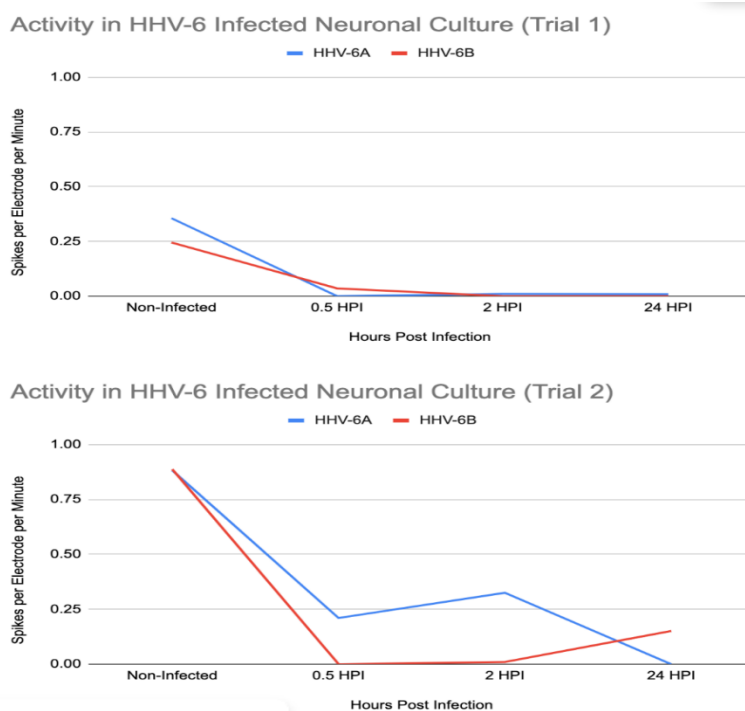
Figure 4-3 These graphs show activity measured in two different trails with dHNSCs uninfected and infected dHNSCs with HHV-6A and HHV-6B at 0.5hPI,2hPIand 24hPI.

4.3 Discussion

Following infection with HHV-6A and HHV-6B, we were able to see a decreased activity in infected dHNSCs. Even 30 minutes after infection, the cells' activity had decreased to less than half of the spikes per minute that had previously been noted. Although there was often a drop in activity after infection, there were times when spike activity appeared to rise. In comparison to half an hour after infection, there was a recovery in the HHV-6A-infected culture in trial 2. In Trial 2, the activity of infected HHV-6B increased from two hours to twenty-four hours post-infection. Trial 2 also started with increased activity in the cultures. Infection in Trial 1 caused a lot of cell death. Rebounding might signal that cells are healing or that a virus is going into latency.

4.4 Materials and Methods

4.4.1 Preparation of MEA plate

The MEA plates are cleaned with 70% ethanol before being used to culture neurons. To make the plates hydrophilic, place them in a plasma cleaner with oxygen operating at 200 motors. Plates were rinsed three times with 70% ethanol. Plates were coated with cellStart and incubated for 45 minutes in the 37-degree incubator.

4.4.2 dHNSCs culturing

Cells were cultured in the plates as previously explained (chapter 2).

4.4.3 Recording with the Multi-Electrode Array

The program Multi Channel Experimenter is used to collect data in combination with the MEA-2100. To record spike data, MEA plates are put in the MEA 2100. Culture plates with dHNSCs were recorded before HHV6-A and HHV6-B infection and at various points after infection. Changes in field potential caused by neuron firing can be detected if the neuron is adjacent to one of the MEA plate's 60 electrodes. This information can be gathered with minimum disruption to the culture.

4.4.4 Filter and Threshold Settings

The recordings were made without filters so that the raw data could be analyzed visually. After the recordings were made, a 1 Hz high pass filter and a 300 Hz low pass filter were added. The spike detection threshold was set at -17.5 V.

4.4.5 Network Spike Analysis

Each channel corresponding to individual electrodes was visually evaluated to see information obtained from the MEA-2100. Channels with unusually high noise levels were filtered out and deleted (figure. 6 for reference). MEAnalyzer software was used to examine the network of spikes and how they interacted with one another. There are virtual instruments presented onto a virtual workbench using the Multi-Channel Analyzer. Multi-Channel Systems provides extensive instructions for their experimenter, analyzer, and data management software to help you better understand and utilize it. Voltage movement outside of the noise range will be detected and recorded. These voltages are frequently measured in microvolts. To avoid missing spikes when detecting noise, the sensitivity can be increased. To prevent detecting the same event repeatedly, dead times might be set. Filtered data may be used to calculate spikes per second or the average interspike interval for a single cell. Multi-Channel Data Manager converts files to the format required by third-party applications. MEAnalyzer made use of HDF5 files. MEA analyzer contains applications that can assist you in determining the link between spikes. All of this data can be compared to cells post infection, as well as uninfected control cells.
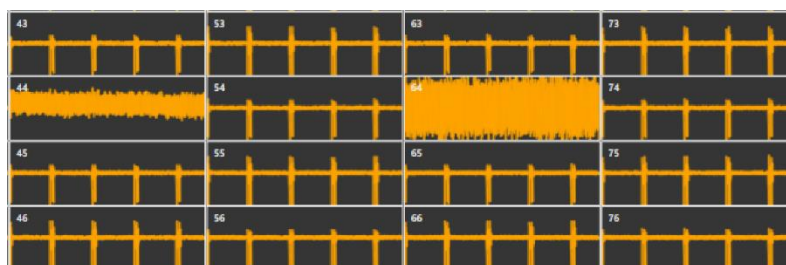

Figure 4-4 This picture shows recordings from an artificial model cell on Multi Channel Analyzer where channels 44 and 64 were showing abnormal levels of noise. These channels would be disregarded for any type of analysis

4.4.6   Individual Spike Analysis

One of the first issues is determining whether the signal is biological or noise. The shape, duration, and size of a spike can all assist in identifying its source. Neurons around the electrode can be seen using microscopes in combination with the MEA 2100. Neurons within the electrode's range can be viewed as a possible source of an action potential(Bar-Gad et al., 2001; Brown, Kass, & Mitra, 2004) if it is found that the change in field potential is due to an action potential. The magnitude of the voltage shift may be measured. This might vary as a result of closeness to the electrode or as a result of HHV-6 infection. The shape formed when cells fire may alter both before and after infection. Examining individual cells provides further information about what happens once the neuronal culture is infected with HHV-6. Using a microscope and looking for patterns in the waveforms or interspike intervals can assist assess how many neurons are touching an electrode.

4.4.7   Eliminating False Signals

To ensure that the MEA was not picking up on false signals, a complete medium was put to a plate with no cells to examine whether any false signals were created. A clean and prepared plate would be used, followed by the addition of a heated medium. We would immediately start recording after inserting the MEA plate into the MEA 2100. Any electrodes that produced electrical recordings that were outside the normal noise range might be discarded.

4.5   References

Asakura, K., Hayashi, S., Ojima, A., Taniguchi, T., Miyamoto, N., Nakamori, C., . . . Honda, Y. (2015). Improvement of acquisition and analysis methods in multi-electrode array experiments with iPS cell-derived cardiomyocytes. *Journal of pharmacological and toxicological methods, 75*, 17-26.

Bar-Gad, I., Ritov, Y. a., Vaadia, E., & Bergman, H. (2001). Failure in identification of overlapping spikes from multiple neuron activity causes artificial correlations. *Journal of neuroscience methods, 107*(1-2), 1-13.

Brown, E. N., Kass, R. E., & Mitra, P. P. (2004). Multiple neural spike train data analysis: state-of-the-art and future challenges. *Nature neuroscience, 7*(5), 456-461.

Burke, D., Kiernan, M. C., & Bostock, H. (2001). Excitability of human axons. *Clinical neurophysiology, 112*(9), 1575-1585.

Buzsáki, G., Anastassiou, C. A., & Koch, C. (2012). The origin of extracellular fields and currents—EEG, ECoG, LFP and spikes. *Nature Reviews Neuroscience, 13*(6), 407-420.

Egert, U., Banach, K., & Meyer, T. (2006). Analysis of cardiac myocyte activity dynamics with micro-electrode arrays *Advances in network electrophysiology* (pp. 274-290): Springer.

Egert, U., & Meyer, T. (2005). Heart on a chip—extracellular multielectrode recordings from cardiac myocytes in vitro *Practical methods in cardiovascular research* (pp. 432-453): Springer.

Erickson, J., Tooker, A., Tai, Y.-C., & Pine, J. (2008). Caged neuron MEA: A system for long-term investigation of cultured neural network connectivity. *Journal of neuroscience methods, 175*(1), 1-16.

Fee, M. S., Mitra, P. P., & Kleinfeld, D. (1996). Automatic sorting of multiple unit neuronal signals in the presence of anisotropic and non-Gaussian variability. *Journal of neuroscience methods, 69*(2), 175-188.

Gross, G. W., Rhoades, B. K., Azzazy, H. M., & Wu, M.-C. (1995). The use of neuronal networks on multielectrode arrays as biosensors. *Biosensors and Bioelectronics, 10*(6-7), 553-567.

Kapucu, F. E., Tanskanen, J. M., Mikkonen, J. E., Ylä-Outinen, L., Narkilahti, S., & Hyttinen, J. A. (2012). Burst analysis tool for developing neuronal networks exhibiting highly varying action potential dynamics. *Frontiers in computational neuroscience, 6*, 38.

Meiry, G., Reisner, Y., Feld, Y., Goldberg, S., Rosen, M., Ziv, N., & Binah, O. (2001). Evolution of action potential propagation and repolarization in cultured neonatal rat ventricular myocytes. *Journal of cardiovascular electrophysiology, 12*(11), 1269-1277.

Miccoli, B., Lopez, C. M., Goikoetxea, E., Putzeys, J., Sekeri, M., Krylychkina, O., . . . Reumers, V. (2019). High-density electrical recording and impedance imaging with a multi-modal CMOS multi-electrode array chip. *Frontiers in Neuroscience, 13*, 641.

Minerbi, A., Kahana, R., Goldfeld, L., Kaufman, M., Marom, S., & Ziv, N. E. (2009). Long-term relationships between synaptic tenacity, synaptic remodeling, and network activity. *PLoS biology, 7*(6), e1000136.

Simeonov, S., & Schäffer, T. E. (2019). Ultrafast imaging of cardiomyocyte contractions by combining scanning ion conductance microscopy with a microelectrode array. *Analytical chemistry, 91*(15), 9648-9655.

Spira, M. E., & Hai, A. (2013). Multi-electrode array technologies for neuroscience and cardiology. *Nature nanotechnology, 8*(2), 83-94.

Vezzani, A., Balosso, S., & Ravizza, T. (2019). Neuroinflammatory pathways as treatment targets and biomarkers in epilepsy. *Nature Reviews Neurology, 15*(8), 459-472.

Zitzmann, F. D., Jahnke, H.-G., Nitschke, F., Beck-Sickinger, A. G., Abel, B., Belder, D., & Robitzki, A. A. (2017). A novel microfluidic microelectrode chip for a significantly enhanced monitoring of NPY-receptor activation in live mode. *Lab on a Chip, 17*(24), 4294-4302.

Chapter V

5.1 Overall conclusion and future direction

Understanding differences in the susceptibility, as well as the immunological and electrophysiology responses of distinct neuronal neurotransmitter phenotypes responses to HHV-6A versus HHV-6B infection, will permit a more critical evaluation of models that seek to explain HHV6-induced neurological disorders(Vezzani, Balosso, & Ravizza, 2019). Combining results presented here from cytokine/growth factor regulation and physiological studies, there is ample evidence to conclude that there are differential impacts of HHV-6A versus HHV-6B infection on nerve cell viability, structure, and function in cultured cells. How this relates to neuronal signaling and neural circuit behavior in other in vitro and in vivo models is the subject of ongoing work in the lab. Furthermore, our lab is interested in examining the effect of coinfection of HHV6-A with HHV6-B, HHV6-A with HHV7, and HHV6-B and HHV7 in differentiated human neural stem cells. Another crucial study that other graduate students will do in our lab is to use different cell types to determine the kinetics of infection. In the future, animal models like mice will be utilized to repeat this experiment to obtain a better understanding of the impact of human herpes virus 6 on the nervous system.

Along with prior reports that support our results, we suggest that each virus may exhibit different levels of virulence on select cell types, with HHV-6A being more virulent despite the apparent advantage of HHV-6B to infect cells more readily with high densities of CD46 and CD134 expression.